ISSN 1408-7073

# RMZ – MATERIALS AND GEOENVIRONMENT

PERIODICAL FOR MINING, METALLURGY AND GEOLOGY

# RMZ – MATERIALI IN GEOOKOLJE

REVIJA ZA RUDARSTVO, METALURGIJO IN GEOLOGIJO

RMZ-M&G, Vol. 58, No. 3 pp. 241–356 (2011)

Ljubljana, September 2011

*Historical Rewiev*

More than 80 years have passed since in 1919 the University Ljubljana in Slovenia was founded. Technical fields were joint in the School of Engineering that included the Geologic and Mining Division while the Metallurgy Division was established in 1939 only. Today the Departments of Geology, Mining and Geotechnology, Materials and Metallurgy are part of the Faculty of Natural Sciences and Engineering, University of Ljubljana.

Before War II the members of the Mining Section together with the Association of Yugoslav Mining and Metallurgy Engineers began to publish the summaries of their research and studies in their technical periodical Rudarski zbornik (Mining Proceedings). Three volumes of Rudarski zbornik (1937, 1938 and 1939) were published. The War interrupted the publication and not untill 1952 the first number of the new journal Rudarsko-metalurški zbornik - RMZ (Mining and Metallurgy Quarterly) has been published by the Division of Mining and Metallurgy, University of Ljubljana. Later the journal has been regularly published quarterly by the Departments of Geology, Mining and Geotechnology, Materials and Metallurgy, and the Institute for Mining, Geotechnology and Environment.

On the meeting of the Advisory and the Editorial Board on May 22$^{nd}$ 1998 Rudarsko-metalurški zbornik has been renamed into "RMZ - Materials and Geoenvironment (RMZ -Materiali in Geookolje)" or shortly RMZ - M&G.

RMZ - M&G is managed by an international advisory and editorial board and is exchanged with other world-known periodicals. All the papers are reviewed by the corresponding professionals and experts.

RMZ - M&G is the only scientific and professional periodical in Slovenia, which is published in the same form nearly 50 years. It incorporates the scientific and professional topics in geology, mining, and geotechnology, in materials and in metallurgy.

The wide range of topics inside the geosciences are wellcome to be published in the RMZ -Materials and Geoenvironment. Research results in geology, hydrogeology, mining, geotechnology, materials, metallurgy, natural and antropogenic pollution of environment, biogeochemistry are proposed fields of work which the journal will handle. RMZ - M&G is co-issued and co-financed by the Faculty of Natural Sciences and Engineering Ljubljana, and the Institute for Mining, Geotechnology and Environment Ljubljana. In addition it is financially supported also by the Ministry of Higher Education, Science and Technology of Republic of Slovenia.

Editor in chief

# Table of Contents – Kazalo

## *Original Scientific Papers – Izvirni znanstveni članki*

*Preliminary notes – Predhodna objava*



*Event notes – Novice*

# The effect of defects on tensile strength of the continuous steel casting products

# Vpliv napak na natezno trdnost kontinuirno ulitih jeklenih proizvodov

Mirko Gojić[1,*], Ladislav Lazić[1], Stjepan Kožuh[1], Ladislav Kosec[2]

[1]University of Zagreb, Faculty of Metallurgy, Aleja narodnih heroja 3, 44103 Sisak, Croatia
[2]University of Ljubljana, Faculty of Natural Sciences and Engineering, Aškerčeva 12, 1000 Ljubljana, Slovenia

*Corresponding author. E-mail: gojic@simet.hr

**Received:** May 23, 2011 **Accepted:** October 6, 2011

**Abstract:** The goal of this paper is to determine the influence of defects on tensile strength of continuous casting steel products made from low alloy Mn-V steel. The microstructure was determined by optical microscopy and scanning electron microscopy. The composition of non-metallic inclusions were determined by energy dispersive X-ray spectroscopy. The microstructural analysis has shown that there are significant differences between the microstructure near the surface and in the central zone of the round cross-section. It was found that a significant decrease in tensile strength can be correlated the presence of alumina and sulphide inclusions as well as dendritic structure.

**Povzetek:** Namen članka je določiti vpliv napak na natezno trdnost kontinuirno ulitih jeklenih proizvodov, izdelanih iz Mn-V maloogljičnega jekla. Mikrostruktura je bila analizirana z optičnim mikroskopom in vrstičnim elektronskim mikroskopom. Kemična sestava nekovinskih vključkov je bila opredeljena z energijsko disperzijsko spektroskopijo rentgenskih žarkov. Mikrostrukturna analiza je pokazala občutno razliko med mikrostrukturo blizu površine in tisto v centralni coni prečnega prereza. Ugotovili smo, da je občuten padec natezne trdnosti v korelaciji s prisotnostjo aluminatnih in sulfidnih nekovinskih vključkov in tudi z dendritsko strukturo.

*Original scientific paper*

**Key words:** low alloy steel, solidification, non-metallic inclusions, continuous casting
**Ključne besede:** malooglјično jeklo, strjevanje, nekovinski vključki, kontinuirno litje

## Introduction

It is known that continuous casting of steels involves many physical phenomena (fluid flow, heat transfer, solidification etc.).[1–4] The flow of liquid steel inside the strand influences the quality of solidified steel, solidification structure, inclusion distribution and segregation.[5] One of the factors in connecting the quality of steel products is the cleanness of the steel, which refers to the non-metallic inclusion content in the steel. The presence of the defects from the steelmaking process can initiate a local weakness of the steel and its failure during application. Among others, low alloy steels are used commonly for oil country tubular goods (OCTG). The main reasons for this application are excellent hardenability, high strength, good toughness and high resistance to sulphide stress corrosion cracking (SSCC) as a form of hydrogen embrittlement.[6] Since these steels are used under complex loads, their defects (especially non-metallic inclusions) should be strictly controlled to decrease their negative effects.[7] Limitation of non-metallic inclusions and reduction of centreline segregation have a very important role in increasing the resistance of low alloy steels to hydrogen induced cracking (HIC) and sulphide stress cracking (SSC). Non-metallic inclusions in steel are originated from deoxidation, reoxidation, segregation and chemical reactions with the refractories.[8, 9]

Since mechanical properties and resistance to corrosion are influenced by the presence of defects in the steel, the objective of this paper is to establish the type, size and distribution of non-metallic inclusions and dendritic structure across the cross-section of the continuous casting products, as well as their impact on tensile strength. The obtained results will serve in the subsequent thermal stress analyses, questioning whether the temperature differences, appearing across the cross-section of the products heated in the rotary-hearth furnace, lead to thermal stresses which exceed the tensile strength of the final products and cause stress cracks in the structure. The investigation methodology consists of testing the tensile strength of the specimens taken at different places of cross-section of cast products, as well as examinations of the microstructural features of steel structure and defects

on the tested tensile specimens using optical microscope (OM) and scanning electron microscope (SEM) methods, respectively.

## Materials and methods

The cast steels for this investigation were produced in an electric arc furnace. The range of composition of the steel under investigation is given in Table 1. As can be seen, the steel grade corresponds to the low alloy Mn-V steel. The molten steel is continuously cast in the round cross-section with the diameter of 410 mm. Specimens for tensile tests were machined from the round cross-section in accordance with ASTM standards.[10] The specimens were taken from the mid-thickness location in two series all over the cross-section, starting from the surface, across the central zone to the opposite end (Figure 1). In this sequence, the specimens were tested at test temperatures from 100 °C up to 650 °C, with the step of 50 °C. The specimens were elongated to fracture on Zwick 50 kN tensile testing machine. The specimens for metallographic analysis were grinded and polished. After that the specimens were etched by a nital solution consisting of 5 % nitric acid in ethyl alcohol. Metallographic analysis was carried out on both etched and non-etched samples. Microstructural examination was carried out using an optical microscope (OM) and scanning electron microscope (SEM) equipped with energy dispersive X-ray spectrometry (EDX). EDX unit was used for the spot aimed chemical X-ray microanalysis. Fraction of inclusions was determined by quantitative metallogra-

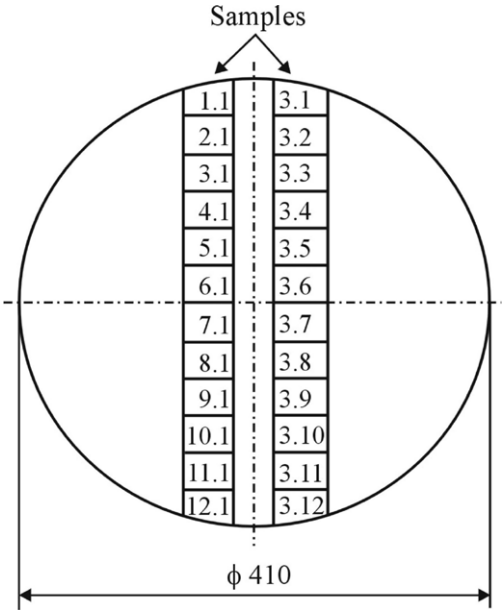


**Figure 1.** Schematic illustration of samples taken for the tensile test.

**Table 1.** Chemical composition of the investigated steel in mass fractions, *w*/%

| C | Mn | Si | Al | V | $P_{max}$ | $S_{max}$ |
|---|---|---|---|---|---|---|
| 0.30–0.34 | 1.15–1.30 | 0.15–0.35 | 0.02–0.04 | 0.15–0.18 | 0.025 | 0.025 |

phy method using optical microscopy Olympus BX61. There measurements were made on specimens from the outer and inner regions. Fractographic analysis of tensile test specimens after fracture was carried out using SEM.

## Results and discussion

In order to remove the flawed layer produced by polishing and in order to reveal the microstructural details, the specimen surfaces were etched by the nital solution. Optical and SEM micrographs of the etched specimens at surface and central zone of the round cross-section are shown in Figures 2, 3 and 4. The OM and SEM micrographs of the specimens near to the surface (Figures 2a and 3a) shows the pearlite-ferrite microstructure consisting of ferrite within the eutectoid structure. Ferritic grains are mostly surrounded by

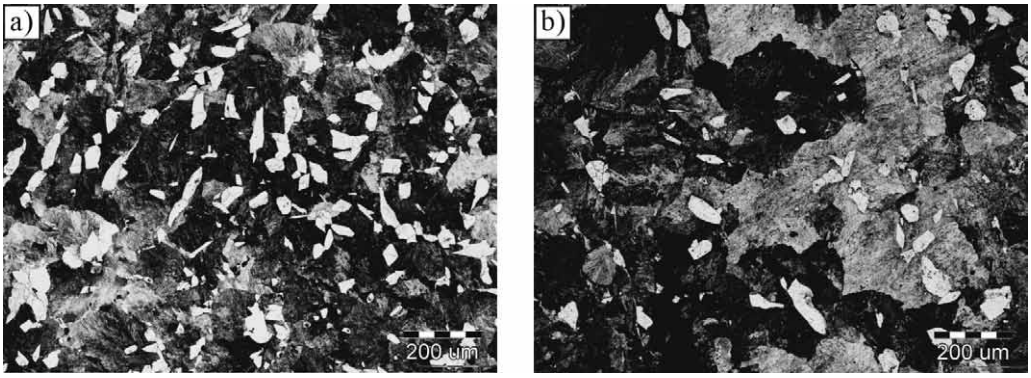


**Figure 2.** Microstructures of the steel product near the outer surface (a) and in the central zone (b) obtained using OM on specimens etched by nital solution.

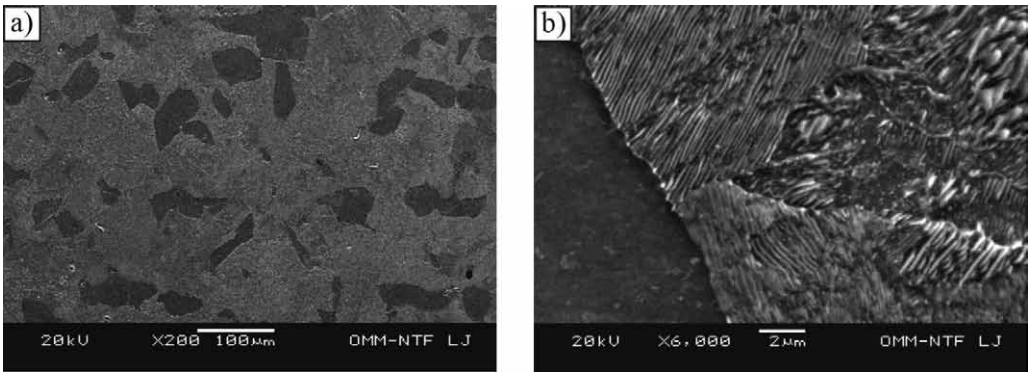


**Figure 3.** Microstructures of the steel product near the outer surface obtained using SEM at different magnifications.

the pearlitic grains. This pearlite can be characterized as lamellar (Figures 3b and 4b). The specimens in the central zone (Figures 2b, 3b and 4) also have pearlite-ferrite microstructure comprising randomly-oriented grains, characteristic for a central equiaxed zone. The grains are of different size and form. Grains are larger compared with the surface samples. The coarse-grain structure resulted from the slow cooling rate at the casting core. The grain

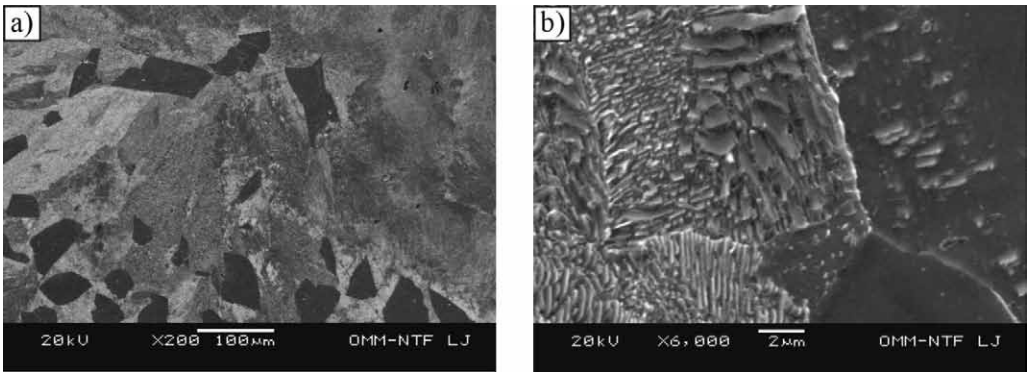


**Figure 4.** Microstructures of the steel product in the central zone obtained using SEM at the different magnification.

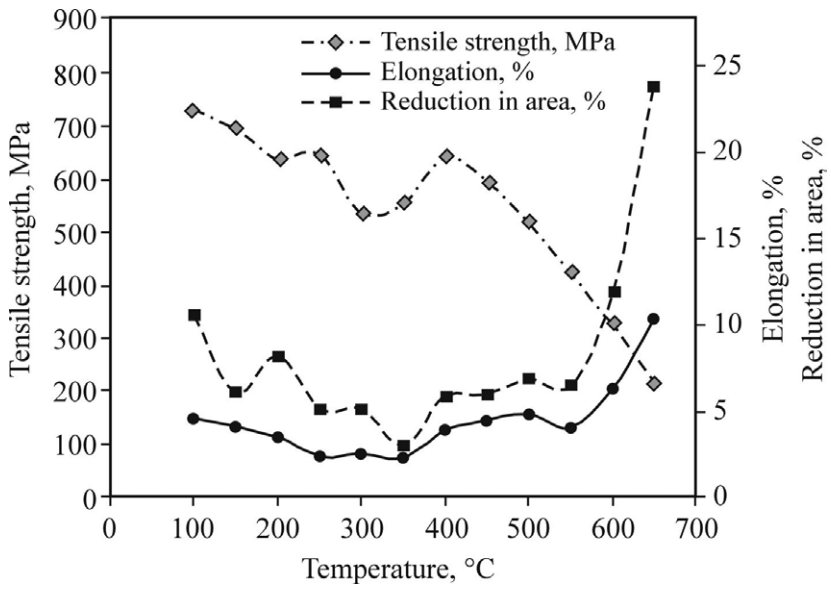


**Figure 5.** Variations of the tensile strength, elongation and reduction in area with the testing temperature.

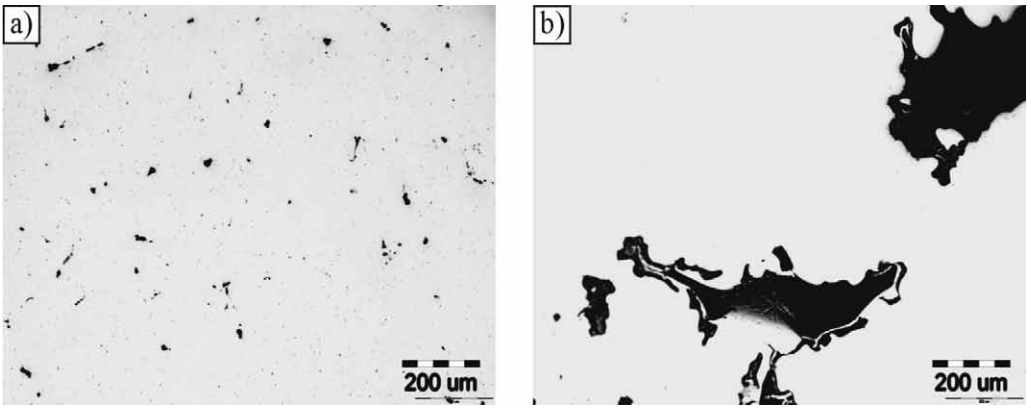


**Figure 6.** Microstructures of the steel product near the outer surface (a) and in the central zone (b) obtained using OM on non-etched specimens.

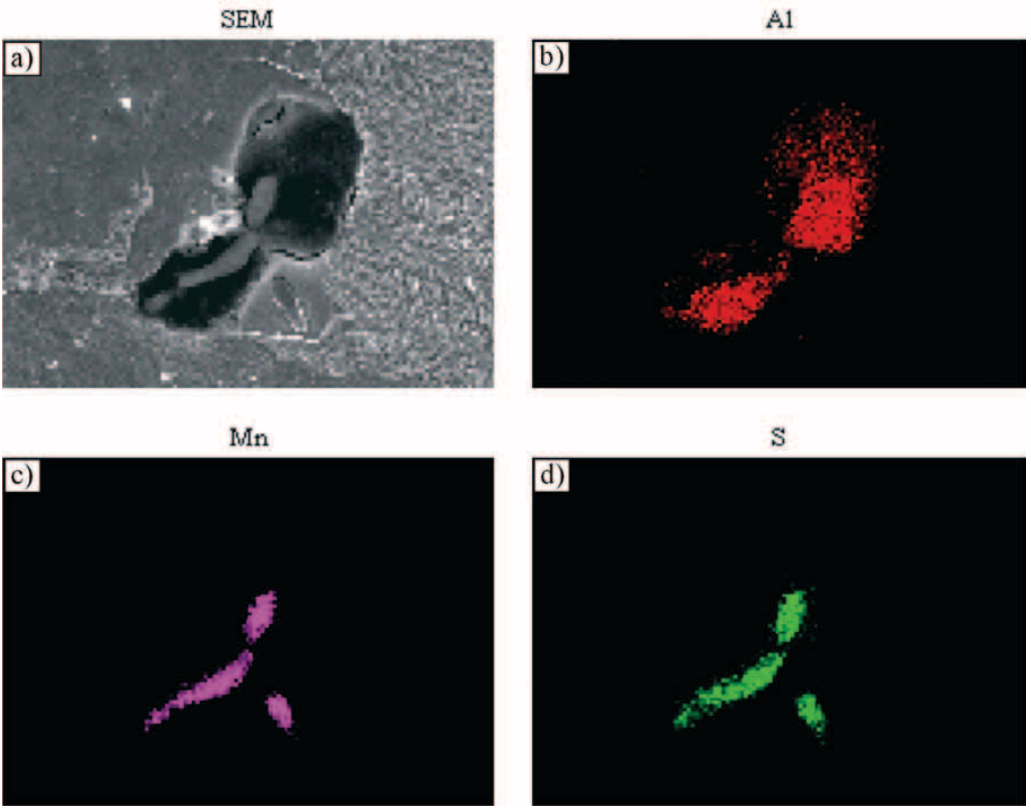


**Figure 7.** Microstructures of the steel product at the ferrite/pearlite interface obtained using SEM (a) and elemental maps for aluminium (b), manganese (c) and sulphur (d).

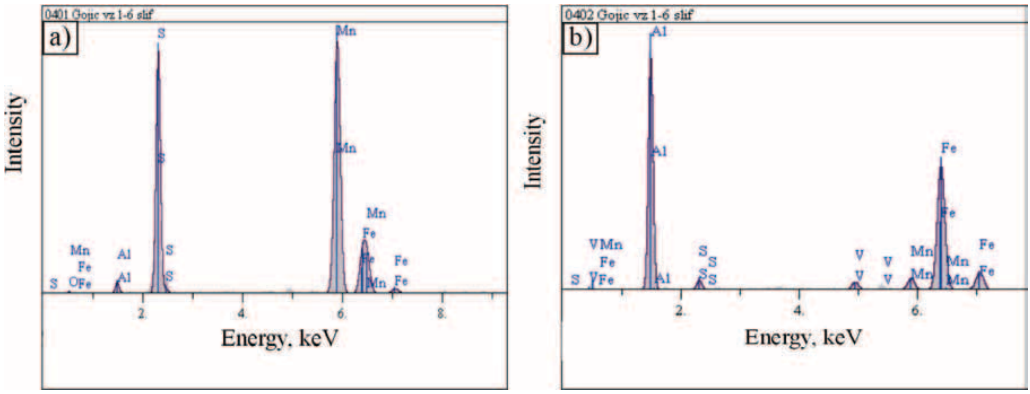


**Figure 8.** EDX spectra of particles enriched with sulphur (a) and aluminium (b) at the ferrite/pearlite interface shown in Figure 7a.

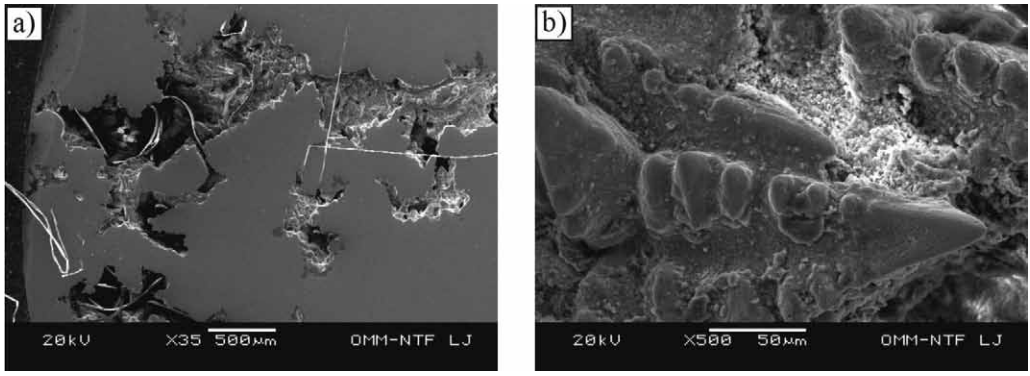


**Figure 9.** Microstructures of the steel product in the central zone obtained using SEM at different magnifications, 1st position.

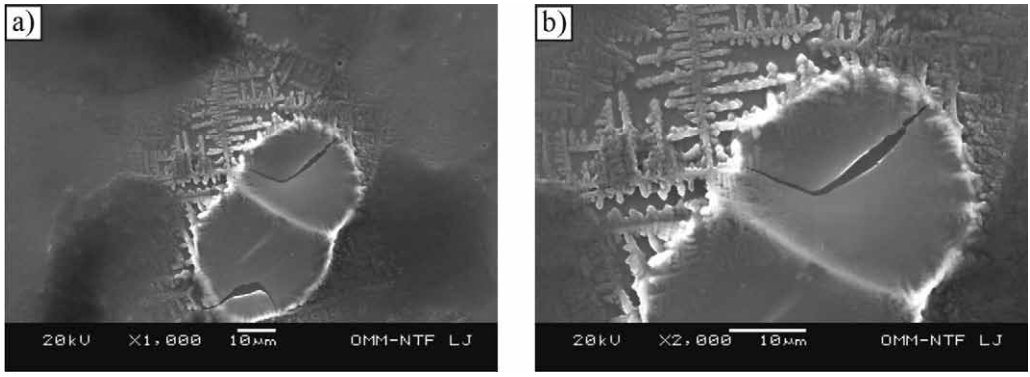


**Figure 10.** Microstructures of the steel product in the central zone obtained using SEM at different magnifications, 2nd position.

boundaries between ferrite and pearlite are clearly visible (Figures 3b and 4b).

The values of tensile strength are obtained by conducting tensile stress-strain tests at elevated temperatures. Figure 5 shows the influence of temperature on tensile strength. It was found that tensile strength decreases with increasing temperature. However, for specimens cut from the central zone of the round cross-section, the hot tensile strength suddenly dropped in the temperature range from 250 °C to 350 °C. The reason of this phenomenon may be only in the metallurgical cleanness of the cast steel.

The optical, SEM and EDX analysis of the specimens at surface and core of the cast steel are shown in Figures 6, 7, 8, 9 and 10. Figure 6a shows the presence of inclusions on non-etched surface. Fine inclusions distributed uniformly at surface were found. There is no important porosity. In the Figures 6b, 7, 8, 9 and 10 many inclusions and dendritic structure in the central part of the round cross-section may be seen. Numerous inclusions are probably segregated between dendrites. Fraction of inclusions into outer regions of the cast steel was 1.55 %, while the fraction of inclusion into core of the cast steel was 2.50 %.

The high deflection region of hot tensile strength ranging from 250 °C to 350 °C (Figure 5) can be connected with microstructural change. It is likely to be attributed to the presence of non-metallic inclusions (Figures 6–9a) and coarser dendritic structure with a small proportion of equiaxed grains in the core of continuous cast products (Figures 9b and 10).

The inclusions segregate in the inter-dendritic regions of the solidifying steel because they were not able to float out. They formed in molten steel before the solidification or after beginning of solidification in interdendritic regions. The composition of inclusions was analysed by EDX-method (Figure 8). The EDX-spectrum shown in Figure 8a illustrates the peaks of manganese and sulphur, while Figure 8b shows peaks of aluminium and iron. Thus the inclusions have complex composition (alumina and sulphide). The formation of alumina and sulphide inclusions as the result of deoxidation and desulphurization processes can be described by the following reactions [11]:

$$3[O] + 2[Al] \rightarrow (Al_2O_3) \quad (1)$$

$$(MnO) + [FeS] \rightarrow (MnS) + (FeO) \quad (2)$$

Alumina inclusions generated by reaction between the dissolved oxygen and the added aluminium deoxidant are typical deoxidation inclusions in steels. They are hard and non-deformable and tend to form oxide clusters. Angular aluminium oxide inclusions are probably more deleterious than

particles with rounded shapes. Small sulphide inclusions can be harmful, especially for steel used for exploitation of oil and natural gas. Manganese sulphide can decrease the plasticity of steel during rolling due to its low melting temperature.

According to their composition, the inclusions might be endogenous, i.e. product of the deoxidation and precipitation during cooling and solidification. Inclusions being formed during the solidification process in interdendritic spaces, termed secondary inclusions, may be either pushed by the advancing solid-liquid interface, i.e. by the thickening dendrite arm, or trapped within the dendrite arm as the solid front moves (for example alumina). The structure, distribution of segregations and non-metallic inclusions, as well as other qualitative characteristics, differ widely between individual cross-sections because the shape and size of the cross-section of continuous castings influence the crystallization process. The manner of final meetings of the crystallization fronts depends on the shape of the casting (mould) cross-section. For the circular or square cross-section the crystallization fronts meet in one point and for the rectangular cross-section in one line. The latter is more favourable in view of the distribution of non-metallic inclusions and segregations.

The fracture surfaces reflect the changes in microstructure. Scanning electron fractograph (Figure 11) of the broken surface specimen near to the surface shows mostly the mixture of ductile and transgranular cleavage fracture surfaces. Ductile fracture is a result of decohesion along the non-metallic inclusion/matrix interfaces. This fracture is characterized by void nucleation, growth and coalescence. Even at small plastic strains the non-metallic inclusions will be released from the ductile matrix and in that way they cause the nucleation of voids, which grow with increasing load. Some of cleavage facets were initiated by inclusions (Figure 11b). Obtained microstructural results in the central zone of the steel products (Figures 9 and 10) are confirmed by fractographic analysis. Scanning electron fractograph of the broken core specimen shows the predominant dendritic structure (Figure 12) which serves as an initiation centre of cleavage. As it can be seen, specimens in the central zone show interdendritic fracture morphology (Figures 12a and 12b) with primary and secondary dendrite arms (Figures 12c and 12d). Primary columnar dendrite arm spacing is around 450 μm, while the secondary columnar dendrite arm spacing ranges from 10 μm to 100 μm, which is according to the results of investigation by Fujda et al.[12]

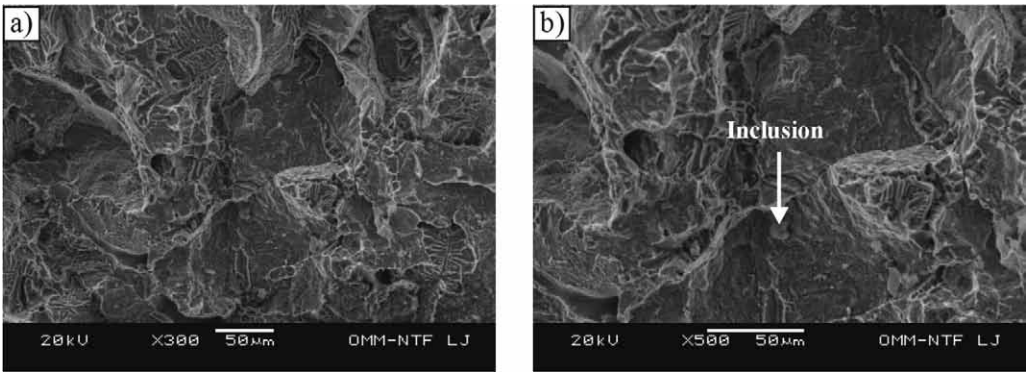


**Figure 11.** SEM micrographs of fracture surface near the surface of the round cross-section at different magnifications.

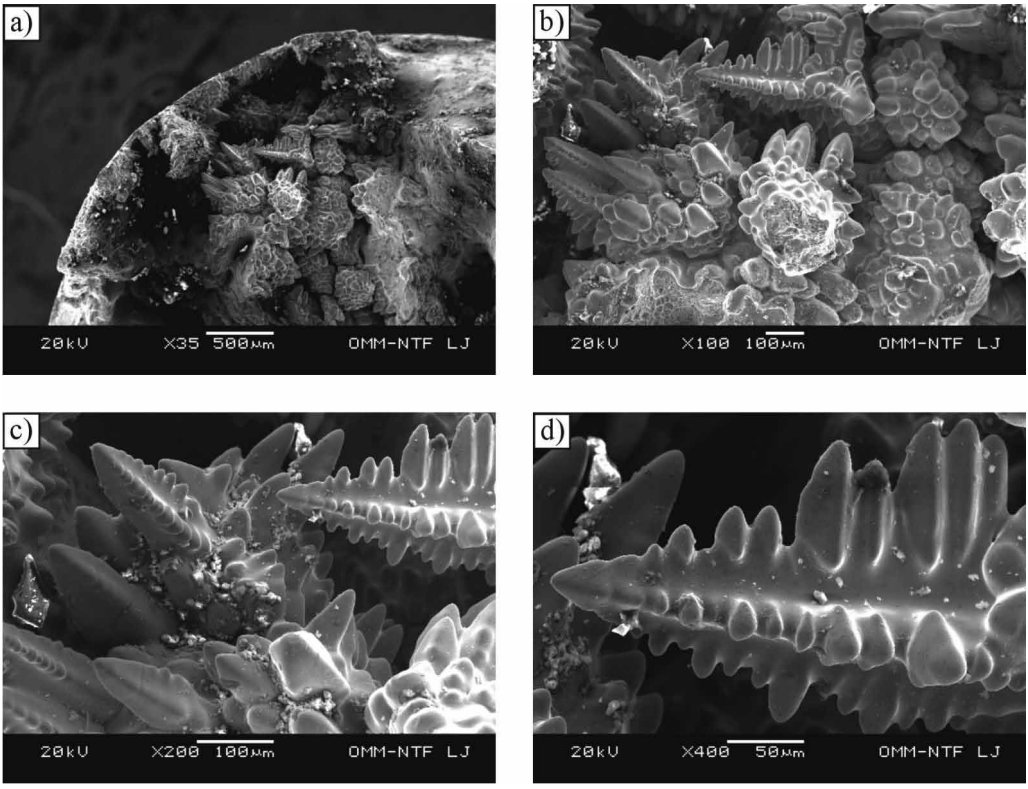


**Figure 12.** SEM micrographs of fracture surfaces in the central zone of the round cross-section at different magnifications.

It is known that solidification grain structure of the cross-section of continuous casting consists of an outer equiaxed zone comprising fine, randomly-oriented grains, an intermediate columnar zone comprising elongated, oriented grains and a central equiaxed zone, again comprising randomly-oriented grains. Thus the steel solidification in casting is dendritic. Each equiaxed grain contains one dendrite, with many dendrite arms. Many secondary dendrite arms grow from a single primary dendrite arm. Due to the anisotropy of properties, such as solid/liquid interface energy and growth kinetics, dendrites will grow in a preferred crystallographic direction that is closest to the heat flow direction, whereas cells grow with their axes parallel to the heat flow direction without regard to the crystal orientation. The columnar grains always grow out from the mould (which is the heat sink) in direction which is opposite to that of the heat flow, while equiaxed growth takes place in a supercooled melt which acts as their heat sink. Thus, the growth direction and the heat flow direction are the same in equiaxed growth. The grain size often, but not always, decreases with increasing cooling rate. Fineness of the dendritic structure, the primary and secondary arm spacings, always decreases with increasing cooling rate. The characteristic of the continuous casting is a high solidification rate in the direction of casting (mould) centre. As a general rule, the characteristic of continuous casting is a high solidification rate in the direction of the mould centre.

## Conclusions

Results show that tensile strength of the low alloy Mn-V continuous casting steel decreased by increasing temperature testing. Characteristic decreasing of tensile strength in the central zone of continuously cast round cross-section with diameter of 410 mm is the result of microstructural changes. Different microstructures are observed depending on the depth under the surface of the round cross-section. Central zone samples showed higher content of non-metallic inclusions and dendritic structure. These inclusions are alumina and sulphides. They are the results of chemical reactions during deoxidation and solidification of the steel.

## References

[1] Yasuda, H., Toh, T., Iwai, K., Morita, K. (2007): Recent progress of EPM in steelmaking, casting, and solidification processing. *ISIJ International*, *47*, pp. 619–626.

[2] De Barcellos, V. K., Da Silva Gschwenter, V. L., Kytönen, H., Dos Santos, C. A., Spim, J., Louhenkilpi, S., Miettinen, J.

(2010): Modelling of Heat Transfer, Dendrite Microstructure and Grain Size in Continuous Casting of Steels. *Steel Research Int.*, *81*, pp. 461–471.

[3] Kitamura, S. (2010): Importance of Kinetic Model in the Analysis of Steelmaking Reactions. *Steel Research Int.*, *81*, pp. 766–771.

[4] Domitner, J., Kharicha, A., Grasser, M., Ludwig, A. (2010): Reconstruction of Three-Dimensional Dendritic Structures Based on the Investigation of Microsegregation Patterns. *Steel Research Int.*, *81*, pp. 644–651.

[5] Javurek, M., Barna, M., Rockenschaub, K., Lechner, M. (2008): Flow Modelling in Continuous Casting of Round Bloom Strands with Electromagnetical Stirring. *Steel Research Int.*, *79*, pp. 617–626.

[6] Gojić, M., Kosec, B., Anžel, I., Kosec, L., Prelošćan, A. (2007): Hardenability of steels for oil industry. *Journal of Achievement in Materials and Manufacturing Engineering*, *23*, pp. 23–26.

[7] Gojić, M., Kosec, L., Matković, P. (2003): Embrittlement damage of low alloy Mn-V steel.*Engineering Failure Analysis*, *10*, pp. 93–102.

[8] Thunman, M., Sichen, D. (2008): Origins of Non-metallic Inclusions and their Chemical Development during Ladle Treatment. *Steel Research Int.*, *79*, pp. 124–132.

[9] Pfeiler, C., Thomas, B. G., Wu, M., Ludwig, A., Kharicha, A. (2008): Solidification and Particle Entrapment during Continuous Casting of Steel. *Steel Research Int.*, *79*, pp. 599–607.

[10] ASTM, A370-94. Standard test method and definitions for mechanical properties of steel products, ASME, New York, 1994.

[11] Gojić, M., Kožuh, S., Kosec, B. (2010): SEM and EDX analysis of continuous casting of steel. *Acta Metallurgica Slovaca Conference-special issue*, *15*, pp. 235–237.

[12] Fujda, M., Longauerová, M. (2006): Morphology of fine surface cracks on low carbon steel CC slab enriched by copper. *Acta Metallurgica Slovaca*, *12*, pp. 243–249.

# An analysis of the quasi-chemical model of a ternary solution: On the counting of pairs

# Analiza kvazikemičnega modela ternarne raztopine: O štetju parov

Jiawen Chen[1, *]

[1]University of Cambridge, Materials Science and Metallurgy, Cambridge CB2 3QZ, U. K.

*Corresponding author. E-mail: jiawen.chenn@gmail.com

**Received:** September 5, 2011 **Accepted:** September 6, 2011

**Abstract:** The quasi-chemical model of a ternary solid solution was proposed in 1971 by Alex and McLellan. The model begins with the counting of different kinds of pairs between nearest atoms in a ternary crystal. The formulae of two pairs used in the model has been shown to be incorrect. A solution is suggested. A new quasi-chemical model of the solid solution developed from this work can be useful in physical metallurgy.

**Izvleček:** Kvazikemični model ternarne trdne raztopine sta predlagala Alex in McLellan leta 1971. Začne se s štetjem različnih vrst parov med najbližjimi atomi v ternarnem kristalu. Prikazana je nepravilna formulacija dveh parov, uporabljenih v modelu, in predlagana pravilna rešitev. Nov kvazikemični model za trdne raztopine, razvit v tem delu, je lahko uporaben v fizikalni metalurgiji.

**Key words:** theory; statistical mechanics; ferritic steels
**Ključne besede:** teorija, statistična mehanika, feritna jekla

## Introduction

A statistical treatment of ternary metals, e.g. Fe-Mn(Cr,Al)-C(N,H) or Nb-Ti(V,Mo,Zr,Ta)-O(C,N), can yield thermodynamic properties which could be diffcult to obtain experimentally. As an example, the carbon-carbon interac-

*Original scientific paper*

tion energy in the ferrite phase in steel can be calculated by fitting the experimentally determined Gibbs free energy to a function deduced from a simple quasi-chemical model.[1, 2] Many recent publications[3, 4] use data that are derived from the quasi-chemical model of a ternary system proposed by ALEX & MCLELLAN.[5] The current work demonstrates a fundamental problem in the model and suggests a solution, which will lead to a correct quasi-chemical model of the ternary system.

A solid phase of two or more kinds of atoms is a solid solution. The forces between the atoms in solid solution are short-ranged. Guggenheim showed that the second nearest neighbour interaction energy is negligible, if it varies as $r^{-6}$.[6] Most solution models consider only the nearest neighbour interactions.

The energy of a solid solution is the sum of the interaction energy of all kinds of pairs. Let us consider a binary model containing A and B atoms, and we interchange an A atom and a B atom on any two sites. Whatever the initial arrangement around the two sites, if the number of A-A pairs increases or decreases by $N$, then the number of B-B pairs will change by the same amount $N$, and the number of A-B pairs will change by $-2N$. Therefore, the properties of the solid solution depends only on the change of combined energy $N(e_{AA} + e_{BB} - 2e_{AB})$

For a non-ideal solution, i.e. $e_{AA} + e_{BB} \neq 2e_{AB}$, if $e_{AA} + e_{BB} < 2e_{AB}$, the attractive force between unlike atoms is stronger, therefore there will be a tendency for each atom to be surrounded by unlike atoms. On the other hand, if $e_{AA} + e_{BB} > 2e_{AB}$, the solution tends to segregate into A-rich and B-rich regions.

A quasi-chemical solution model accounts for the non-random distribution of atoms. It starts with the partition function , which equals the sum of all microstates the system can occupy.

$$\Omega = \sum_i \exp\left\{-\frac{E_i}{kT}\right\}$$

where $k$ is the Boltzmann constant and $1/kT$ is the inverse temperature; $E_i$ is the energy level of microstate $i$. Each microstate has a unique arrangement of atoms. Hence, $E_i$ is the function of numbers of different pairs and associated interaction energies. Thermodynamic quantities like the Gibbs free energy and the activity of a solute can be deduced from the partition function. An exact solution of the partition function in two dimensions was obtained by ONSAGER.[7] The partition function has not been evaluated exactly for a three dimensional lattice.

The system researched in the work by Alex and McLellan contains A, B and c atoms. A and B form a substitutional solution, and may interchange positions on the sites. Whereas c atom occupy

sites in the space between the A and B atoms. It is an interstitial solute of the solvent A and B. Figure 1 shows a body-centered cubic (BCC) lattice model.

The number of A, B and c atoms are designated as $N_A$, $N_B$ and $N_c$ respectively. The ratio of interstitial sites per lattice atom is $\beta$. Therefore the number of empty sites $e$ equals $(N_A + N_B)\,\beta - N_c$. The pairs of nearest neighbouring atoms are separated by half the lattice parameter $a/2$ and can be divided into two groups (Figure 2).

The number of nearest interstices and the number of nearest lattice atoms to any interstice are designated as $Z_1$ and $Z_2$ respectively. In the BCC structure, $Z_1$ equals 4, and $Z_2$ equals 2 (Figure 3).

## The difficulty

Alex and McLellan proposed a set of formulae counting the numbers of the seven kinds of pairs for the construction of a quasi-chemical model.

For the first group of pairs, it starts with the number of pairs between atom c and site e, which is simply designated as $Z_1\lambda_1$. Then the number of c-c pairs equals the total interstitial pairs con-

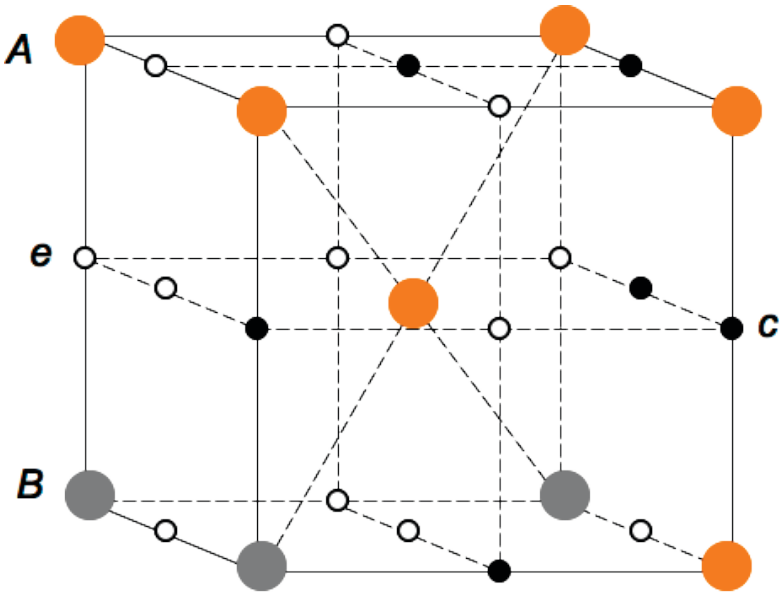


**Figure 1.** The ternary system consists of three types of atoms: type A, type B and type c. Atoms A and B form the BCC lattice, and atom c and empty sites e are the octahedral sites in BCC structure.

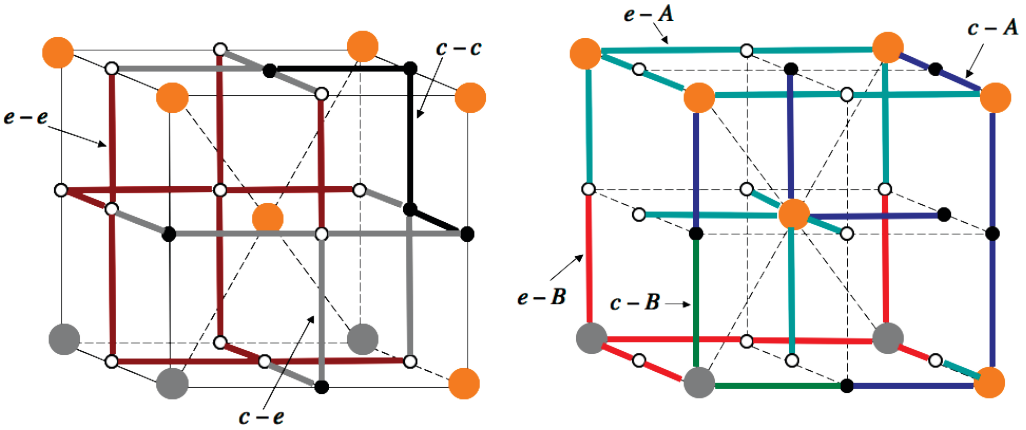


**Figure 2.** The left shows the pairs between interstices, i.e. c-e, c-c and e-e, and the right shows the pairs between interstice and a main lattice atom, i.e. c-A, c-B, e-A and e-B.

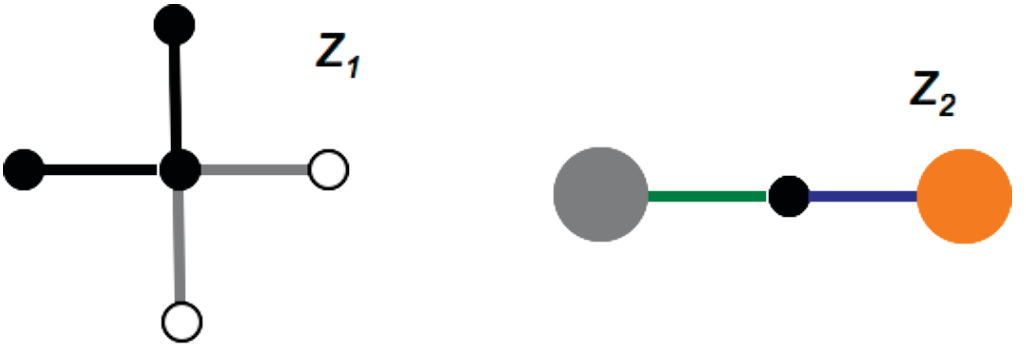


**Figure 3.** $Z_1$ is the number of nearest interstices to any interstice. $Z_2$ is the number of main lattice atoms to any interstice.

**Table 1.** Formulae of the number of pairs used in a ternary quasi-chemical model[5]

| Type of pair | Count |
|---|---|
| c-e and e-c | $Z_1\lambda_1$ |
| c-c | $(Z_1N_c - Z_1\lambda_1)/2$ |
| e-e | $[Z_1 (N_a + N_b)\beta - (Z_1N_c - Z_1\lambda_1) - 2 Z_1\lambda_1]/2$ |
| c-A | $Z_2\lambda_2$ |
| c-B | $Z_2N_c - Z_2\lambda_2$ |
| e-A | $Z_2N_a - Z_2\lambda_2$ |
| e-B | $Z_2N_b - (Z_2N_c - Z_2\lambda_2)$ |

necting to c, $Z_1N_c$, minus those connecting c to e, and then divided by 2 as the same pair is double counted by either c of the pair. The same logic applies to the e-e pairs.

For the second group of pairs, first the number of pairs between c and A is designated as $Z_2\lambda_2$. Then the number of c-B pairs equals all the pairs connected to c minus the c-A pairs. The formulae of the numbers of e-A and e-B pairs are problematic, which will be discussed below. The list of the formulae of the counting of the pairs used by Alex & McLellan is shown on Table 1.

Let us take a closer look at the number of e-A pair and e-B pair. A simple sum of the formulae of e-A and e-B pairs in Table 1 yields the equation for the total number of pairs connecting e to A or B atoms.

$$[Z_2N_A - Z_2\lambda_2] + [Z_2N_B - (Z_2N_C - Z_2\lambda_2)] = Z_2\,(N_A + N_B) - Z_2N_C \quad (1)$$

Equation 1, in principle, should equal the number of all pairs connecting to both c and e, $Z_2\,(N_A + N_B)\beta$, minus c-A and c-B pairs

$$Z_2\,(N_A + N_B)\beta - Z_2N_c \quad (2)$$

However, clearly the two equations are not equal, as $\beta$ equals 3 for a BCC lattice.

## The solution

To solve the problem, a new variable, $Z_3$ is needed. It is the number of nearest interstices to an A atom or a B atom (Figure 4). For both body-centered cubic metal, e.g. ferrite in steel and face-centered cubic metal, e.g. austenite in steel, $Z_3$ equals 6.

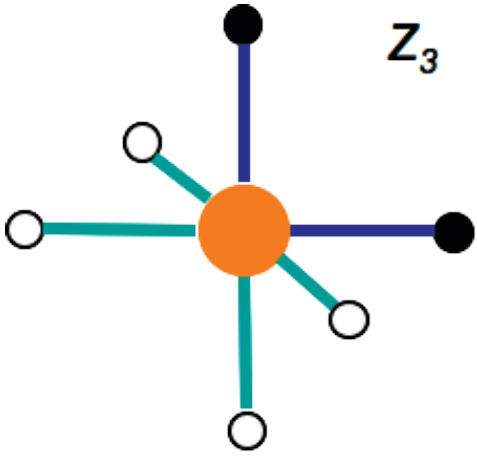


**Figure 4.** $Z_3$ is the number of nearest interstices to a lattice atom.

**Table 2.** The comparison of the formulae of e-A and e-B pairs.

| Type of pair | Old count | New count |
|---|---|---|
| e-A | $Z_2N_A - Z_2\lambda_2$ | $Z_3N_A - Z_2\lambda_2$ |
| e-B | $Z_3N_B - (Z_2N_C - Z_2\lambda_2)$ | $Z_2(N_A + N_B)\beta - Z_3N_A - (Z_2N_C - Z_2\lambda_2)$ |

The number of *e-A* pairs equals the total number of pairs connecting *A* to interstices, $Z_3N_A$, minus c-A pairs

$$Z_3N_A - Z_2\lambda_2$$

And the number of e-B pairs equals all the pairs connecting e to lattice atoms, $Z_2[(N_A + N_B)\beta - N_c]$, minus e-A pairs

$$Z_2[(N_A + N_B)\beta - N_c] - (Z_3N_A - Z_2\lambda_2)$$

or

$$Z_2(N_A + N_B)\beta - Z_3N_A - (Z_2N_c - Z_2\lambda_2)$$

The new and old formulae are compared in Table 2

## Conclusion

A careful investigation of the quasi-chemical model of a ternary solid solution proposed by ALEX & MCLELLAN[5] has revealed a mistake in two formulae counting the number of pairs. The solution to the flaw proposed in this work will give a new quasi-chemical model of the solid solution, which will produce different functions of thermodynamic properties. It would be interesting to investigate the compatibility of the new quasi-chemical model of the ternary system with the model of a binary system[2] at the limits where $N_B \rightarrow 0$, or the interaction energy $e_{BX} \rightarrow e_{AX}$, where X represents the interstitial atom in the system.

## References


[1] J. A. LOBO & G. H. GEIGER (1976): Thermodynamics and Solubility of Carbon in Ferrite and Ferritic Fe-Mo Alloys. *Metallurgical Transactions* A; 7A:1347.

[2] R. B. MCLELLAN & W. W. DUNN (1969): A Quasi-Chemical Treatment of Interstitial Solid Solutions: Its Application to Carbon Austenite. *J. Phys. Chem. Solids*; 30:2631–2637.

[3] L. M. YU, F. X. YIN & D. H. PING (2007): Natural Mechanism of the Broadened Snoek Relaxation Profile in Ternary Body-centered-cubic Alloys. *Phys. Rev. B*; 75(17):174105.

[4] M. GRUJICIC & X. W. ZHOU (1993): Monte-carlo Analysis of Short-range Order in Nitrogen-strengthened Fe-Ni-Cr-N Austenitic Alloys. *Materials Science and Engineering A*, 169:103–110.

[5] K. ALEX & R. B. MCLELLAN (1971): A Quasi-Chemical Approach to the Thermodynamics of Ternary Solid Solutions Containing Both Substitutional and Interstitial Solute Atoms. *J. Phys. Chem. Solids*; 32:449–457.

[6] E. A. GUGGENHEIM (1952): *Mixtures*. Oxford University Press, Oxford.

[7] L. ONSAGER (1944): Crystal Statistics. I. A Two-Dimensional Model with an Order-Disorder Transition. *Phys. Rev.*; 65:117–149.

# Finite element solution strategy to analyze heterogeneous structures

# Strategija analize heterogenih struktur z metodo končnih elementov

Martin Lamut

[1]CO Vesolje-SI, Aškerčeva 12, 1000 Ljubljana, Slovenia

*Corresponding author. E-mail: martin.lamut@space.si

**Received:** September 19, 2011 **Accepted:** November 2, 2011

**Abstract:** In this contribution a general strategy for solving a coupled micro-macro problems is presented which enables analyses of modern heterogeneous materials. It provides an efficient problem solving tool to structures with complex microstructures, used in a demanding structural components. The method uses a nested finite element solution strategy called multilevel finite element approach-ML-FEM. Within the ML-FEM framework one conducts an embedded microscale computation in order to obtain quantities required at the macroscopic level. The application of ML-FEM circumvents the need to construct an explicit macroscale constitution formulation, considering increased computational costs. Increased computation is linked to detailed microscopic analysis for which the statistical representative volume element-RVE is needed. RVE will be derived based on the convergence criterion. In this work a general method for calculation of the consistent macroscopic stiffness matrix via sensitivity analysis of a micro level is shown. As an example the proposed method is applied on a simple test specimen under compression consisting microstructures with porosities and stiff inclusions.

**Povzetek:** V tem delu je bila razvita splošna strategija za reševanje vezanih mikro-makro sodobnih heterogenih materialov. Strategija je učinkovito orodje pri reševanju problemov s kompleksno mikrostrukturo, uporabljeno v zahtevnih inženirskih komponentah. Strategija uporablja večnivojski način reševanja problemov, kjer na mikroskopski in makroskopski ravni poteka analiza z metodo končnih elementov

*Original scientific paper*

(ML-FEM). Pri tej metodi reševanja makroskopska konstitutivna zveza ni več potrebna, saj je le-ta na račun povečanega računskega časa pridobljena z natančno mikroskopsko analizo. Ta je izvedena na statističnem reprezentativnem volumnu (RVE), katerega velikost določimo s konvergenčnim merilom. Metoda je splošen način reševanja makroskopske togostne matrike preko občutljivostne analize mikroskopskega nivoja. Lastnosti metode so bile preizkušene na enostavnem tlačnem preizkusu za porozno mikrostrukturo in mikrostrukturo s togimi vključki.

**Keywords:** Heterogeneous materials, multiscale analysis, macroscopic tangent computation, sensitivity analysis
**Ključne besede:** heterogeni materiali, mikro-makro analize, makroskopska togost, občutljivostna analiza

## INTRODUCTION

Heterogeneous materials used in engineering sciences have physical properties that vary throughout their microstructures. Heterogeneities, such as inclusions, pores, fibers and grain boundaries, have a significant impact on the observed macroscopic behavior of multi-phase materials. In engineering some typical examples are metal alloy systems, various composites, porous and cracked structures, polymeric blends and polycrystalline materials.

To describe the macroscopic overall characteristics of heterogeneous structures is a vital problem in many engineering applications. The ability to convey information across length scales is essential for a better understanding of the sources of physical behavior observed on higher scales. Using micromechanical models of the microstructural elements, homogenization techniques allow an efficient and correct transfer of microscale information to the macroscale analysis. The fundamental methodology of homogenization is the characterization of the macroscopic behavior of the heterogeneous material by appropriately identifying and testing a statistically representative micromechanical sample. Once an appropriate sample is identified it can be used in the multiscale analysis methodology. The most straightforward way is to use the multilevel finite element method ML-FEM[1–5]. When analyses at both levels are made in the context of FEM, it can be referred to as the $FE^2$ method[6, 7]. The application of ML-FEM circumvents the need to construct an explicit macroscale constitution formulation, though at an increased computational cost. The con-

stitutive equations are written only on microscopic scale and homogenisation and localization equations are used to compute the macroscopic strains and stresses knowing the mechanical state at microscopic level.

By analyzing the engineering structure, the point of interest is usually localized in the so called critical region, where detailed analyses are needed. So to further increase the efficiency of the computation the structure can be divided into subdomains, critical region and the rest of the structure. In the critical region an embedded ML-FEM computation is conducted, while elsewhere a classical homogenization technique is used. In either case a statistical micromechanical model or representative volume element (RVE) will be needed.

The purpose of this contribution is mainly two fold. First, the statistical RVE size will be derived based on convergence criterion of the several parameters being monitored. The second purpose of this work tackles the efficiency of multilevel computation. Since a conventional way of macroscopic tangent computation in a condensation procedure, necessitate the computation of a Shur complement. It inflicts for increasingly complex microstructure higher memory allocation demands that may not be met by today's computers. Therefore, as an alternative, a tangent computation technique based on a sensitivity analysis of a microscopic level will be presented.

## Methods

### Numerical RVE size

In order to estimate the effective properties of heterogeneous material, most of the micro-macro methods assume the existence of a micromechanical sample that is statistically representative of the microstructural features. The usual approach[8] is to determine a relation between averages, $\boldsymbol{E}^*$, defined through $\langle\sigma\rangle_{RVE} = E^*\langle\varepsilon\rangle_{RVE}$ . Here $\sigma$ and $\varepsilon$ are the stress and strain fields within a statistically representative volume element. The RVE is considered both smaller enough than the macro scale media and bigger enough than the heterogeneities on the micro scale, without introducing non-existing properties (e.g. anisotropy).

In this contribution, macroscopically isotropic materials are considered, therefore the two linear elastic constants (bulk and shear moduli) describing the form of $\boldsymbol{E}^*$can be computed using:

$$3K^* = \frac{\left\langle \frac{tr\sigma}{s} \right\rangle_{RVE}}{\left\langle \frac{tr\varepsilon}{s} \right\rangle_{RVE}}$$

$$2G^* = \sqrt{\frac{\langle \sigma' \rangle_{RVE} : \langle \sigma' \rangle_{RVE}}{\langle s' \rangle_{RVE} : \langle \varepsilon' \rangle_{RVE}}} \qquad (1.1)$$

where $\boldsymbol{\sigma}$' and $\boldsymbol{\varepsilon}$' denotes the deviatoric part. Macroscopically isotropic heterogeneous structure is achieved by random particle distribution at the microscale. Therefore, for a given sample size, multiple distributions of particles are possible. In order to capture a statistical measure of the range of responses from different distributions, a simple averaging of three samples per RVE size was used.

To model random porous microstructures a matrix containing randomly distributed pores throughout a square L × L was considered. The size of the particles were determined relatively to unit length of the RVE such that $0.1 < 2r < .15$. Mechanical properties of the matrix material was $K$ = 167 GPa and $G$ = 77 GPa. In order to determine a suitable RVE size, one must monitor the range of estimates to $\boldsymbol{E}^*$ for successively larger samples, shown on Figure 1. The following sequences of particles per sample are used ($N$): 2, 4, 15 and 32. Relying on the expectation as RVE size increases indefinitely the effective properties of material constants ($K$, $G$) will converge towards $\boldsymbol{E}^*$.

For numerical simulation of the response a 2D quadrilateral plane strain 2 ×2 Gauss rule elements were used. To determine the effective bulk and shear moduli, since the effective response is assumed isotropic, only one test loading is necessary $\varepsilon_{11} = 0.01005$. In Table 1, the perturbation magnitudes are shown for various quantities as a function of pore number in the sample.

Besides convergent material properties, the RVE must be tested upon the influence of the microstructural geometry

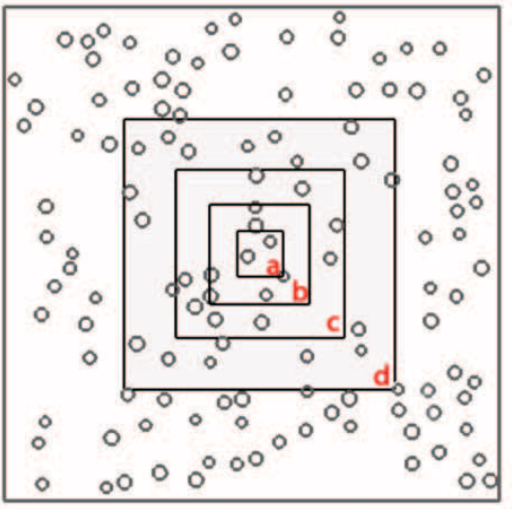


**Figure 1.** A series of test samples with increasing size, the volume fraction of particles is fixed at 0.6 %.

**Table 1.** Perturbation magnitudes for shear and bulk moduli as a function of particles number ($N$).

| $N$ | RVE size | $\frac{K}{\frac{K_{32}-K_N}{K_{32}}}$ | $\frac{G}{\frac{G_{32}-G_N}{G_{32}}}$ |
|---|---|---|---|
| 2 | 0.73 | 0.018 | 0.018 |
| 4 | 1 | 0.021 | 0.023 |
| 15 | 2 | 0.013 | 0.013 |
| 32 | 3 | 0.002 | 0.005 |

properties. This can be done by tracking various quantities such as: strain energy function, maximal stresses, averaged stresses in the particles or matrix etc. In this work the maximal effective stress was considered (von Misses). To guarantee the mixed stress fields besides the previously used normal test loading $\varepsilon_{11}$ = 0.01005 the shear loading condition was used $\varepsilon_{12}$ = 0.01005 all the rest stays the same as described previously. Figure 2 is showing the convergence of the max. effective stress in the RVE by increasing its size.

Based on the tests the statistical RVE size 2 (approximately 15 particles) is chosen. This size is used in all subsequent analysis. The outline of the determination of the RVE size and ef-

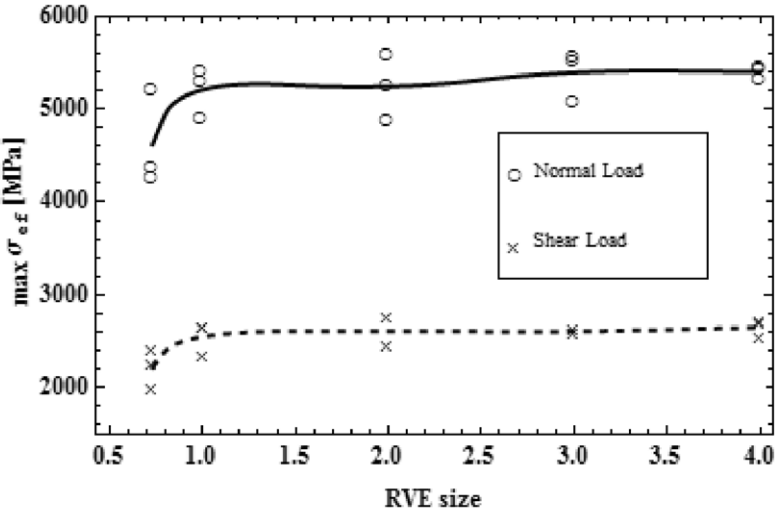


**Figure 2.** Max. effective stress for two loading cases depending upon RVE size

**Table 2.** Perturbation magnitudes of max. $\sigma_{\text{eff}}$ for normal and shear load condition as a function of particles number ($N$).

| $N$ | RVE size | $\frac{\sigma_{eff.32} - \sigma_{eff.N}}{\sigma_{eff.32}} \times 100\%$ $F_n$ | $\frac{\sigma_{eff.32} - \sigma_{eff.N}}{\sigma_{eff.32}} \times 100\%$ $F_s$ |
|---|---|---|---|
| 2 | 0.73 | 14,4 | 16.2 |
| 4 | 1 | 3.6 | 3.8 |
| 15 | 2 | 2.9 | 1.5 |
| 32 | 3 | 0.15 | 1.5 |

fective material constants are made for particles representing voids. The same procedures are used to determine the size and effective material constants also for microstructure with stiff inclusions. All the values are given in the Results & discussion section.

**Multilevel finite element - principle**

The material under consideration is assumed to be macroscopically homogeneous, so that continuum mechanics can be used to describe macroscopic behavior. However, at the micro level is the material configuration heterogeneous, consisting of many distinguishable components e.g. grains, cavities, hard inclusions. The microscopic length scale is much smaller than the characteristic length of the macroscopic structure, therefore in this case a hypothesis on periodicity of the microstructure is acceptable. The multilevel finite element strategy may be described by the following subsequent steps: [9, 10]

1. Determination of a statistical representative volume element (RVE), used in homogenization and in embedded multilevel analysis.
2. The macroscopic structure to be analyzed is discretized by finite elements. The external load is applied by an incremental procedure.
3. Macroscopic deformation gradient tensor $(\boldsymbol{F}_M)$ is calculated for every integration point of the macrostructure in a multilevel subdomain.
4. From the macroscopic deformation tensor appropriate boundary conditions are derived to be imposed on the RVE that is assigned to this point.
5. Upon the solution of the boundary value problem for the RVE, the macroscopic stress tensor $(\boldsymbol{P}_M)$ is obtained by averaging the resulting RVE stress field over the volume of the RVE.
6. Additionally, the local macroscopic consistent tangent is derived from the sensitivity analysis of the RVE.

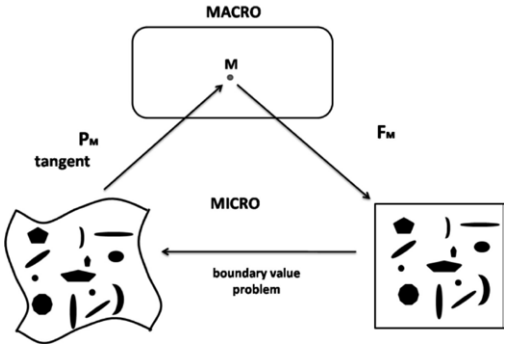


**Figure 3.** Shematic diagram of the ML-FEM model.

This framework is schematically illustrated in Figure 3. In the subsequent sections these issues are discussed in more detail.

**Linking macroscopic and microscopic levels**

The actual coupling between the macroscopic and microscopic scales is based on averaging theorems. The energy averaging theorem, known in

the literature as the **Hill** condition or macrohomogeneity condition[11, 12], requires that the macroscopic volume average of the variation of work performed on the RVE is equal to the local variation of the work on the macroscale. Formulated in terms of a deformation gradient tensor and the first Piola-Kirchhoff stress tensor, the work criterion in differential form is written:

$$\left\langle \mathrm{P}m \cdot d\mathrm{F}m \right\rangle = \left\langle \mathrm{P}_M \right\rangle \left\langle d\mathrm{F}_M \right\rangle \qquad (2.1)$$

In words, this equality states that in the transition from the microscopic scale to the macroscopic scale, energy is conserved.

It is well known that this criterion is not satisfied for arbitrary boundary conditions (BC) applied to the RVE. Classically three types of RVE boundary conditions are used, i.e. prescribed displacements, prescribed tractions and prescribed periodicity. Periodicity here is referring on an assumption on global periodicity of the microstructure, suggesting that the whole macroscopic specimen consists of spatially repeated unit cells. Among them the periodic BCs show a more reasonable estimation of the effective properties. This was supported and justified by numbers of authors[13–16]. The periodicity conditions for the microstructural RVE are written in a general format as:

$$\overrightarrow{x^+} - \overrightarrow{x^-} = \mathrm{F}_M \cdot \left( \overrightarrow{X^+} - \overrightarrow{X^-} \right)$$
$$\overrightarrow{p^+} = \overrightarrow{p^-}, \qquad (2.2)$$

where $\vec{x}$ and $\vec{X}$ represents the actual and initial position vector and $\vec{p}$ the boundary traction of the RVE. In the equation (2.1) the macroscopic first Piola-Kirchhoff stress tensor ($\boldsymbol{P}_{\mathbf{M}}$) and the macroscopic deformation gradient tensor ($\boldsymbol{F}_{\mathbf{M}}$) are the fundamental kinetical and kinematical measures which are defined in terms of the volume average of their microscopic counterparts. Every time that the work criterion is satisfied, the volume average of the macroscopic above mentioned measures can be obtained through the knowledge of boundary information only.

$$F_M = \left\langle F_m \right\rangle_{RVE} = \frac{1}{V_{RVE}} \int_{\mathrm{RVE}} F_m \mathrm{dV} = \frac{1}{V_{RVE}} \int_{\Gamma} \vec{x} \vec{N} \mathrm{d}\Gamma \qquad (2.3)$$

$$P_M = \left\langle P_m \right\rangle_{RVE} = \frac{1}{V_{RVE}} \int_{\mathrm{RVE}} P_m \mathrm{dV} = \frac{1}{V_{RVE}} \int_{\Gamma} \vec{p} \vec{X} \mathrm{d}\Gamma \qquad (2.4)$$

Here, $V_{RVE}$ is undeformed RVE, $P_m$ and $F_m$ are microscopic stress tensor and deformation gradient tensor, respectively, $\Gamma$ represents the boundary of the RVE, while $\vec{N}$ represents the normal vector to the surface of RVE.

**Macroscopic tangent computation**

In the realization of the multilevel FEM approach, the macroscopic constitutive formulation is not explicitly obtained from the experimental data. Instead, the needed stiffness matrix at every macroscopic integration point has to be determined directly from the numerical relation of the macroscopic stress ($\boldsymbol{P}_{\mathbf{M}}$) and macroscopic deformation gradient ($\boldsymbol{F}_{\mathbf{M}}$) at that point[15, 17, 18]. The weak form of the macroscale problem in the absence of body forces and acceleration can be written in variational form as:

$$\delta\Pi = \int_{V_0} \delta F_M \cdot P_M dV \tag{2.5}$$

To solve the macroscopic primal problem within ML-FEM setting, at i-th iteration step of a standard Newton-Raphson solution scheme, the following linearization needs to be computed.

$$\int_{V_0} \delta F_M \cdot P_M^{i+1} dV \approx \int_{V_0} \delta F_M \cdot P_M^{i} dV + \int_{V_0} \delta F_M \cdot \frac{DP_M^i}{DF_M} \Delta F_M dV \tag{2.6}$$

The macrolevel element tangent stiffness matrix and the residual force vector can be obtained with the knowledge of the stress ($\boldsymbol{P}_{\mathbf{M}}$) and macroscopic tangent ($\partial P_M/\partial F_M$) obtained from the RVE analysis, since $F_M$ is explicit function of node displacements. The ($\boldsymbol{P}_{\mathbf{M}}$) can be obtained directly from RVE analysis by using averaging theorem equation (2.4), while for the determination of the macroscopic tangent a RVE sensitivity analysis is performed. For the sensitivity problem[19] the residuals and the vector of unknowns are defined as a function of sensitivity parameters, which are in this case the elements of tensor ($\boldsymbol{F}_{\mathbf{M}}$). The sensitivity problem can then be obtained from the primal problem by differentiating the response functional and the residuals with respect to macroscopic deformation gradient ($\boldsymbol{F}_{\mathbf{M}}$), and the following system on the microlevel has to be solved:

$$\frac{\partial \psi_m}{\partial a}\frac{D_a}{D\phi} = -\frac{\partial \psi_m}{\partial \phi} \tag{2.7}$$

where, $\boldsymbol{\Psi}_{\mathbf{m}}$ represents response functional on the microlevel, **a** is a set of unknowns (displacements), while $\boldsymbol{\phi}$ represents arbitrary sensitivity parameter in our case $\boldsymbol{F}_{\mathbf{M}}$.

With the assembling of the macroscopic stiffness matrix is the problem on the macro level fully described and can be solved to produce an update of the macroscopic displacement field.

**Remark 1:** for consistency the particular type of BC employed for the comp. of $K$ must match the type of BC employed in the computation of $P$.

## Results & discussion

In order to evaluate the presented ML-FEM strategy a simple compression test, Figure 4a, of a homogeneous matrix material with 6 % volume fraction of randomly distributed voids or stiff inclusions has been examined. The material parameters used in the analysis are: shear modulus of matrix material and stiff inclusions are $G_m$ = 77 GPa and $G_i$ = 307 GPa respectively, bulk modulus of matrix material and stiff inclusions are $K_m$ = 167 GPa and $K_i$ = 667 GPa respectively. For the homogenized part the effective material constants are calculated from RVE tests presented in the **Numerical RVE size** section: voided microstructure $G$ = 72 GPa and $K$ =156 GPa, microstruc-

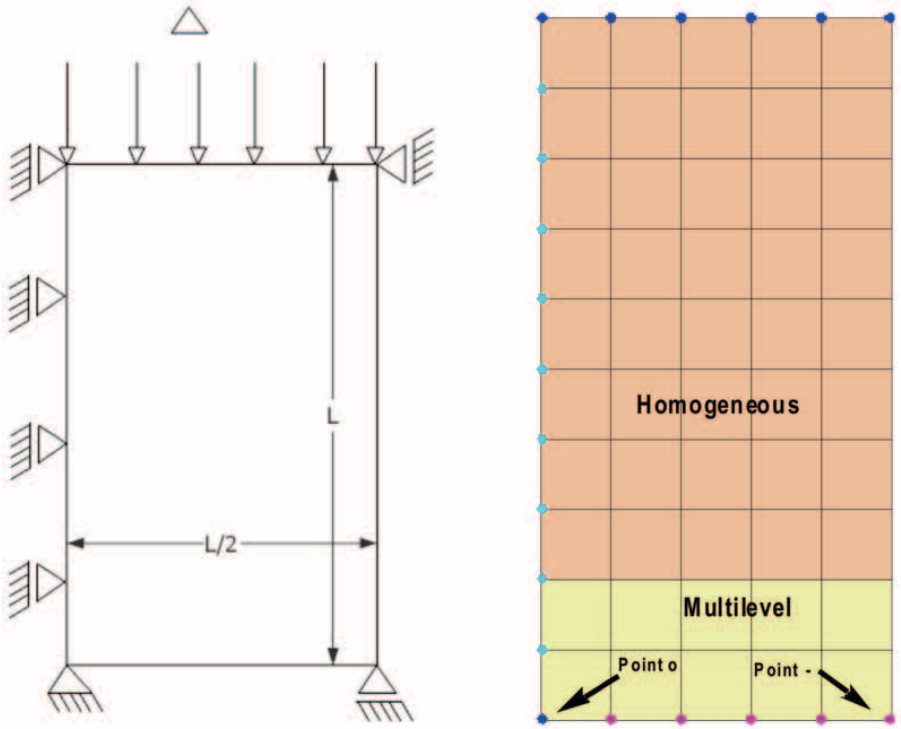


**Figure 4.** a) Axisymmetric model of compresion test. b) Axisymmetric numerical model: two subdomains with critical points indicated.

ture with stiff inclusions $G$ = 90 GPa and $K$ = 194 GPa. On the macroscopic level a 2D quadrilateral plane strain 2 × 2 Gauss rule elements were used. Load was applied incrementally: load displacements $\Delta$ = 1 unit relative to $L$. The multilevel algorithm has been implemented into computer program AceFEM[20], where a special macroscopic element can be readily defined in open source code.

Figure 4b shows a discretized numerical model where the homogenized and multilevel subdomains are clearly indicated. In the later, two critical points are marked where a detailed RVE analysis has been done. From Figure 4b a straightforward estimate, regarding the considered test, can be done about the amount of computation needed for each macroscopical load increment: number of elements in the multilevel subdomain times the Gauss points per elements. For the present test it takes, 18 Elements × 4 Gauss points, RVE analyses for each load increment. In order to further speed up the analysis and to make it more useful for complicated engineering applications, multilevel algorithm was set up for parallel computations.

In Figure 5 the contour plots of the equivalent Misses stress considering the two microstructures are compared.

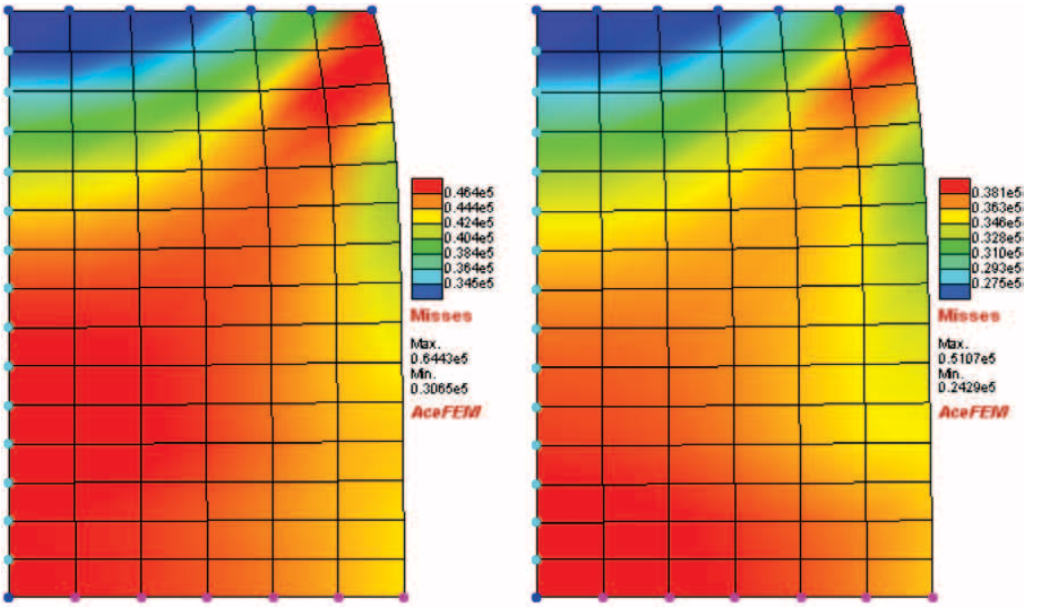


**Figure 5.** Effective stress in the macrostructure 2D a) stiff inclusions, b) voided microstructure.

As expected the microstructure with stiff inclusions produces higher stresses but the interesting point is that the contour plots are not the same which would be the case for completely homogenized structure. The influence of more realistic model on the microscopic level is clearly visible even in a simple case considered.

The detailed analyses of the RVE at the critical points for both microstructures are depicted in Figures 6 and 7. It can be seen that the voids act as a stress concentrator and that some stress concentration regions can be seen between neighboring voids, Figure 6. The RVE taken from macroscopic point (o) is subjected to mainly hydrostatic compression stresses, while RVE from point (-) is exposed to some amount of deviatoric stresses as well. This phenomenon has greater influence on the voided microstructure, where higher

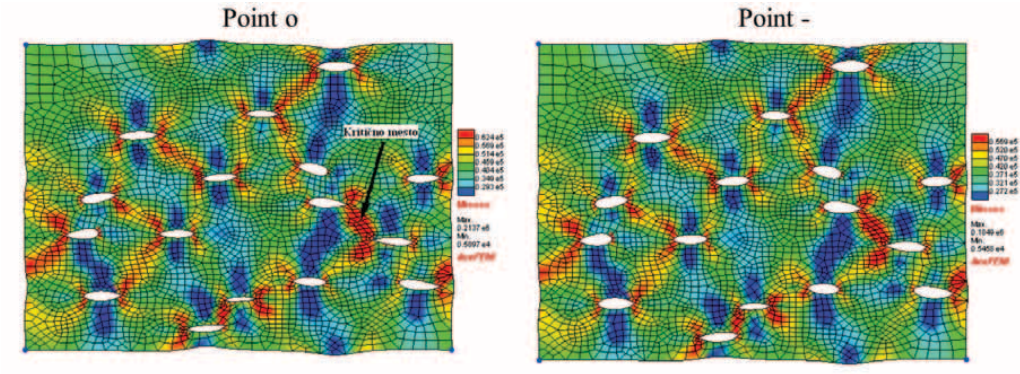


**Figure 6.** Effective stress in the RVE from the critical point of the macrostructure voided microstructure.

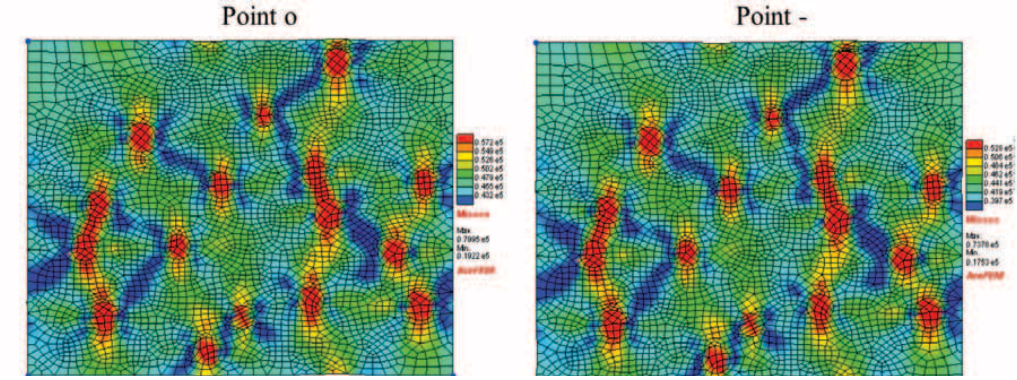


**Figure 7.** Effective stress in the RVE containing stiff inclusions from the critical point of the macrostructure.

effective stresses are observed in the mainly hydrostatic region. Generally by comparing the microscopic and macroscopic stress fields a substantially higher stresses are observed on the microscopic level. So by simultaneously examining RVE at critical macro points, while deforming the macro structure, a deeper understanding of deformation mechanisms can be obtained, which can be very helpful in studying the damage mechanisms and densification in various engineering materials.

## Conclusions

Firstly it was shown how to determine a statistical representative volume element (RVE), which was later used in the homogenization process and as well in embedded multilevel analysis. A multilevel finite element analysis strategy for the simulation of the mechanical behavior of heterogeneous materials has been outlined. The performance of the method was illustrated by the modeling of simple compression test. Two different microstructures were tested: first including voids and second with hard inclusions embedded in the matrix. The presented multilevel finite element analysis strategy provides an efficient approach to determine the macroscopic response of heterogeneous materials with accurate account for microstructural phenomena. In the ML-FEM strategy the computational efficiency hinges on the correct and effective macroscopic tangent computation, in this work this is done by sensitivity analysis of the microscopic level. It enables a problem solving tool for a variety of different micro-macro problems which includes complex microstructures.

## References

[1] KOUZNETSOVA, V., BREKELMANS, W. A. M., BAAIJENS, F. P. T. (2001): An approach to micro-macro modeling of heterogeneous materials, *Comp. Mech.*, Vol. 27, pp. 37–48.

[2] TEMIZER, I., WRIGGERS, P. (2008): On the computation of the macroscopic tangent for multiscale volumetric homogenization problems, *Comput. Methods Appl. Mech. Engrg.,* Vol. 198, pp. 495–510.

[3] SMIT, R. J. M., BREKELMANS, W. A. M., MEIJER, H. E. H. (1998): Prediction of the mechanical behavior of nonlinear heterogeneous systems by multi-level finite element modeling, *Comput. Methods Appl. Mech. Engrg.*, Vol. 155, pp. 181–192.

[4] MIEHE, C., KOCH, A. (2002): Computational micro-to-macro transitions of discretized microstructures undergoing small strains, *Archive of Applied Mechanics*, Vol. 72 pp. 300–317.

[5] MIEHE, C. (2003): Computational micro-to-macro transitions for dis-

cretized micro-structures of heterogeneous materials at finite strains based on the minimization of averaged incremental energy, *Comput. Meth. Appl. Mech. Eng.,* Vol. 192, pp. 559–591.

[6] Feyel, F., Chaboche, J. L. (2000): $FE^2$ multiscale approach for modelling the elastoviscoplastic behaviour of long fibre SiC/Ti composite materials, *Comput. Methods Appl. Mech. Engrg.,* Vol. 183, pp. 309–330.

[7] Feyel, F. (1999): Multiscale $FE^2$ elastoviscoplastic analysis of composite structures, *Comput. Mat. Sci.*, Vol. 16, pp. 344–354.

[8] Zohdi, T. I., Wriggers, P. (2001): Computational Micro-macro Material Testing, Arch. *Comput. Methods Eng.,* Vol. 8, pp. 131–228.

[9] Lamut, M. (2010): *Mikro in makromehansko modeliranje kompozitnih materialov.* Ph. D. Thesis. Ljubljana: University of Ljubljana 2010; 87 p.

[10] Lamut, M., Korelc, J., Rodič, T. (2011): *Multiscale modelling of heterogeneous materials, Math. Tech.,* Vol. 45, pp.421–426.

[11] Hill, R. (1963): Elastic properties of reinforced solids : some theoretical principles, *J. Mech. Phys. Solids.,* Vol. II, pp. 357–372.

[12] Hill, R. (1972): On constitutive macro-variables for heterogeneous solids at finite strain, *Proc. R. Soc. Lond. A.*, Vol. 326, pp. 131–147.

[13] Terada, K., Hori, M., Kyoya, T., Kikuchi, N. (2000): Simulation of the multi-scale convergence in computational homogenization approaches, *International Journal of Solids and Structures,* Vol. 37, pp. 2285–2311.

[14] Khisaeva, Z., F., Ostoja-Starzewski, M. (2006): On the Size of RVE in Finite Elasticity of Random Composites, *J. Elasticity*, Vol. 85, pp. 153–173.

[15] Sluis, O., Schreurs, P. J. G., Brekelmans, W. A. M., Meijer, H.E.H. (2000): Overall behaviour of heterogeneous elastoviscoplastic materials: effect of microstructural modelling, *Mechanics of Materials*, Vol. 32, pp. 449–462.

[16] Temizer, I., Wriggers, P. (2008): On the computation of the macroscopic tangent for multiscale volumetric homogenization problems, *Comput. Methods Appl. Mech. Engrg.*, Vol. 198, pp. 495–510.

[17] Temizer, I., Zohdi, T. I. (2007): A numerical method for homogenization in non-linear elasticity, *Comput. Mech.,* Vol. 40, pp. 281–298.

[18] Miehe, C. (1996): Numerical computation of algorithmic (consistent) tangent moduli in large-strain computational inelasticity, *Comput. Methods Appl. Mech. Engrg.,* Vol. 134, pp. 223–240.

[19] Korelc, J. (2009): Automation of primal and sensitivity analysis of transient coupled problems, *Comput. Mech.*, Vol. 44, pp. 631–649.

[20] Korelc, J. (2007): AceGen & AceFEM user manual, FGG-UL.

# Tracing coalbed gas dynamics and origin of gases in advancement of the working faces at mining areas Preloge and Pesje, Velenje Basin

# Spremljanje sestave premogovega plina in izvor plinov z napredovanjem čela delovišč na pridobivalnih (rudarskih) območjih jam Preloge in Pesje, Velenjski bazen

Tjaša Kanduč[1,*], Janja Žula[2], Simon Zavšek[2]

[1]Jožef Stefan Institute, Jamova 39, SI - 1000 Ljubljana, Slovenia
[2]Velenje Coal mine, Partizanska 78, SI - 3320 Velenje, Slovenia

*Corresponding author. E-mail: tjasa.kanduc@gmail.com

**Received:** May 9, 2011 **Accepted:** September 7, 2011

**Abstract:** During excavation of lignite in the Velenje Coal Mine coalmine, seam problems with gas outbursts occur. Geochemical investigations are designed to help predict, prevent, and manage coal mine gas outbursts and to study their origin and mechanisms. However, geochemical studies of the coalbed gases in the Velenje basin have been initiated since year 2000. Temporal changes in chemical and isotopic composition of "free" seam gases were observed as a function of the advancement of the working face –120/B, G2/C and –50/B within boreholes jpk-28/10, jpk-30/10, jpk-31/10, jpk-22/09 and jpk-23/09. Mass spectrometry and isotope mass spectrometry methods were used to determine gas composition and perform gas characterization. Coalbed gases in the Velenje basin are highly variable in both their concentrations and stable isotope composition. Major gas components are $CO_2$ and methane. Concentrations and isotopic studies revealed several genetic types of coalbed gases: endogenic $CO_2$ (including $CO_2$ originating from dissolution of carbonates), microbial methane and $CO_2$.

**Izvleček:** Med izkopavanjem lignita se lahko pojavljajo plinski izbruhi, zato je pomembno izvajati nadzorne meritve premogovnih plinov na odkopih. Geokemične raziskave premogovnega plina so pomembne

*Original scientific paper*

za razumevanje mehanizma nastanka, preprečevanja in napovedovanja plinskih izbruhov. Raziskave premogovnega plina v Velenjskem bazenu potekajo od leta 2000. Časovne spremembe v kemijski in izotopski sestavi "prostih" premogovnih plinov smo spremljali kot funkcijo približevanja čel delovišč 120/B, G2/C in –50/B v vrtinah jpk-28/10, jpk-30/10, jpk-31/10, jpk-22/09 in jpk-23/09. Sestavo in izotopsko sestavo premogovnih plinov smo določili z metodama masne spektrometrije in izotopske masne spektrometrije. Premogovni plini v Velenjskem bazenu se spreminjajo tako po vsebnosti kot tudi po izotopski sestavi. Glavni plinski komponenti sta $CO_2$ in metan. Raziskave vsebnosti in stabilnih izotopov premogovnih plinov kažejo različne izvore plinov: endogeni $CO_2$, (vključno s $CO_2$, ki nastaja zaradi raztapljanja karbonatov) ter mikrobni metan in $CO_2$.

**Key words**: coalbed gas composition, working faces, carbon isotopes, gas origin, Velenje basin
**Ključne besede**: sestava premogovnih plinov, odkopi, ogljikovi izotopi, izvor plinov, Velenjski bazen

## INTRODUCTION

An increasing demand for coal, as a result of changes in the availability and cost of other fossil fuels, has re-focused attention on the problem of outbursting in deeper coal mines. When the rate of advance of the cutting face is slow, better opportunities for the slow escape of the gases under high pressure in the virgin coal exist. However, at the faster rates of advance of the coal face now required, less time is available for the equalization of gas pressures and mining induced stresses. Thus, the hazard of instantaneous outbursting of gas and coal is increased, although under favorable circumstances some control may be achieved by gas drainage (SMITH & GOULD, 1980). It is generally assumed that the pressure and volume of gases held within the virgin coal play a major part in producing outbursts; however, some doubt still exists as to whether outbursts are actually triggered by gas pressure or by stresses induced in the rock itself during mining operations (FLORES, 1998).

The most trivial definition of coalbed gas is "gas from coal". Coalbed gas usually consist of hydrocarbons (mainly methane), $CO_2$ in concentrations from 0 to greater than 99 %, and occasionally small percentages of nitrogen (CLAYTON, 1998). A numbers of models were developed

to describe sources of hydrocarbon gases (Shoell, 1983, Kotarba, 1990, Scott, 1993, Kotarba, 2001, Aravena, 2003). Stable carbon isotope analyses of methane and $CO_2$ can be applied to identify the origin of coalbed gases, their migration pathways, and accumulation processes. There are three main sources of hydrocarbon gases and $CO_2$ in sedimentary basins: abiogenic, microbial and thermogenic gas (Scott, 1993). In general, thermogenic gases are typically associated with high rank coal, whereas microbial gases are typically associated with low rank coals and could have been produced throughout the basin history, as long as the coalbeds were never pasteurized. Abiogenic sources of gas are typically found in deep subsurface (Sherwood Lollar et al., 2006).

Details of isotopic composition of different lithotypes of lignite and the origin of coalbed $CO_2$ gas based on tectonic events during formation of the basin using cluster analysis and CDMI index (carbon dioxide methane index) of different gases are presented in Kanduč et al. (2005a) and Kanduč & Pezdič (2005b). The study revealed levels of microbial methane and $CO_2$, and endogenic $CO_2$. Unexpected organic arsenic compounds found in Velenje lignite indicated their relation with biogeochemical degradation of organic material (Šlejkovec & Kanduč, 2005c).

The aim of the study is to explain concentrations and origin of gases as a function of the advancement of the working faces –120/B, G2/C and –50/B in mining areas of Preloge South, Preloge North and Pesje in Velenje Basin.

## Materials and methods

### Sampling procedure

Sampling of coalbed gas was performed at working faces –120/B (mining area Preloge South), G2/C (Preloge North) and –50/B (Pesje) from November 2009 till November 2010, in the lignite seam of the Velenje basin with purpose to determine concentrations ($CO_2$, methane, $N_2$ and $O_2$) and $\delta^{13}C$ of methane and $CO_2$ from pillar coal in advancement with the working face (Figure 1). Boreholes were drilled in pillar coal to a depth of 20 m. After drilling, the capillary tube was inserted in the borehole. Boreholes (jpk-28/10 - Preloge South, jpk-30/10, jpk-31/10 - Preloge North, jpk-22/09 and jpk-23/09 - Pesje) and working faces (–120/B, G2/C, and –50/B) are shown on Figure 1. "Free gas" emitted from the borehole was collected in a 50 mL plastic syringe and then transferred to a 12 mL evacuated ampoule with a septum. After sampling "free gas" from the boreholes, the ampoules were stored at normal atmospheric conditions un-

til analysis. Free gas includes both the volatiles filling the pores and cracks within the coal structure and some gas degassed from the coal during drilling and sampling (KOTARBA, 2001). Some boreholes were compressed in advancement of the working faces, which caused too much air contamination in boreholes and therefore unable the interpretation. In this study only data of coalbed gases, which contained below 50 % of air were used for interpretation.

**Analytical procedure**

Determinations of the concentrations of methane, $CO_2$, nitrogen, oxygen and argon were performed using a home-made mass NIER spectrometer. The method of singular decomposition of matrix was used, to obtain the simultaneous analysis of the gases. The precision of the method was ±3 %.

Isotope composition of methane, $CO_2$ was determined using an Europa 20-20 continuous flow isotope ratio

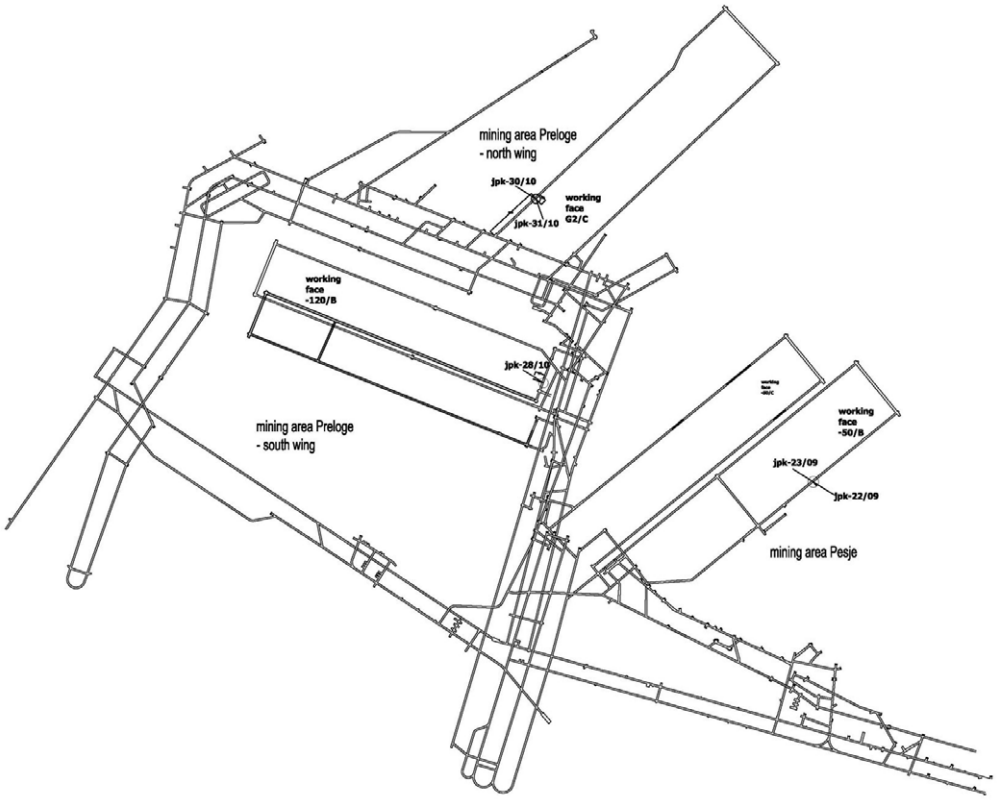


**Figure 1.** Map of sampling locations of coalbed gases from the lignite strata at working faces (–120/B – Preloge South, G2/C – Preloge North and –50/B - Pesje)

mass spectrometer with ANCA – TG preparation module. First water was removed and then $CO_2$ was directly analyzed for $^{13}C$ content. For methane measurements first $CO_2$ was removed and then methane was combusted over hot 10 % platinum CuO (1000 °C). The methane completely converted to $CO_2$ was then directly analyzed for isotopic composition of carbon ($\delta^{13}C$). Working standards calibrated to IAEA (International Atomic Energy Agency) reference materials were used with value of –3.2 ‰ for $CO_2$ and value of –47.5 ‰ for methane relatively to VPDB (Vienna Pee Dee Belemnite). Analytical precision for carbon isotope composition is estimated to be ±0.2 ‰. The stable carbon isotopes are presented in the δ – notation relative to VPDB standards and expressed in parts per million (Coplen, 1996) as follows (O'Neil, 1979):

$$\delta^{13}C_{vz} = \frac{R_s - R_{RM}}{R_{RM}} \cdot 1000 \quad [‰] \qquad (1)$$

Where:
$R_s$ – ratio $^{13}C/^{12}C$ in sample
$R_{RM}$ – ratio $^{13}C/^{12}C$ in reference material

## Results and discussion

"Free gases" accumulated within the lignite coal seam showed a considerable variability in concentrations and isotopic composition. Due to air contamination within boreholes and the capillary system samples were recalculated on an air - free basis. Major gas components were $CO_2$ and methane. Only one sample from our study had nitrogen, meaning that it was in excess. Concentrations of $CO_2$ varied from 20.8 % to 86.9 %, methane from 13.1 % to 58.9 %. Geochemical index CDMI ($(CO_2/ (CO_2 + CH_4) \times 100$ %) vary from 26.1 % to 86.9 % and stable isotope ratios varied in the following ranges: $\delta^{13}C_{CO2}$ from –12.5 ‰ to 2.3 ‰ and $\delta^{13}C_{CH4}$ from –69.1 ‰ to –26.9 ‰ (Table 1).

High correlation (*r* between 0.95 and 1) is obtained between methane and $CO_2$ concentrations (Figure 2) in a lignite seam within boreholes as a function of the advancement of the working faces (–120/B, G2/C and –50/C). Working faces from different mining areas (Preloge North, Preloge South and Pesje) have different composition of coalbed gases. At all investigated mining areas Preloge South (–120/B), Preloge North (G2/C) and Pesje (–50/B) $CO_2$ prevails under methane (Figure 2). The highest $CO_2$ concentrations are observed in mining are Preloge South (except 1 sample) where $N_2$ concentrations were in excess of air (Table 1). The results of areas of high and low methane concentrations (Figure 2) are in physicochemical properties of $CO_2$ and methane (Atkins, 1994). Fissures generated

**Table 1.** Composition of coalbed gases and isotopic composition of carbon ($\delta^{13}C$) of coalbed gases ($CO_2$ and methane) at working faces: –120/B, G2/C and –50/B within boreholes jpk – 28/10, jpk – 30/10, jpk – 31/10, jpk – 22/09 and jpk – 23/09. CDMI index = $(CO_2/(CO_2 + CH_4) \times 100\ \%)$

**Working face -120/B, borehole jpk-28/10, mining area Preloge South**

| Date of sampling | Distance of the working face (m) | $CH_4$ (vol. %) | $CO_2$ (vol %) | $N_2$ (vol. %) | CDMI index (%) | $\delta^{13}C_{CO2}$ (‰) | $\delta^{13}C_{CH4}$ (‰) |
|---|---|---|---|---|---|---|---|
| March 3, 2010 | 191 | 13.1 | 86.9 | 0.0 | 86.9 | -5.7 | -62.7 |
| March 12, 2010 | 160 | 58.9 | 20.8 | 20.3 | 26.1 | -7.9 | -64.4 |
| March 17, 2010 | 151 | 13.8 | 86.2 | 0.0 | 86.2 | -7.1 | -63.1 |
| April 9, 2010 | 92 | 17.5 | 82.9 | 0.0 | 82.6 | -4.8 | -50.6 |
| May 4, 2010 | 45 | 20.5 | 79.5 | 0.0 | 79.5 | -9.6 | -69.1 |
| May 11, 2010 | 37 | 19.8 | 80.2 | 0.0 | 80.2 | -8.1 | -62.7 |
| May 13, 2010 | 32 | 23.0 | 77.0 | 0.0 | 77.0 | -8.6 | -62.9 |
| May 14, 2010 | 31 | 20.0 | 80.0 | 0.0 | 80.0 | -8.5 | -61.9 |
| May 18, 2010 | 30 | 24.3 | 75.7 | 0.0 | 75.7 | -12.5 | -63.3 |
| June 1, 2010 | 30 | 29.1 | 70.9 | 0.0 | 70.9 | -7.6 | -51.1 |

**Working face G2/C, borehole jpk-30/10, mining area Preloge North**

| Date of sampling | Distance of the working face (m) | $CH_4$ (vol. %) | $CO_2$ (vol %) | $N_2$ (vol. %) | CDMI index (%) | $\delta^{13}C_{CO2}$ (‰) | $\delta^{13}C_{CH4}$ (‰) |
|---|---|---|---|---|---|---|---|
| August 18, 2010 | 341 | 42.2 | 57.8 | 0.0 | 57.8 | 1.8 | -31.0 |
| August 31, 2010 | 316.4 | 43.5 | 56.5 | 0.0 | 56.5 | -1.1 | -37.2 |
| September 22, 2010 | 307.5 | 46.1 | 53.9 | 0 | 53.9 | -6.6 | -29.8 |
| November 30, 2010 | 152.1 | 42.3 | 57.7 | 0.0 | 57.7 | 0.9 | -50.0 |

**Working face G2/C, borehole jpk-31/10, mining area Preloge North**

| Date of sampling | Distance of the working face | $CH_4$ vol. % | $CO_2$ vol % | $N_2$ vol. % | CDMI index (%) | $\delta^{13}C_{CO2}$ (‰) | $\delta^{13}C_{CH4}$ (‰) |
|---|---|---|---|---|---|---|---|
| August 20, 2010 | 335.3 | 45.7 | 54.3 | 0.0 | 54.3 | -1.7 | -45.5 |
| August 27, 2010 | 316.4 | 30.7 | 69.3 | 0.0 | 69.3 | -9.1 | |
| September 22, 2010 | 307.5 | 36.6 | 63.4 | 0.0 | 63.4 | -3.9 | -60.4 |
| November 30, 2010 | 152.1 | 43.3 | 56.7 | 0.0 | 56.7 | -0.7 | -50.3 |

**Working face -50/B, borehole jpk-22/09, mining area Pesje**

| Date of sampling | Distance of the working face | $CH_4$ vol. % | $CO_2$ vol % | $N_2$ vol. % | CDMI index (%) | $\delta^{13}C_{CO2}$ (‰) | $\delta^{13}C_{CH4}$ (‰) |
|---|---|---|---|---|---|---|---|
| November 16,2009 | 267 | 41.3 | 58.7 | 0.0 | 58.7 | 2.28 | -26.9 |
| December 14, 2009 | 214 | 19.9 | 80.1 | 0.0 | 80.1 | -4.76 | -44.4 |
| January 11, 2010 | 181 | 33.1 | 66.9 | 0.0 | 66.9 | -0.70 | -42.6 |
| February 22, 2010 | 79 | 24.5 | 75.5 | 0.0 | 75.5 | -2.1 | -58.0 |
| February 24, 2010 | 76 | 28.0 | 72.0 | 0.0 | 72.0 | -4.4 | -60.6 |
| March 15, 2010 | 35 | 42.1 | 57.9 | 0.0 | 57.9 | -0.1 | -48.3 |
| March 22, 2010 | 26 | 27.6 | 72.4 | 0.0 | 72.4 | 1.0 | -56.6 |

**Working face -50/B, borehole jpk-23/09, mining area Pesje**

| Date of sampling | Distance of the working face | $CH_4$ vol. % | $CO_2$ vol % | $N_2$ vol. % | CDMI index (%) | $\delta^{13}C_{CO2}$ (‰) | $\delta^{13}C_{CH4}$ (‰) |
|---|---|---|---|---|---|---|---|
| November 16,2009 | 267 | 38.7 | 61.3 | 0.0 | 61.3 | 0.44 | -49.4 |
| February 22, 2010 | 79 | 24.5 | 75.5 | 0.0 | 75.5 | -2.2 | -58.3 |
| February 24, 2010 | 76 | 28.0 | 72.0 | 0.0 | 72.0 | -4.4 | -60.6 |
| March 8, 2010 | 48.2 | 19.2 | 80.8 | 0.0 | 80.8 | -1.3 | -54.6 |
| March 15, 2010 | 35 | 26.0 | 74.0 | 0.0 | 74.0 | -2.5 | -59.6 |

with advance of the working face enable migration of methane through lignite seam in surrounding strata or to a surface, while $CO_2$ remains adsorbed in lignite seam.

Figures 3 A, B and C show concentrations of $CO_2$ and methane at researched mining areas (Preloge North, Preloge South and Pesje) in advancement of the working face (–120/B, G2/C and –50/B). Generally, at all working faces it was observed that methane migrates faster than $CO_2$ with advance of the working face, therefore the trend of maximum of methane concentration coincides with minimum $CO_2$ concentrations (Figures 3 A, B and C). Temporal changes of coalbed concentrations ($CO_2$ and methane) fluctuate with the rate of advancement of working faces (Figures 3 A, B and C). At the working face –120/B it was observed that at the distance of the working face 92 m (rate of advancement of working face 2.5 m/d) caused highest concentrations in methane and lowest concentration in $CO_2$ (Figure 3 A). At the distance of the working face 45 m (rate of advancement of the working face cca. 2 m/d) the next maximum of $CO_2$ was detected, coinciding with minimum of methane concentrations. After May 13 the rate of working face approaching to borehole jpk-28/10 gradually slowed down (rate of advancement

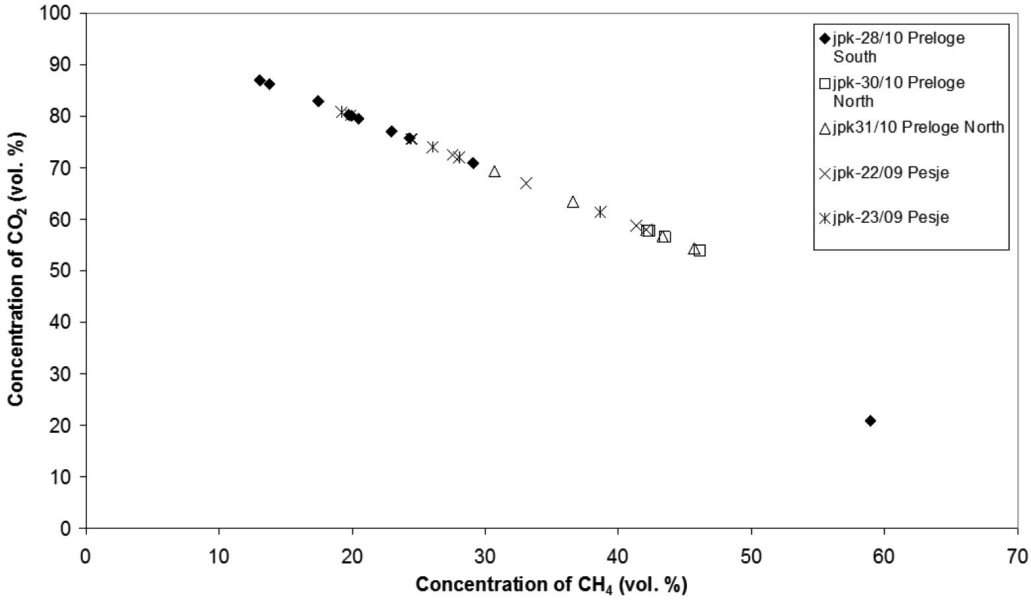


**Figure 2.** Concentration of $CO_2$ versus concentration of methane in lignite seam in advancement of the working faces (–120/B Preloge South, G2/C Preloge North, –50/B Pesje)

of working face cca. 1 m/d) causing lower fluctuations in concentration of $CO_2$ and methane. At the working face G2/C no trends of increasing/decreasing of $CO_2$ and methane concentrations are observed, probably due to constant approaching of the working face with average rate 1.9 m/d to the boreholes jpk-30/10 and jpk-31/10 (Figure 3 B). The rate of advancement of the working face –50/B was from 0.9 m/d to 2.4 m/d. Maximum methane and minimum methane concentrations were traced within borehole jpk-22/09 at the distance of the working face 35 m (rate of advancement of working face cca. 2.2 m/d) (Figure 3 C). Approaching of the working face also influence on stress situation at working face (Figure 4). During excavation of lignite secondary fissures are generated due to rearrangement of primary stress conditions, enabling releasing of coalbed gas preserved in pores of coalbed reservoir. These stress conditions are presented in Figure 4 modified after WILLIAM (1999). Results of changing of stresses were investigated by three axis cells build in lignite structure. The research revealed that at the distance of 120 m from the working face vertical stresses start to increase. At the distance of 80 m from the working face shearing and collapsing of lignite structure occur; vertical stresses continue to increase while horizontal and transverse stresses decrease. At the distance of the working face 30–50 m from three axis cell vertical stresses are so high that the lignite structure collapse (ZAVŠEK, 1990). Research of temporal variations of concentrations ($CO_2$ and methane) within borehole 780H IV at working face -80c similar trends as at working faces –120/B, G2/C and–50/B in concentrations of $CO_2$ and methane were observed; at the distance of the working face 177 m and 122 m maximum concentrations of methane were traced and coincide with minimum concentrations of $CO_2$ (KANDUČ, 2004). Besides the rate of advancement of the working face concentrations of methane and $CO_2$ measured in lignite seam within boreholes (jpk-28/10, jpk-30/10, jpk-31/10, jpk-22/09 and jpk-23/09) also depends on permeability and porosity of lignite seam. When methane and $CO_2$ reaches strata with high permeability such as fault zones, their concentrations start to increase, therefore also areas with high concentrations of methane and $CO_2$ might be expected. $CO_2$ behaves at certain condition (above its critical temperature 31.1 °C and critical pressure 7.39 MPa, expanding to fill its container like a gas but with a density like that of a liquid) as supercritical fluid (ATKINS, 1994), meaning that could be at liquid and gas phases. The conditions of critical temperature and pressure for $CO_2$ are possibly reached at working faces causing its adsorption (liquid phase)/desorption (gas phase). Areas with high $CO_2$ content (CDMI index) might be potentially danger-

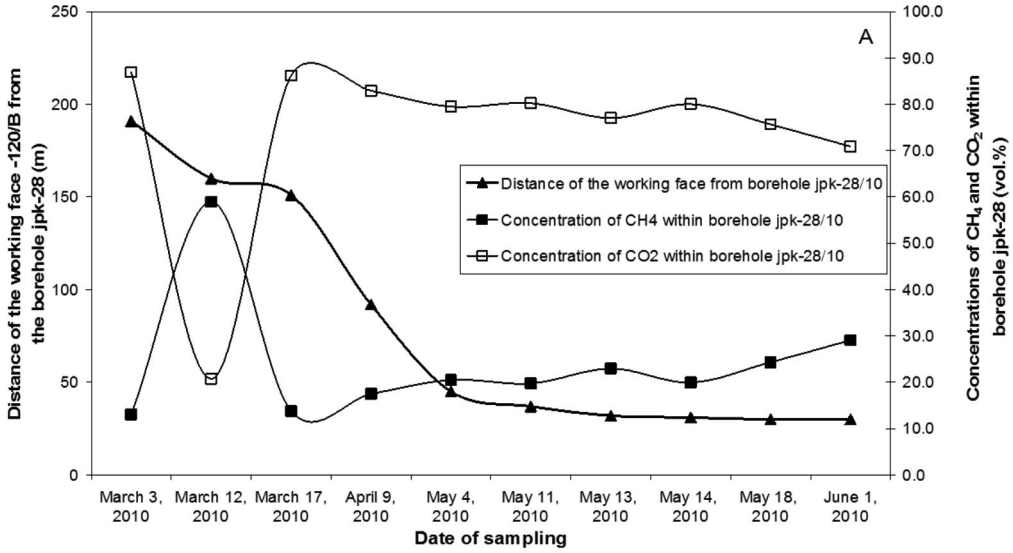


**Figure 3A.** Concentration of methane and $CO_2$ versus date of sampling in advancement of the working face –120/B (Preloge South)

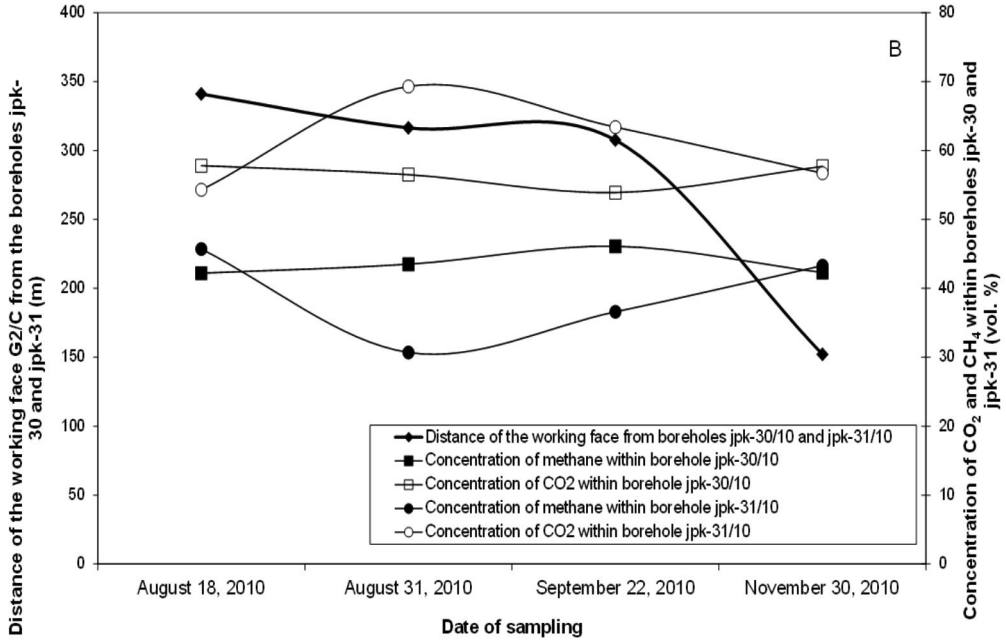


**Figure 3B.** Concentration of methane and $CO_2$ versus date of sampling in advancement of the working face G2/C (Preloge North)

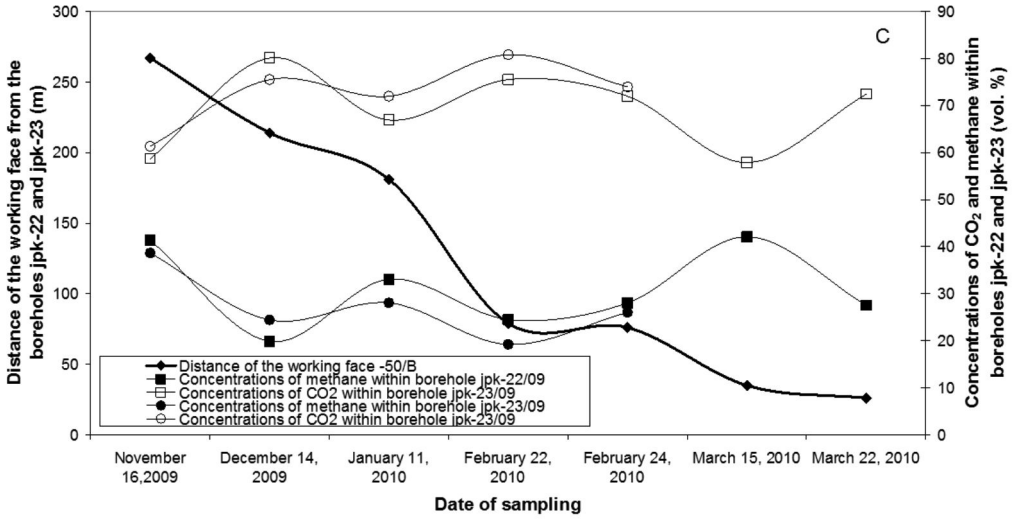


**Figure 3C.** Concentration of methane and $CO_2$ versus date of sampling in advancement of the working face –50/B (Pesje)

ous for gas outbursts (CLAYTON, 1998). Anyway, investigation of gas concentrations at each working face should be further related to petrological characteristics of lignite (lithotype type e. g. xylite, detrite), tectonically characteristics (characteristics of fault zones) and geotechnical conditions (pressures, porosity and permeability) to get better insight to coalbed gas migration as well sorption/desorption processes, especially $CO_2$ through lignite.

Interpretation of coalbed gases from investigated mining areas of Pesje and Preloge was performed according to previous study of tracing inorganic and organic carbon cycles in different geological media (calcified xylite, carbonate lenses in the lignite seam, lignite and Pliocene, Triassic and Lithotamnium aquifers) (KANDUČ et al., 2010, in review). From the results it was concluded that coalbed gases in the Velenje Basin are mainly microbial (bacterial) origin, while $CO_2$ could be also endogenic. Microbes that generate methane (methanogens) could have either of been deposited with the coal sediments in the geologic past or transported in more recently with active groundwater recharge. To thrive methanogens require an anoxic, aqueous environment with organic carbon substrates and the absence of other free-energy electron acceptors, such as $NO_3^-$ and $SO_4^{2-}$. Fermentative bacteria degrade complex organic matter in coalbeds (e.g. structures of carbohydrates, proteins and lipids that originate in vegetation and sediments) to simpler molecules including acetate ($CH_3COOH$), fatty

acids, $CO_2$ and $H_2$ gas. Acetogenic bacteria thrive on fatty acid products to produce acetate, with $CO_2$ and $H_2$ by products (Kotelnikova, 2002). The products of these reactions support a variety of methanogens. Some methanogens use an acetate food source to produce $CO_2$ and methane, according to following reactions:

$$CH_3COOH \rightarrow CH_4 + CO_2$$
Acetate fermentation (2)

While other methanogens use the hydrogen gas to reduce $CO_2$:

$$CO_2 + 4H_2 \rightarrow CH_4 + 2H_2O$$
$CO_2$ reduction (3)

or

$$HCO_3^- + 4H_2 \rightarrow CH_4 + 2H_2O + OH^-$$
$CO_2$ reduction (4)

We applied diagrams $\delta^{13}C_{CH4}$ versus $\delta^{13}C_{CO2}$ (Figure 5) to explain the origin of methane and $\delta^{13}C_{CO2}$ versus CDMI index (Figure 6) to explain the origin of $CO_2$. $\delta^{13}C_{CH4}$ (Figure 4) in the Velenje basin indicate the successive origin of methane: microbial ($CO_2$ reduction) with $\delta^{13}C_{CH4}$ values from –40 ‰ to –50 ‰, microbial (acetate fermentation) with $\delta^{13}C_{CH4}$ less than –50 ‰ and mixed origin between these two (Clayton, 1998). Enrichment with $^{13}C$ in methane could be also due to microbial oxidation of methane, which results in an enrichment of residual methane with the $^{13}C$ isotope and depletion of $^{12}C$ in generated $CO_2$ (Figure 5).

It is known that coalbed lignite strata were formed in the Pliocene in a calm sedimentary environment (Markič & Sachsenhofer, 1997), but the proportion of early stage microbial gas retained in the lignite structure (Smith & Pallaser, 1996) is difficult to estimate. Microbial methane in Velenje basin was generated by microbial reduction and/or by microbial fermentation. Also recent microbial activity (methanogenic and methanotrophic bacteria) might generate microbial

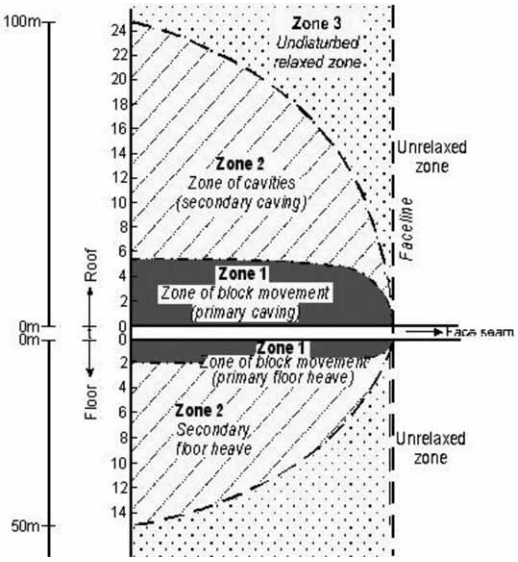


**Figure 4.** Geomechanical conditions and generation of secondary fissures due to longwall method of excavation of lignite, causing a realese of coalbed gases inside of demolished zone (adapted after Williams, 1999)

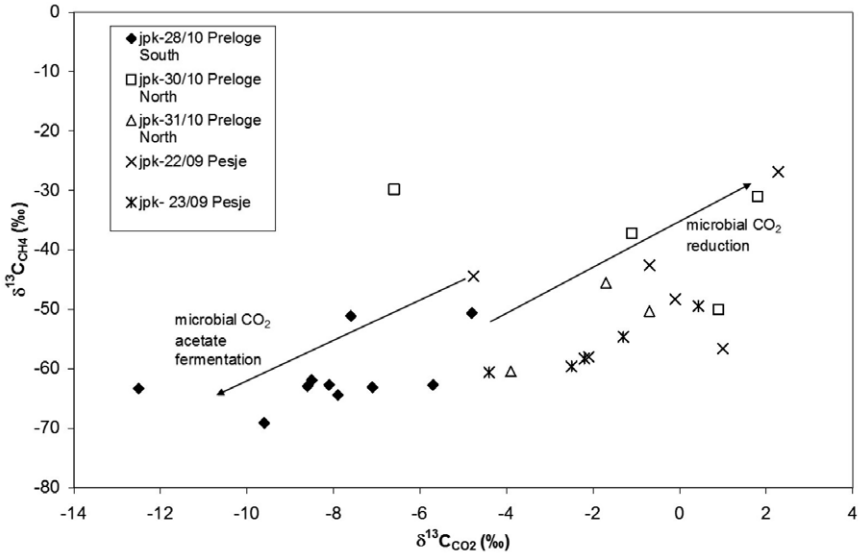


**Figure 5.** Interpretation of the origin of methane in the Velenje basin using $\delta^{13}C_{CH4}$ versus $\delta^{13}C_{CO2}$ in a lignite seam at boreholes (jpk – 28/10, jpk – 30/10, jpk – 31/10, jpk – 22/09 and jpk – 23/09) in advancement of the working faces (–120/B, G2/C and –50/B)

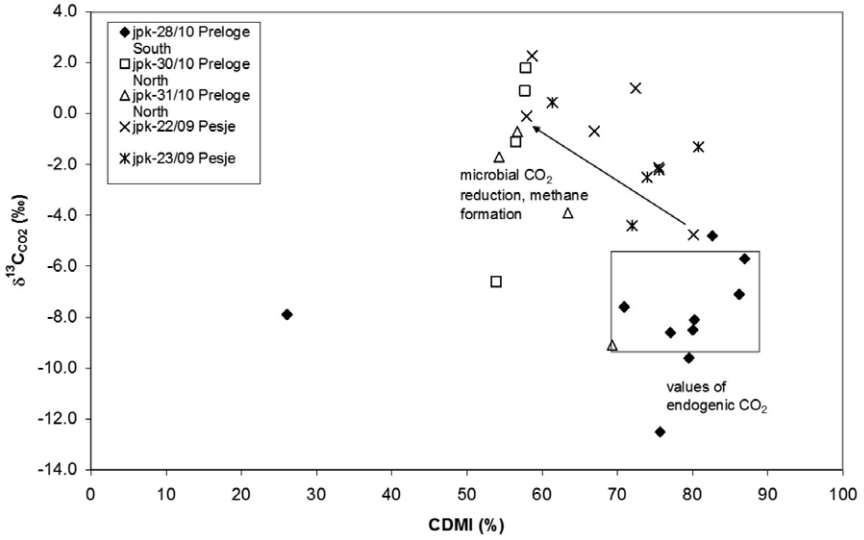


**Figure 6.** Interpretation of the origin of $CO_2$ at working faces (–120/B, G2/C in –50/B) using $\delta^{13}C_{CO2}$ versus CDMI index in a lignite seam in boreholes (jpk – 28/10, jpk – 30/10, jpk – 31/10, jpk – 22/09 and jpk – 23/09) ahead of the working faces (–120/B, G2/C and –50/B)

gas (Kotelnikova, 2002). Methane and $CO_2$ were/are generated by microbial fermentation process while methane was/is generated by $CO_2$ reduction process. $CO_2$ generated by fermentation process is characterized by $\delta^{13}C_{CO2}$ similar that organic matter around –25 ‰, while microbial reduction process results in an enrichment with the $^{13}C$ of residual $CO_2$ (Figures 5 and 6). Microbial $CO_2$ reduction is characteristic in mining area Preloge North, while at Preloge South $\delta^{13}C_{CH4}$ indicate bacterial origin via fermentation. At mining area Pesje both microbial ($CO_2$ reduction and methane fermentation) processes generated methane formation (Figure 5).

The origin of $CO_2$ is interesting due to its relation with outbursts in coalmines. High concentrations of carbon dioxide in seam gases in Australian coals occur in regions of igneous activity and associated faulting and this component has been described as being of presumed pneumatolytic origin (Smith & Gould, 1980). In our study CDMI index versus $\delta^{13}C_{CO2}$ (Figure 5) was used to explain the origin of $CO_2$ (Kotarba, 2001) and indicate endogenic $CO_2$ (including $CO_2$ originating from carbonates) and $CO_2$ of microbial origin in relation to microbial methane (working face Preloge North, jpk-30/10) discussed above. At working face Pesje –50/B (jpk-22/09 and jpk-23/09) $\delta^{13}C_{CO2}$ indicate microbial and endogenic origin (Figure 6). Typical endogenic values of $\delta^{13}C_{CO2}$ are about –7 ‰ (Kotarba, 2001) and high CDMI index found in our study (at working face Preloge South, jpk-28/10) are probably related to the tectonics of the Šoštanj and Smrekovec faults at the time of formation of the Velenje basin.

$\delta^{13}C_{CO2}$ derived from carbonates is dependent on $\delta^{13}C$ of carbonates and the temperature of their degradation. The resulting products are clay minerals and $CO_2$. Supposing that dolomites underwent thermal decomposition and are located below lignite seam along the Šoštanj fault zone values of $\delta^{13}C_{CO2}$ from –2 ‰ to –6 ‰ might indicate $CO_2$ of thermal decomposition of dolomites (Figure 6). This source of $CO_2$ has similar values as endogenic $CO_2$ from the fault zones and can not be distinguished with $\delta^{13}C_{CO2}$.

Also secondary processes should be considered since they might camouflage the origin of gases. Migration of gases as a secondary process caused by reduction of pressure in lignite seam causes enrichment in light $^{12}C$ isotope in methane and in $CO_2$. During migration of coalbed gases, gases of different origin might be mixed together and complicate interpretation of gas origin.

## CONCLUSIONS

Gas outbursts remain for coalminers one of the main problems in the Velenje coalmine, therefore geochemical investigations are one of the important parameters used in case of prediction or prevention gas outbursts.

Concentrations of methane and $CO_2$ change in advance of the working face. Areas with high $CO_2$ concentrations accompany with low methane concentrations and could be related with the rate of advancement of the working face. The rate of advancement of the working face is one of the crucial parameters influencing on gas composition at working faces.

Concentrations and stable isotope studies of coalbed gases at working faces allow the possible interpretation of the origin of coalbed gas in the Velenje basin. Considering also the results of previous studies, it can be concluded that coalbed $CO_2$ from investigated working faces is endogenic and bacterial origin. Methane is microbial origin (formed through microbial fermentation and/or $CO_2$ reduction). Secondary processes like migration, adsorption/desorption and mixing of gases of different origin during excavation complicate the interpretation of gas origin and were neglected in interpretation of the origin of coalbed gases. Examination of the origin of nitrogen (at locations with excess of nitrogen) in coalbed gases from Velenje Basin needs further research.

## Acknowledgements

This study was conducted in the framework of project Z1-2052 funded by the Slovenian Research Agency (ARRS) and the Velenje Coalmine d.d. The authors are also grateful to Mr. Tedej Zagoričnik, Mr. Robert Lah and Mr. Stojan Žigon for technical support, assistance in the field sampling and laboratory analyses. Sincere thanks to Dr. Jennifer McIntosh for improving the English of the manuscript.

## REFERENCES

ARAVENA, R., HARRISON, S. M., BARKER, J. F., ABERCROMBIE, H. & RUDOLPH, D. (2003): Origin of methane in the Elk Valley coalfield, southeastern British Columbia, Canada. *Chem. Geol.*; Vol. 195, pp. 219–227.

ATKINS, P. W. (1994): Physical Chemistry, fifth ed. Oxford Univ. Press, Oxford, pp. 1031.

CLAYTON, J. L. (1998): Geochemistry of coalbed gas – A review. *Inter. J. Coal Geol.*; Vol. 35, pp. 159–173.

COPLEN, T. B. (1996): New guidenices for reporting stable hydrogen, carbon and oxygen isotopes ratio data. *Geochim. Cosmochim. Acta*.; Vol.

60, pp. 390–3360.

Flores, R. M. (1998): Coalbed methane: From hazard to resource. *Inter. J. Coal Geol.*; Vol. 35, pp. 3–26.

Kanduč, T. (2004): *Isotopic characteristics of coalbed gases in Velenje Basin*. Master Thesis. Ljubljana: University of Ljubljana 2004; pp. 78 (in Slovene).

Kanduč, T., Markič, M. & Pezdič, J. (2005a). Stable isotope geochemistry of different lithotypes of the Velenje lignite (Slovenia), *Geologija;* Vol. 48, pp. 83–92.

Kanduč, T. & Pezdič, J. (2005b). Origin and distribution of coalbed gases from the Velenje Basin, Slovenia. *Geochem. J.*; Vol. 39, pp. 397–409.

Kanduč, T. & Šlejkovec, Z. (2005c). Unexpected arsenic compounds in low-rank coals. *Environ. Sci. Technol.;* Vol. 39, pp. 3450–3454.

Kanduč, T., Markič, M., Zavšek, S. & McIntosh, J. (2010). Methanogenesis in the Pliocene Velenje Coal Basin, Slovenia, inferred from stable carbon isotopes. *Inter. J. Coal Geol.* (in review).

Kotarba, M. (1990): Isotopic geochemistry and habitat of the natural gases from the Upper Carboniferous Zacler coal – bearing formation in the Nowa Ruda coal district (Lower Silesia, Poland). *Org. Geochem.;* 16, pp. 549–560

Kotarba, M. J. (2001): Composition and origin of coalbed gases in the Upper Silesian and Lublin basins, Poland. *Org. Geochem.;* 32, pp. 163–180

Kotelnikova, S. (2002): Microbial production and oxidation of methane in deep subsurface. *Earth – Science Reviews*. ; Vol. 58, pp. 367–395.

Markič, M. & Sachsenhofer, R. F. (1997): Petrographic composition and depositional environments of the Pliocene Velenje lignite seam (Slovenia). *Inter. J. Coal Geol.* 33, pp. 229–254

O'Neil, J. R. (1979): Stable Isotope Geochemistry of Rocks and Minerals. - V: Lectures in Isotope Geology, Jager, E., Hunzinger, J. C., (Eds). - Springer Verlag, 235–263, Berlin.

Scott, A. R. (1993): Composition and origin of coalbed gases from selected basins in the United States. *Proceeding of the 1993 International Methane Symposium, Birmingham, Alabama*. Vol. 1, pp. 207–222.

Sherwood Lollar, B., Lacrampe-Couloume, G., Slater, G. F., Ward, J., Moser, D. P., Gihring, T. M., Lin, L.-H. & Onstott, T. C. (2006): Unravelling abiogenic and biogenic sources of methane in the Earth's deep subsurface. *Chem. Geol.*; Vol. 226, pp. 328–339.

Shoell, M. (1983): Genetic characterization of natural gases. *Amer. Ass. Petrol. Geol. Bull.;* Vol. 67, pp. 2225–2238.

Smith, J. W. & Pallaser, R. (1996): Microbial origin of Australian coalbed methane. *Amer. Ass. Petrol. Geol. Bull.;* Vol. 80, pp. 891–897.

Smith, J. W. & Gould, K. W. (1980): An isotopic study of the role of carbon dioxide in outbursts in coal

mines. *Geochem. J.*; Vol. 14, pp. 27–32.

ZAVŠEK, S. (1990): Projekt raziskovalne proge na k. +75 v jami Škale, projektna štrudija, rudarski project, REK Velenje, DO Rudnik Lignita Velenje. Velenje: Premogovnik Velenje, Hidrogeološki oddelek, pp. 30 (in Slovene).

WILLIAM, D. J. Fugutive emissions from coal mining (online). 1999, November 23.12.2003 [citirano 11. 11. 1999]. Dostopno na svetovnem spletu:<http://www.atse.org.au>.

# Sediment transport and sedimentation in a coastal ecosystem – a case study

# Sedimentni transport in sedimentacija v priobalnem ekosistemu - zgled študije

B. K. Purandara[1], B. Venkatesh[1] & V. K. Choubey[2]

[1]Regional Center, National Institute of Hydrology, Hanuman Nagar, Belgaum – 590 001 Karnataka, India
[2]NIH, Roorkee - 2447667, Uttarakhand, India

*Corresponding author. E-mail: purandarabk@yahoo.com

**Received:** August 27, 2011 **Accepted:** November 2, 2011

**Abstract:** The determination and interpretation of particle grain-size has a fundamental role in hydraulics, geomorphology and sedimentology. The study of textural parameters of the sediments is of paramount utility in differentiating various depositional environments. The present study is carried out along the Central Kerala coast. Grain-size data have been collected from various sources. Apart from collected data, few representative surface sediment samples from the downstream of important rivers like Pamba, Manimala, Muvattupuzha, Minachil and Periyar which debauches into Vembanad lake have been collected. Surface and suspended sediment samples were also collected from the Vembanad lake area where the rivers join the lake and the adjacent nearshore area. Beach sediments were also collected from the selected locations. The study revealed a systematic change in grain-size pattern from moving from one environment to another. Coastal waters showed significant quantities of suspended sediment which resulted in the formation of mud banks (wave dampening). It is also observed that the accumulation of finer sediments aid in protecting the coast during southwest monsoon season. A socio-economic survey has been conducted in the study area to know the importance and significance of the rare coastal phenomena known as mud banks. Mud banks acts as a treasure house for fishes.

*Original scientific paper*

**Izvleček:** Določanje in interpretacija zrnavosti ima bistveno vlogo v hidravliki, geomorfologiji in sedimentologiji. Preučevanje strukturnih značilnosti sedimentov je izjemno pomembno pri razločevanju različnih sedimentacijskih okolij. To študijo so opravili ob obali osrednje Kerale (Indija). Podatke o zrnavosti so zbrali iz različnih virov. Razen tega so vzeli nekaj značilnih površinskih vzorcev naplavin iz spodnjega teka pomembnejših rek, ki se izlivajo v jezero Vembanad, kot so Pamba, Manimala, Muvattupuzha, Minachil in Periyar. Površinski in suspendirani sediment so vzorčili pri izlivu rek na območju jezera Vembanad in v okolici. Nadalje so vzorčili tudi obalni sediment v izbranih točkah. Študija je razkrila sistematično spreminjanje zrnavosti na prehodih od enega okolja do drugega. Ugotovili so, da priobalne vode vsebujejo znatne količine suspendiranega sedimenta, kar vodi do nastanka blatnih usedlin ("wave dampening"). Opazili so tudi, da kopičenje zelo drobnozrnatih usedlin pripomore k varovanju obale v obdobjih jugozahodnega monsuna. Na preučevanem območju so opravili tudi družbeno-ekonomsko raziskavo za oceno pomembnosti redkega obalnega pojava, znanega kot blatni nasipi. Blatni nasipi so prava zakladnica za ribe.

**Key words:** grain-size, lake, suspended sediments, mud bank, nearshore, beach

**Ključne besede:** zrnavost, jezero, suspendirane usedline, blatni nasip, priobalno okolje, obala

## INTRODUCTION

The various processes involved in the movement of water and its relationship to depositional patterns have attracted the scientists and engineers from various fields. Tides, freshwater outflow, and waves cause complicated water movement which transport, fractionate and modify the properties of particulate matter in coastal regions. These area differ geomorphologically, but have the common feature that suspended matter is carried back and forth, deposited, and eroded many times before it finally settles, either permanently or for a long period. Although the problem of the source of the sediments is often very complex, the process of sorting and grain size selection usually establishes an equilibrium between the bottom, suspended matter and the water.

Sediment granulometry have been studied using grain-size statistics. Review of this work has been given by

(Folk & Ward, 1957; Folk, 1966; Friedman, 1961, 1967; Veerayya et al. 1975; Rawlison,1984; Purandara, 1993; Pathani,1997; Kumar et al, 2000; Ganesan, 2004; Sanil et al., 2006; Purandara, 2008).

Kerala coast is one of the most dynamic and distinctive areas with variety of natural resources and facilities and there has always been a zone of hectic human activity. In the coastal areas, numerous problems such as devastation of natural habits due to erosion, pollution, siltation, over population, salt water intrusion, flooding etc are encountered. This part of the coastal area is known for highest density of population in the world.

The present study is an attempt to understand the distribution pattern of sediments in rivers, lake, beach and adjoining shelf. The study has been conducted along the central Kerala coast, between Azhikode in the north to Purakkad in the south (south of Alleppey). This stretch of coastal land is important for their unique formation of `Mud banks'. Mud banks are natural smooth water anchorages formed at particular locations along the Kerala coast during the southwest monsoon season. It extends outwards up to a distance of 3–4 km from the shore. These are semicircular in shape, with their northern and southern edges defined by two crescentic lines of breakers running outwards to the sea. The formation of mud banks play a major role in moulding the socio-economic set up of the coastal people by providing a stable fishing ground during the monsoon season. Mud banks affect the coastal processes by damping the waves in the following ways:

- traps the littoral material transported from the updrift side thereby preventing its downcoast movement,
- causes refraction of waves on its sides, (iii) protects the beach in particular from erosion.

## Study area

Geologically, the study area is covered by the Tertiary and Recent sediments which rests directly upon the Archaean crystalline complex consisting of khondalites, leptynites, charnockites and mica hornblende gneisses. The entire wetland ecosystem comprises of four major rivers that debouches into the Vembanad lake which fringes the coastal tract with an outlet to sea. The sediments brought by the rivers first settles in the lake and then it filters out to the sea through the estuary. The estuarine region presents a stable marine condition for major part of the year. During the monsoon period temporary halocline formed with fresh to brackish wa-

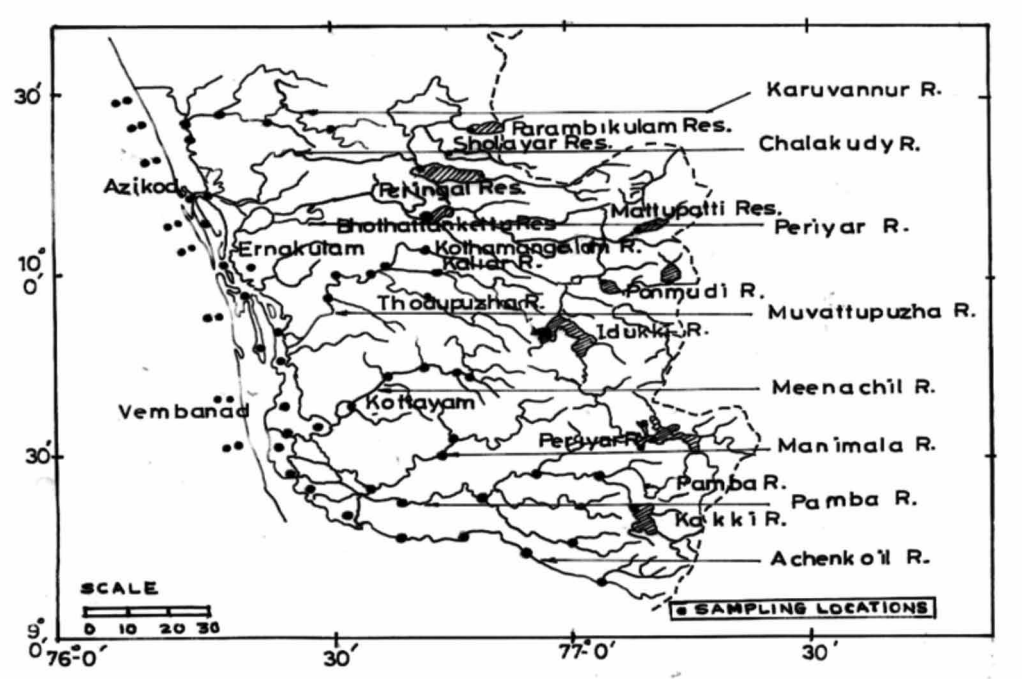


**Figure 1.** Study Area map with sediment sampling locations

ter condition exists at the surface, and marine condition continues to prevail at the bottom. The estuarine region is highly productive and the underlying sediments are correspondingly rich in organic matter content. The coastal sedimentary basins of the Kerala form the eastern margin of a bigger basin extending westward over the continental shelf. In the nearshore, gradients are 20 m/km to 80 m/km. The sediments present in the Kerala coastal basin include primarily Miocene sediments overlain by a thin section of Quarternary sediments. Present study has been carried out along the Central Kerala coast (Figure 1) to understand the distribution pattern of sediments. Surficial sediments from the rivers (downstream areas of Pamba, Manimala, Minachil, Muvattupuzha and Periyar) Vemband lake, mud banks and shelf were collected and sedimentological analysis were carried out.

## METHODOLOGY

### Field Investigations

Sediment samples were collected from the downstream region of the rivers Pamba, Manimala, Minachil, Muvattupuzha and Periyar (up to 30 km) were collected from the mid-stream channel at an interval of about 2 km to 10 km to

the point of origin of the rivers. Sediment samples were collected during pre-monsoon and post-monsoon season. Samples were collected from the beach, mud bank and non-mud bank areas of the continental shelf. Surficial sediments were collected by using van Veen grab and water sampling for suspended sediments and salinity determinations were carried out by using Hi-Tech water bottles at different depths.

## Laboratory Investigations

### *Textural analysis*

Textural analysis include both sieve and pipette analysis. Samples collected from the Vembanad lake and mud bank region was subjected to combined sieve and pipette analysis. For pipette analysis known quantities of dried sediments were dispersed overnight in a solution of sodium hexametaphosphate. The silt and clay fractions were separated by sieving the dispersed sediments through 230 μm mesh sieve. The coarse fractions remained in the sieve were dried and analysed. Statistical parameters like mean, standard deviation, skewness and kurtosis were determined by the method suggested by Folk & Ward (1957).

## Results and discussion

The size analysis of the sediments collected from various rivers, namely, Pamba, Minachil, Muvattupuzha and Periyar reveal that the downstream sediments are very fine in size and the upstream sediments are medium to coarse grained. This is clear from the polymodal nature of the sediments in the upstream. The decreasing tendency of grain-size with distance has been attributed to various hydraulic processes associated with the sediment movement which mainly depends on the travel distance.

However, the present investigations reveal that the distribution of sediment varies widely, particularly in the downstream regions as shown in figures 2a, 2b & 2c. The variation is more pronounced in the river Pamba where there is a sudden change of grain size at a distance of 22 km from the river mouth. This is attributed to the change in river pattern and also due to the confluence of Puthan ar which supplies comparatively finer sediments to the main stream by depositing the coarser sediments in the meandering course. It can also be explained on the basis of irregular mixing up of the estuarine and nearshore sediments. The mixing up process is influenced by the tidal currents, waves and coastal currents which push the sediment towards the estuarine region and from there it reaches the river mouth and vice versa.

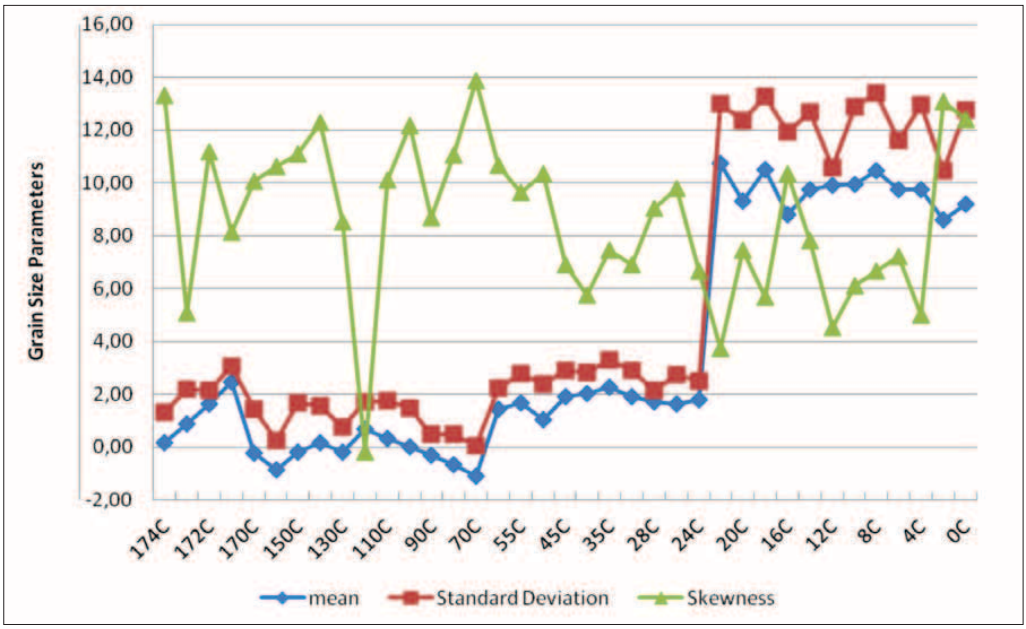


**Figure 2a.** Plots showing variation of Grain size parameters (Phi mean size, Standard deviation and Skewness) with Distance (upstream to downstream) along the river Pamba

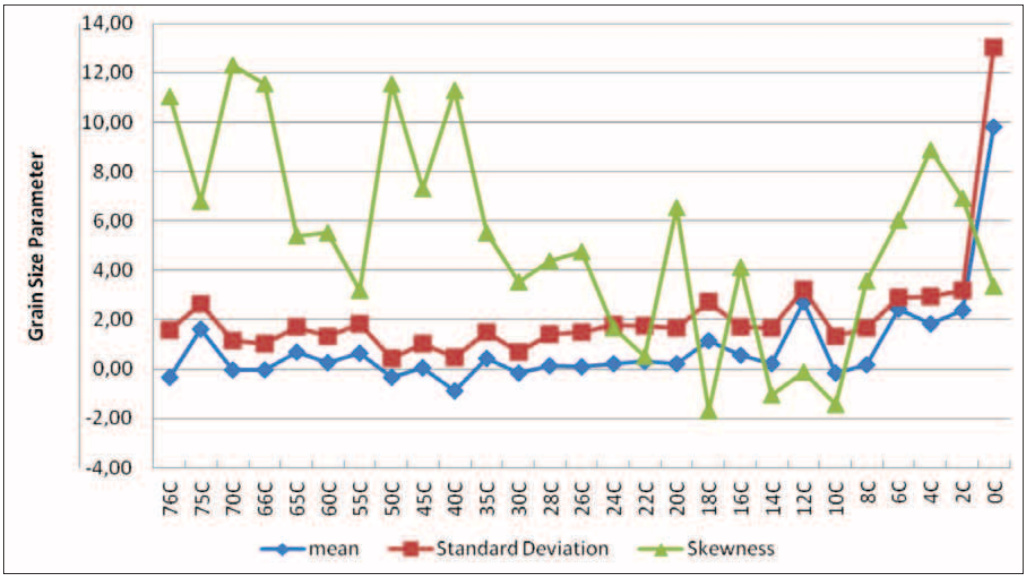


**Figure 2b.** Plot showing variation of Grain size parameters (Phi mean size, Standard deviation and Skewness) with Distance (upstream to downstream) along the river Minachil

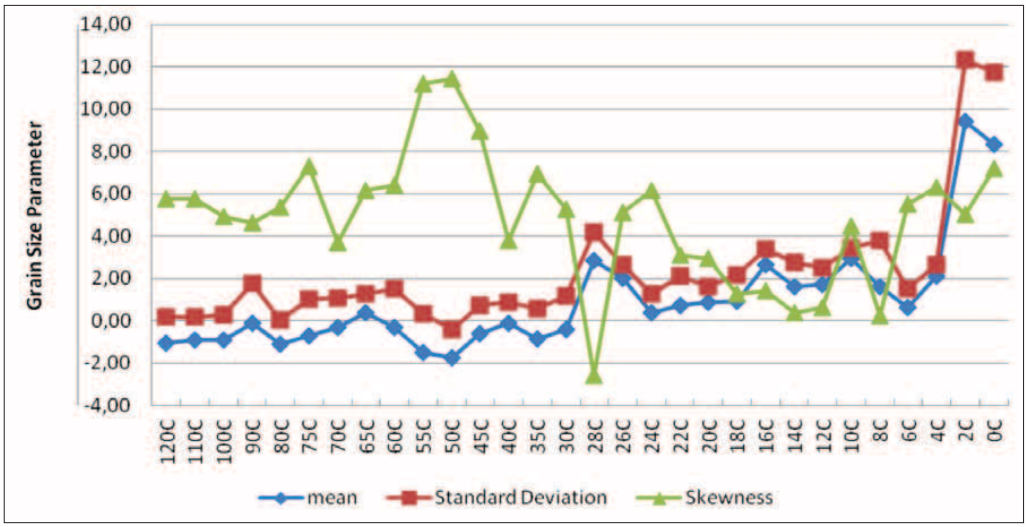


**Figure 2c.** Plot showing variation of Grain size parameters (Phi mean size, Standard deviation

Grain-size analysis (phi mean size, standard deviation and skewness) of the sediments carried out for all the four rivers in the downstream region are poorly sorted to very poorly sorted. The upstream sediments of Pamba, Minachil and Muvattupuzha show almost a constant value and are poorly sorted. The coarseness and poor sorting of the sediments may be due to its high energy conditions, relative proximity of the source area and the influx of the sediments from the tributaries. The poor sorting of the sediments towards Pamba from Muvattupuzha are noted both in the downstream and upstream region. Generally, river sands display better sorting towards downstream due to progressive sorting based on size. Here, instead, in the downstream area, a complex distribution pattern is observed. This may be due to its sharp decrease in the competency of the transporting agent, intensive mixing of sediments in the river mouth and an increase in depth which is observed during the field investigations. The decrease in velocity is responsible for the sudden deposition of coarser sediments which mixes with the finer sediments. The skewness of the sediments vary between positive to very negative values both in the upstream and downstream region. In general, most of the downstream sediments show a negative skewness or nearly symmetrical distribution. The negative skewness of sediments could be attributed to the addition of material to the coarser terminal, or subtraction of fines from the normal population. This is evident from the observation that the finer sedi-

ments are added through bank erosion and the tidal currents carry finer sediments during the flood tides.

The CM pattern (Figure 3) of the rivers of Central Kerala, closely resembles the pattern of river Mississippi. From the diagram, it is clear that the majority of the samples fall in region IV of PASSEGA & BYRAMJEE (1969) showing graded suspension with high turbulence. A small percentage of the samples fall in region I showing rolling with high energy environment. This shows that the river sediments are mainly transported either as graded suspension or bottom suspension with minor rolling and uniform suspension (PURANDARA, 1990). It is also assumed that particles of graded suspension are lifted by bottom turbulence and the sorting of the deposit is due to settling out of a bottom current (PASSEGA & BYRAMJEE, 1969). It is also important to note that the diameter of the coarsest grain of a graded suspension deposit indicates slow bottom currents. Sediments in the deposits having median values lower than 15 μm never

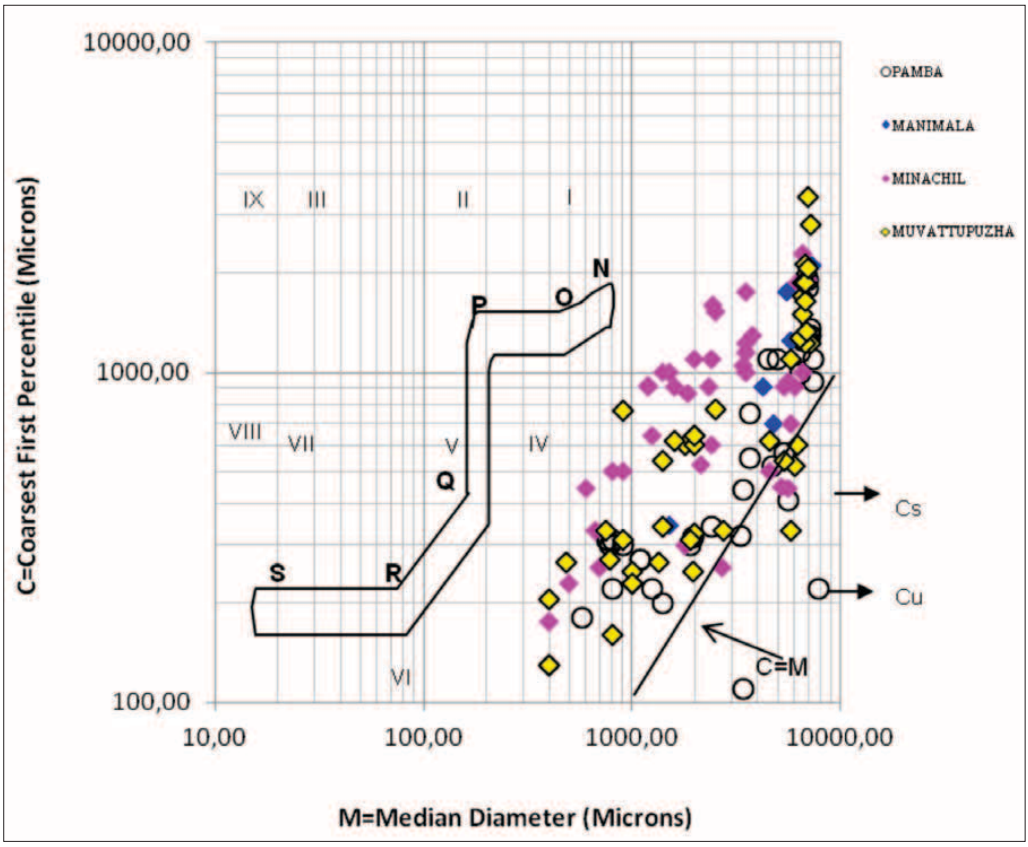


**Figure 3.** CM pattern diagram of selected rivers of central Kerala

show proportionality between C and M. They are too fine to be sorted by bottom currents. Hence, the uniform suspension is shown by fine particles of the downstream region where the competency of the river decreases and depth of water increases.

The phi mean size of the Vembanad lake sediments varies between 2.5 and 10.55. The average phi mean is 8.21 in the pre-monsoon and 6.4 for the post-monsoon sediments. The standard deviation varies from 1.39 phi to 4.54 phi (pre-monsoon) and 1.95 phi to 3.85 phi (post monsoon). The skewness varies between 0.38 and 0.48 phi during both the seasons. Lake sediments are platykurtic in nature. The kurtosis value ranges from 0.55 to 0.98 during Pre-monsoon and 0.31 to 0.98 during post-monsoon. Sorting of the sediments is poorer during post-monsoon and comparatively better sorted during pre-monsoon season. The kurtosis value shows decrease from pre-monsoon to post-monsoon season.

The CM pattern drawn for the pre-monsoon and post-monsoon sediments of Vembanad lake (Figure 4) show that the segment PM is missing during the pre-monsoon and post-monsoon seasons. In the case of pre-monsoon sediments, it contains QR and RS segments. Cluster of very fine sediments are noted due to its constant mean size and percentile values. In the pre-monsoon season, majority of the sediments are grouped below the coarsest percen-

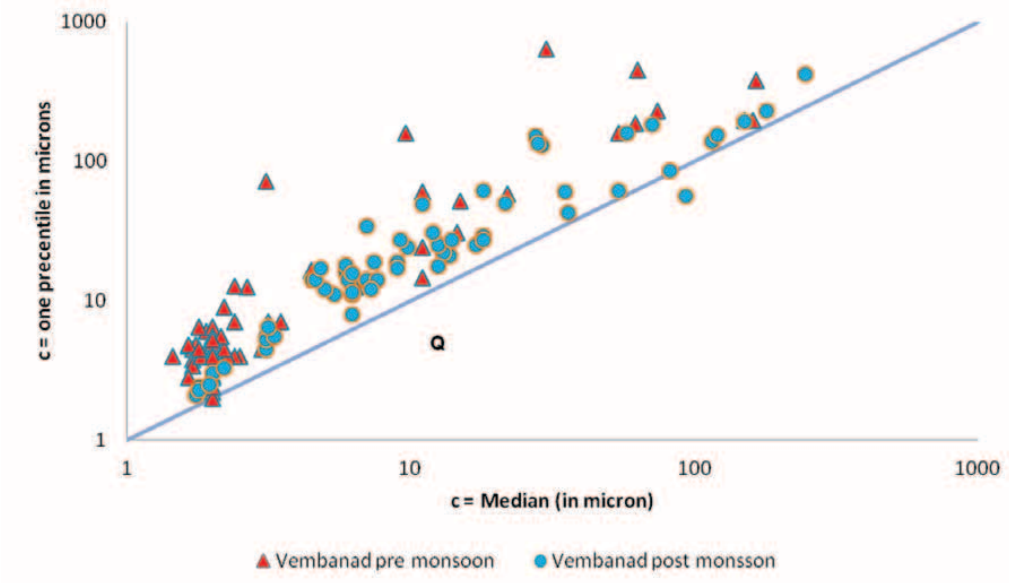


**Figure 4.** CM pattern diagram of Vembanad lake sediments (a) pre-monsoon; (b) post-monsoon

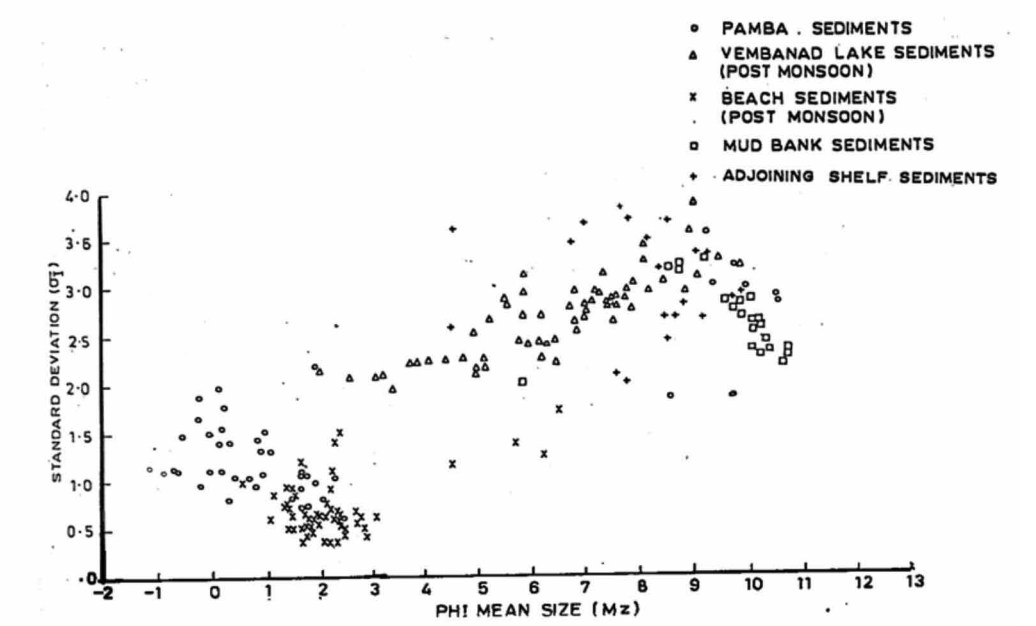


**Figure 5.** Scatter plot - Phi mean versus Standard deviation

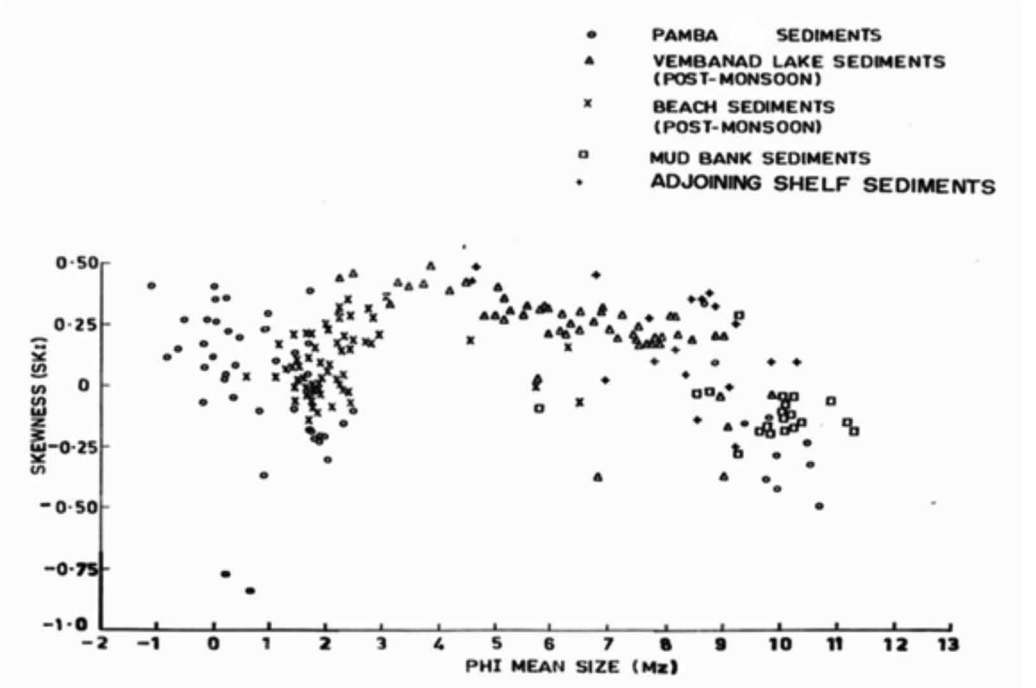


**Figure 6.** Scatter plot- Phi mean versus Skewness

tile of 31 μm and the median less than 3 μm. The total sediments in uniform suspension and graded suspension are less. The plot drawn for post-monsoon sediments indicates that the sediments are transported mostly by uniform suspension and graded suspension. The maximum size of the grains transported is 650 μm in size during pre-monsoon and it is 420 μm during post-monsoon.

The textural analysis of the beach sands showed that generally, sediments are finer during May and also immediately after the offset of monsoon. The finer size of the sediments may be due to the action of sediments by waves and currents along the beaches at certain places. The formation of mud bank is also significant in depositing the sediments along the coast. Most of the beach sediments are moderately sorted (Figure 5). The range of standard deviation is from moderately sorted to well sorted. Generally, the better sorting of the sediments could be due to the constant action by waves and currents. The skewness value of the pre-and post monsoon sediments varies widely. However, majority of the sands are nearly symmetrical in nature. In general, some of the beach sands are positively skewed. The positive skewness in beach sands as in the case of river sands may be because of the infiltration of fines.

The micro-environmental delineation of granulometric characteristics of the beach sediments are attempted. The size varies from coarse to very fine sand (Figure 5, 6). It is observed that beach sands relatively finer during May and immediately after the offset of monsoon. Most of the beach sands are moderately sorted and nearly symmetrical. Sediment movement in a coastal environment indicates that the various transport mechanisms remain active and it tend to retain the sediments as far as possible in the nearshore environment. In fact, very limited quantity of sediments brought by rivers and other geological agents passes to offshore. In the first stage, the sediments are filtered through estuary and escape into the nearshore and are mostly accumulated as suspended matter due to settling, scour lag effect and salinity variation. Only coarser denser materials are transported further offshore. This kind of accumulation of fine sediments in the nearshore region lead to the formation of mud banks. Mud banks are smooth water tracts along the study area formed during southwest monsoon season. This zone is relatively calm due to the dampening of the waves. The sediment characteristics of this region shown that the percentage of clay increase from May to August and there is a considerable decrease after September. The sediment with grain size less than 1 μm exceeds more than 50 %. During the south-west monsoon, the overflowing rivers of central Kerala are the major contributors of the

sediments through the lake and estuary. These overloaded sediments brought by rivers as suspension and bed load may be filtered through the estuarine mouth and will be transported to the nearshore zone. The transportation of sediments through such a long distance will bring very finer sediments and may remain in suspension due to lower salinity. Due to high concentration of suspended sediments (100 mg/L to 900 mg/L in the surface layer and 120 mg/L to 3600 mg/L in the bottom waters), waves are unable to reach the coast and are dampened completely. This process is very clear from the results which showed that there is a considerable increase in the concentration of suspended sediments from May to August and then a gradual decrease as observed by (KURUP, 1977; RAMACHANDRAN & MALLIK, 1985; PURANDARA & DORA, 1991). Furthermore, it explains that the accumulation of sediments take place in the low energy environment as the waves cannot reach the shore. This clearly indicates the gradual decrease of grain-size when transported to the sea through rivers and estuary. The confinement of suspended matter within a certain region, combined with movement by tidal and density currents, has an important selective effects on the sediment distribution on the continental shelf. In many areas distributional patterns are closely related to water movements including that of waves. Deeper portions on the shelf are often sufficiently quiet for mud deposition, but the deposits are coarse since no fine grained suspended matter is available. Conversely, muddy deposits may form in rough water if sufficient fine grained materials are supplied.

## CONCLUSIONS

In summary, the movement of sediments in coastal sedimentary environments shows that various transport mechanisms are responsible for holding the material within these regions. The study reveal that the accumulation of fine grained sediments and suspension are mainly due to settling, tidal movements and scour lag effects. The size of the particles mainly depends on local conditions and also on the accumulation process but the retention is usually most effective for fine grained matter. Further, it is important to note that the confinement of suspended matter within a certain region, combined with movement by tidal and density currents, has an important selective effect on the grain-size distribution of the deposit. (POSTMA, 1967) explained similar condition while dealing with estuarine sedimentation.

A socio-economic survey was conducted by contacting the farmers in the region and they expressed the view that the formation of mud banks is a boon to them because, the waters in

the region is enriched with nutrients and therefore, fishes come closer to the coast during this particular season. Since, offshore movement is restricted during the monsoon season, the availability of fishes in the nearshore region helps them to fetch their livelihood. However, they also opined that, in the recent years the Vembanad lake is facing threat of pollution due to various industries located in and around the lake. The pollutants entering the lake will finally reach to the open sea and may harm the production fishes due to their pollutant. Therefore, it is essential to take control measures while discharging the industrial wastes to lake.

## Acknowledgement

Authors are highly grateful to Sh. R. D. Singh, Director, National Institute of Hydrology, Roorkee for his encouragement. Authors are also grateful to Department of Marine Sciences, Cochin university of Science and Technology for the assistance rendered during the study.

## References

Folk, R. L., Ward, W. C. (1957): Brazos River Bar: A study in the significance of grain-size parameters. *Journal of Sedimentary Petrology*, Vol. 27, pp. 3–26.

Friedman, G. M. (1961). Distinction between Dune, Beach and River sands from their textural characteristics. *Journal of Sedimentary Petrology*, Vol. 31, pp. 514–529.

friedman, G. M. (1967). Dynamic processes and statistical parameters compared for size frequency distribution of beach and river sands. *J. Sediment. Petrol.*, Vol. 37, pp. 327–354.

Ganesan, P. (2004): Delineation of high tide line and seasonal beach profiling at Kalbadevi bay, Maharashtra, central west coast of India. Technical report: NIO/TR-8/2004.

Kumar, S. V., Kumar, K. A., Anand, N. M. (2000): Characteristics of waves off Goa, West coast of India. *Journal of Coastal Research*, V. 16(3), pp. 782–789.

Kumar, S. V., Pathak, K. C., Pednekar, P., Raju, N. S. N., Gowthaman, R. (2006): Coastal processes along the Indian Coastline. *Current Science*, Vol. 91(4), pp. 530–536.

Kurup, P. G. (1977): Stduies on Physica aspects of mud banks along the Kerala coast, Mahasagar- Bull. *National Institute of Oceanography*, 2(3), 25–31.

Passega, R., (1957 Texture as characteristic of clastic deposition.Bull. *Am. Assoc. Petrol. Geologists*, Vol. 41(9), pp. 1952–1984.

Passega, R., Byramjee, R. (1969): Grain size image of clastic deposits. Sedimentology. Vol.13, pp. 233–252.

Postma, H. (1967): Sediment transport and sedimentation in estuaries (ed by G. H. Lauff). *American Associ-*

*ation for Advancement of Science*, pp. 158–179.

PATHANI, R. A. (1997): Significance of grain-size analysis to differentiate microenvironment from Malvan beach, Maharshtra. *Journal Geol. Assn. Res. Centre*, Vol. 5(1), pp. 20–28.

PURANDARA, B. K., UNNIKRISHNAN, V. P., GUPTA, C. S., DORA, Y. L., (1987): Textural and mineralogical studies from Fort-cochin to Chellanam, Kerala. *Journal Geological Society of India*, Vol. 30, pp. 524–530.

PURANDARA, B. K. (1990): Provenance, Sedimentation and Geochemistry of the modern sediments of mud banks off the central Kerala coast, India. *Ph. D. Thesis*, Cochin University of Science & Technology.

PURANDARA, B. K., DORA, Y. L. (1991): Textural variations of Narakkal and Saudi Mud banks, west coast of India. *Journal of Indian Association of Sedimentologists*, Vol. 10, pp. 1–11.

PURANDARA, B. K. (1993): Texture and Mineralogy of Periyar river(southwest coast of India) sediments. IJMS, 22:78–80.

PURANDARA, B. K. (2008): Sediment Observations in Muvattupuzha, Kerala, Southwest India. Proceedings (Abstract volume) National Seminar on Konkan Coast DEED, pp. 74–81.

RAMACHANDRAN, K. K. & MALLIK, T. K. (1985): Mud banks off Kerala Coast- A State of the Art report. *State Committee on Science, Technology and Environment*, Govt. of Kerala.

RAWLISON, S. E. (1984): Environments of deposition, Palaeo-currents, and provenance of Tertiary deposits Kachemaka Bay, Kenai Peninsula, Alaska, *Sedimentary Geology*, 38, pp. 421–442.

SAMSUDDIN, M., SUCHINDAN, G. K., (1987): Beach erosion and accretion in relation to seasonal longshore current variation in the Northern Kerala coast, India. *Journal of Coastal Research*, Vol. 3(1), pp. 55–62.

SAMSUDDIN, M. (1986): Textural differentiation of the foreshore and breaker zone sediments on the northern Kerala coast, India. *Sedimentary Geology*, Vol. 46, pp.135–145.

UNNIKRISHNAN, V. P. (1987): Texture, Mineralogy and Provenance of the beach sands of south Kerala. *Ph. D thesis*. Cochin University of Science and Technology (unpublished).

VEERAYYA, M., VARADACHARI, V. V. R. (1975): Depositional environments of coastal sediments of Calangute, Goa. *Sedimentary Geology*, Vol. 14, pp. 63–74.

# Integrated remote sensing and GIS approach to groundwater potential assessment in the basement terrain of Ekiti area southwestern Nigeria

# Povezava daljinskega ugotavljanja in GIS za oceno potenciala podtalnice v kristalinični podlagi območja Ekiti v jugozahodni Nigeriji

Abel O. Talabi[1, *] & Moshood N. Tijani[2]

[1]University of Ado-Ekiti, Faculty of Science, Department of Geology, Ado-Ekiti, Nigeria
[2]University of Ibadan, Faculty of Science, Geology Department, Ibadan, Nigeria

*Corresponding author. E-mail: soar_abel@yahoo.com

**Received:** March 15, 2011 **Accepted:** September 6, 2011

**Abstract:** Occurrence of groundwater in the Basement Complex terrain of Ekiti area, southwestern Nigeria is controlled by secondary porosities developed through weathering and fracturing of the crystalline bedrocks. Here, the aquifers are characteristically discontinuous (localized) warranting assessment of the groundwater potential of the area to serve as a guide for groundwater exploration. Remote sensing (RS) and Geographical Information System (GIS) have been useful in assessing, monitoring and conserving groundwater occurrence. Hence, this paper presents the integrated approach of RS and GIS to groundwater potential zonation in the study area. Thematic maps of geology, geomorphology, lineament, slope, drainage and drainage density were prepared and integrated using ArcGIS 9.1 software to produce the groundwater potential map of the study area. The GIS evaluation produced a groundwater potential map in which the study area was categorized into zones; very good, good-moderately good and poor. Furthermore, superimposition of the groundwa-

*Original scientific paper*

ter yield data from the study area on the groundwater potential map revealed that there are more number of high-yield wells in the favourable zones (very good to good-moderately good) indicated by the GIS approach. This study highlights that the groundwater potential map would apart from its role as exploration guide be useful for the development of sustainable groundwater scheme in the area.

**Izvleček:** Navzočnost podtalnice v stari podlagi območja Ekiti v jugozahodni Nigeriji je odvisna od sekundarne poroznosti, ki je posledica preperelosti in razpokanosti kristaliničnih kamnin. Značilno za vodonosnike v njih je, da so nepovezani (lokalizirani) in je zato mogoče podatke o potencialu podtalnice v njih uporabiti kot vodilo za njeno sledenje. Daljinsko ugotavljanje (RS) in geografski informacijski sistem (GIS) sta uporabni orodji za ocenjevanje, spremljanje in varstvo podtalnice. V članku je opisana povezana uporaba RS in GIS za zoniranje potenciala podtalnice na raziskovanem ozemlju. Izdelane tematske karte geologije, geomorfologije, lineamentov, nagiba reliefa, površinskih vodnih tokov in njihove gostote so združili s programsko opremo ArcGIS 9.1 v karto potenciala podtalnice raziskovanega ozemlja. Na tej karti, izdelani z uporabo GIS, je ozemlje razdeljeno na območja dobrega, dobrega do zmerno dobrega in slabega potenciala. Ob prekritju karte izdatnosti podtalnice na raziskovanem ozemlju s karto njenega potenciala se je dalje izkazalo, da so visoko izdatni vodnjaki številnejši v ugodnih območjih (z zelo dobrim in dobrim-zmerno dobrim potencialom), kakor so bili določeni z metodologijo GIS. Iz raziskave izhaja, da je karto potenciala podtalnice mogoče uporabiti ne le kot vodilo pri sledenju, vendar tudi za trajnostno gospodarjenje s podtalnico na danem ozemlju.

**Key words:** Remote sensing, GIS, groundwater potential zonation, Ekiti area, Basement Complex, thematic maps, high yield wells.

**Ključne besede:** daljinsko ugotavljanje, GIS, zonalnost vodnega potenciala, območje Ekiti, kristalinična podlaga, tematske karte, vodnjaki visoke izdatnosti

## Introduction

Water is an important constituent of all forms of life and is required in sufficient quantity and acceptable quality to meet the ever increasing demand for various domestic, agricultural and industrial processing operations. This requirement is hardly fulfilled because 97.5 % of the world global water is saline existing in the ocean, 69.5 % of the remaining 2.5 % world global water that is fresh is locked up in glaciers/permafrost while 30.1 % and 0.4 % of it represent groundwater and surface/atmospheric water respectively (http://ga.water.usgs.gov/edu/waterdistribution.html). Surface water on the one hand is prone to seasonal fluctuations and contamination through anthropogenic activities while groundwater on the other hand is more in quantity, readily available as it exists in virtually all geologic formations and is naturally protected from direct contamination by surface anthropogenic activities. In the basement terrain of Ekiti area, south western Nigeria, availability of surface water is seasonal; during the relatively dry period of November to February each year, shallow groundwater in form of hand-dug wells and boreholes remain the only source of water supply as most streams and rivers are dried up. However, the occurrence and movement of groundwater in this crystalline bedrock setting depend on the degree of weathering and extent of fracturing of the rocks (Oloruniwo & Olorunfemi, 1987).

The highlighted scenario warrants a detailed investigation of the groundwater potential characteristics of the area so that an exploration guide as well as sustainable groundwater management strategy can be developed.

Groundwater prospect in an area is controlled by many factors such as geology, geomorphology, drainage, slope, depth of weathering, presence of fractures, surface water bodies, canals and irrigated fields amongst others (Jain, 1998). Slope for example is one of the factors that control the rate of infiltration of rainwater into the subsurface and could therefore be used as an index of groundwater potential evaluation. In the gentle slope area the runoff is slow allowing more time for rainwater to percolate, whereas high slope area facilitate high runoff allowing less residence time for rainwater hence comparatively less infiltration. In one way or the other, each of the listed factors contributes to groundwater occurrence. These factors can be interpreted or analyzed with GIS using RS data. Burrough (1986) defined a GIS ‘‘as a powerful set of tools for collecting, storing, retrieving at will, transforming and displaying spatial data from the real world for a particular set of purpose’’. GIS thus enables a wide

range of map analysis operations to be undertaken in support of groundwater potential zonation of an area.

Several conventional methods exist for the exploration and preparation of groundwater potential map of an area. These methods include; geological, geophysical and hydrogeological. However, RS amongst these methods is considered to be more favourable as it is less expensive and applicable even in inaccessible areas. It is a rapid and cost effective tool in producing valuable data in geology and geomorphology. In classifying groundwater potential zones, visual integration of data generated from remote sensing is feasible but cumbersome. However, with the advent of GIS technologies, the mapping of groundwater potential zones within each geological unit has become easy.

GUSTAFSSON (1993) used GIS for the analysis of lineament data derived from SPOT imagery for groundwater potential mapping in a semi-arid area in south eastern Botswana. Also, JAIN (1998) demonstrated the use of hydro geomorphological map by using Indian Remote Sensing Satellite Linear Imaging Self-Scanning II geocoded data on 1 : 50 000 scale along with the topographic maps to indicate the groundwater potential zones in qualitative terms (i.e., good to very good, moderate to good and poor). Previous research efforts in the study area have been directed at locating and developing potable groundwater using geophysical and geological techniques. Such studies, including the work of REBOUCAS & CAVALCANTE (1989), classified the basement terrains aquifers into three; the weathered basement aquifer, the basement detrital overburden aquifer and the fractured rock aquifer. Also, OYINLOYE & ADEMILUA (2005) examined the nature of aquifer in the crystalline Basement rocks of Ado-Ekiti, Igede-Ekiti and Igbara-odo areas, southwestern Nigeria and concluded that aquifers occurred both in the regolith and fractured basement rocks of the area.

The highlighted previous groundwater investigations concentrated on identifying fracture zones and areas with thick overburden employing geophysical and geological techniques as pathfinders to groundwater availabity. However, basic knowledge of groundwater location, its potential in terms of quantity and availability can provide basis for more rational planning. Therefore, the present study assessed the groundwater potentials of the study area using integrated RS and GIS approach.

## STUDY AREA

The study area (Figure 1) lies between latitudes $7^0$15'–$8^0$5' N and longitudes $4^0$44'–$5^0$45' E and fall within the Basement Complex setting of southwestern

Nigeria. It covers area extent of about 6 353 km$^2$. The study area enjoys tropical climate with two distinct seasons; rainy and dry seasons covering (April to October) and (November to March) respectively. The annual temperature range is between 25 °C and 30 °C while the annual rainfall is 1 500 mm. The study area is drained by many streams and rivers most of which dry off at the pick of the dry season usually between January and February causing supply of water for domestic and agricultural purposes to depend heavily on groundwater system. Groundwater supply in the area is mainly from shallow hand dug wells and limited boreholes. Two major aquiferous units (weathered and fractured layers) have been identified as source of supply to the wells and boreholes (Ademilua & Olorunfemi, 2000).

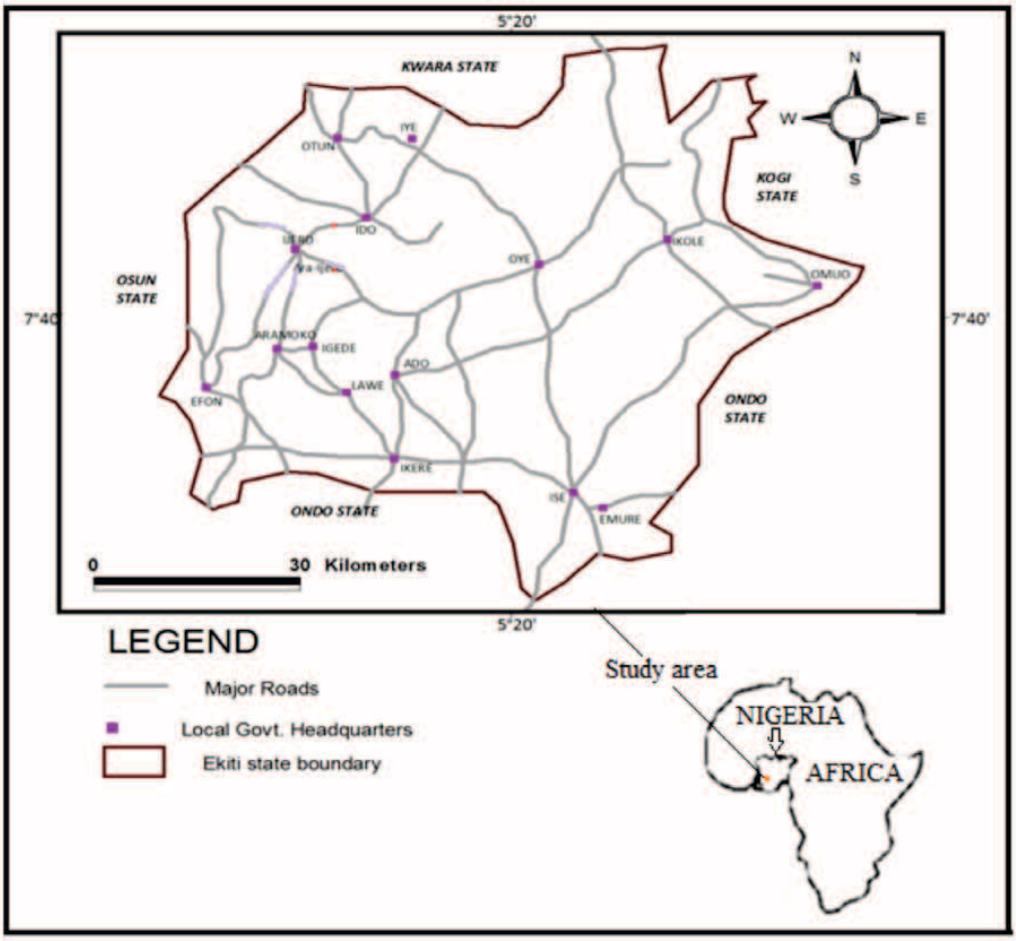


**Figure 1**. Location map of Nigeria showing the study area

The topography is generally undulating with most area lying above 250 m above sea level. The landscape is characterized by old plains, broken steep sided outcrops of dome shaped Inselbergs that may occur singularly or in ridges. Such outcrops exist mainly in form of rugged hills at Ado-Ekiti (central part of study area) and Ikere-Ekiti in the southern part of the study area.

**Geology of study area**

Geologically, the study area is underlain by Precambrian crystalline rocks mostly of igneous-metamorphic origin with isotopic ages greater than 300 Ma to 450 Ma (MATHEIS, 1987). Prominent rock units include porphyritic granite, fine-medium grained granite, granite gneiss, schist/quartz schist, migmatites and charnockite. The gneisses and migmatite are intimately associated such that they are hardly distinguishable on the field. The gneisses and the migmatite rock units are ubiquitous and form the bulk of the rocks in the study area. In some places, these rocks display characteristic feature of banding of varying width (Figure 2). Migmatite is a mixed rock composed of a gneissic host and intruded by the granitic and pegmatitic rocks. It covers over 50 % of the whole study area (Figure 3).

**Figure 2.** Migmatite rock outcrop along a road cut (Iworoko-Ifaki) in the study area.

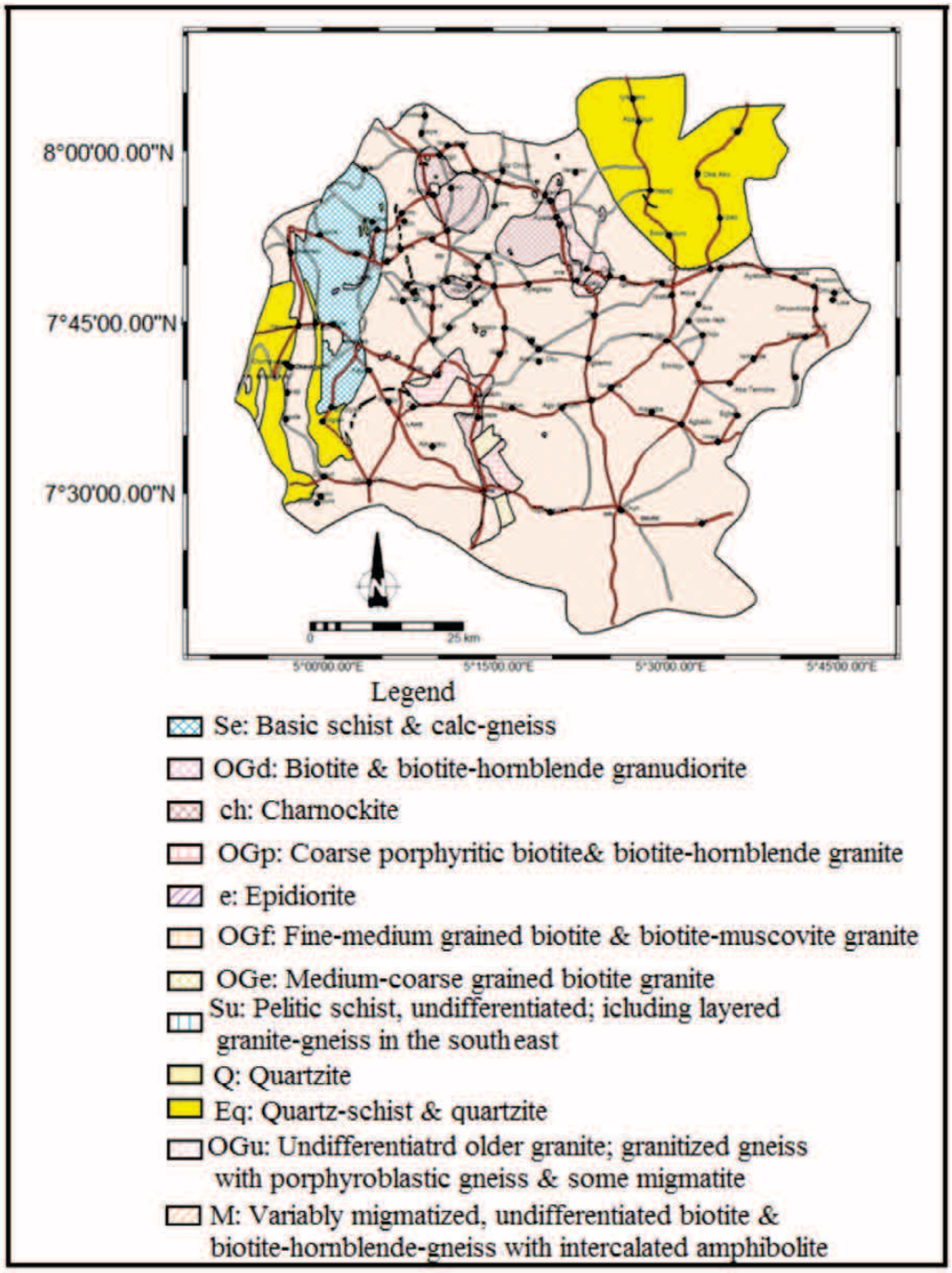


**Figure 3.** Geology Map of the Study Area.

The quartzite occurs as relatively minor concordant layers within the gneiss-migmatite units. On account of high content of late crystallised mineral and consequently resistance to weathering/ erosion, the quartzite tends to stand out as prominent hills and ridges within the study area.

The granitic units occur as intrusive bodies of various dimensions in the pre-existing basement rocks i.e. the gneiss-migmatite units and the schist/ quartz schist bedrock. The granitic units consisting of a suite of porphyritic and non-porphyritic granite rocks as well as medium to coarse grained textural varieties are widely distributed in the study area especially the central and south- eastern part. One striking feature of the granitic unit is the occurrence as picturesque inselbergs (prominent hills) rising sharply above their surrounding plains.

In some places, charnockite, a bluish-green rock, is found associated with the granitic units. The charnockite features prominently at Ikere and Ado towns in the study area.

## METHODOLOGY

System integration, which involves the integration of computer software (AutoCAD 2000, Cad overlay R.14 and ArcGIS 9.1) and hardware, imagery processing, information extraction and analysis formed the basic methodology of this work. System integration involves the use of computer hardware (equipment), software, data and personnel as well as other accessories such as digitizer and scanner at building capable expert system to extract geo-referenced information from the acquired satellite imagery. The processing flow chart of the methodology used in this study is presented in Figure 4. The first step in system integration is to identify data need, conceptualize how it would be captured and display in a GIS platform. The data required and used for this study were identified and their sources verified. The data sources include the Geological Survey Department of Nigeria, Abuja, National Institute of

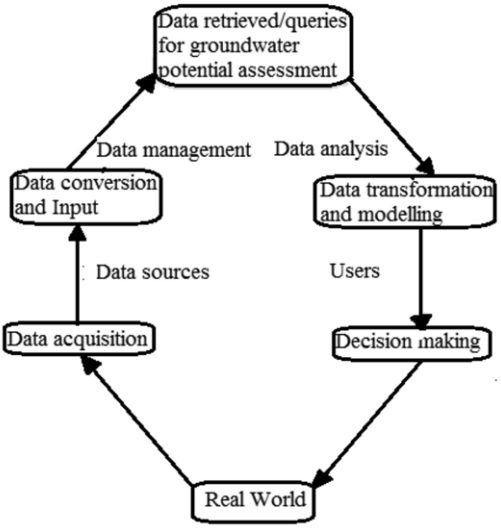


**Figure 4.** GIS in groundwater potential assessment

Remote sensing, Bukuru, Jos, Nigeria and Federal Ministry of Solid Mineral Resources, Abuja, Nigeria.

## Data acquisition, Conversion and Information extraction

The relevant data acquired which include existing analogue maps, charts, plans and records are presented in Table 1. Consequently, assembling and detail data structuring were also carried out before the compilation and digital conversion for logical data structure. The data as highlighted in Table 1 conformed to the National Geospatial Data Infrastructure (NGDI) - an initiative for co-sharing information in a Geoinformation-based economy. Subsequently, the analogue spatial and attribute data acquired were captured, rasterized, georeferenced and manipulated in CAD software (CAD Overlay R14) and converted to GIS supported GeoTIFFs raster format. These were subsequently exported into ArcGIS 9.1 software for further processing which include editing of both spatial and tabular data on a continuous and interactive basis.

As part of the follow up activities, the information required were extracted using supervised, unsupervised and ground truthing approach plus existing data and information. To classify the image into unique characters comprising of pixels with similar spectral characteristics, unique clusters which represent one or more features according to some statistically determined criteria, were also employed. Subsequently, fieldwork was embarked upon to validate GIS processed information. Where outcrops were not visible, the slope and drainage were used to validate the results.

**Table 1.** Relevant spatial data, information extracted and data sources for the research

| Spatial Data | Attribute Data | Source |
|---|---|---|
| Land sat Imagery | Digital Elevation Modeling/ Terrain/Geology | National Institute of Remote Sensing, Bukuru, Jos, Nigeria |
| NigerSat-1 Imagery | Digital Elevation Modeling/ Terrain/Drainage | National Institute of Remote Sensing, Bukuru, Jos, Nigeria |
| Mineral Maps of Nigeria | Metadata | Geological Survey Department of Nigeria, Abuja, Nigeria |
| Aero Magnetic Map of Southwestern Nigeria | Lineation | Ministry of Solid Mineral Resources, Abuja, Nigeria |

**Integration of data**

Consequently, each of the thematic maps in raster format was assigned suitable weightage factor (Table 2) based on previous works of researchers such as SRINIVASA RAO & JUGRAN (2003), KRISHNAMURTHY et al. (1996), SARAF & CHOUDHARY (1998) and PARASAD et al. (2008). Each of the thematic maps such as geology, geomorphology, drainage density, lineament and slope provides certain clue in respect of the occurrence of groundwater. To unify these information, there is the need for integration of the data with appropriate factor. Though, it is possible to superimpose the information manually, however, it is time consuming and may be proned to errors. Therefore, the information were integrated through the application of GIS. Various thematic maps were reclassified on the basis

**Table 2.** Weightage assigned to various thematic maps based on prospective contribution of input factors to groundwater occurrence (SRINIVASA RAO & JUGRAN, 2003).

| Feature | Classification | Weightage |
|---|---|---|
| Geology | Migmatites | 1 |
| | Charnockite | 1 |
| | Granite gneiss | 2 |
| | Granite | 2 |
| | Quartzite/quartzite schist | 3 |
| Geomorphology | Hilly area | 1 |
| | Lowland area | 3 |
| Slope | Extreme steep slope ($76.3^0$) | 1 |
| | Very steep slope ($35.2^0$) | 1 |
| | Steep slope ($30.81^0$) | 1 |
| | Moderate-steep slope ($22.13^0$) | 1 |
| | Moderate slope ($9.21^0$) | 1 |
| | Gentle slope ($8.4^0$) | 2 |
| | Very gentle slope ($4.57^0$) | 3 |
| | Lowland/Nearly Level ($0.25^0$) | 4 |
| Lineaments | Present | 3 |
| | Absent | 1 |
| Drainage density | Low density/coarse texture | 4 |
| | Medium density/medium texture | 2 |
| | High density/fine texture | 1 |
| | Very high density/very fine texture | 1 |
| Drainage density | Low density/coarse texture | 4 |
| | Medium density/medium texture | 2 |
| | High density/fine texture | 1 |
| | Very high density/very fine texture | 1 |

of weightage assigned and processed using the ‘‘Raster Calculator’’ function of Spatial Analysist Extension of ArcGIS 9.1 for integration.The procedure adopt simple arithmetical model to integrate the various thematic maps by averaging of the weightage to produce a final groundwater potential map of the study area. Finally, to validate or authenticate the evaluation method, existing borehole yield data were correlated with the various groundwater potential zones in the study area.

## Results and discussion

Results of the integrated approach of RS and GIS to delineate groundwater potential zones in hard rock terrain of Ekiti area are presented in form of thematic maps (Figures 3, 5 & 7–10).

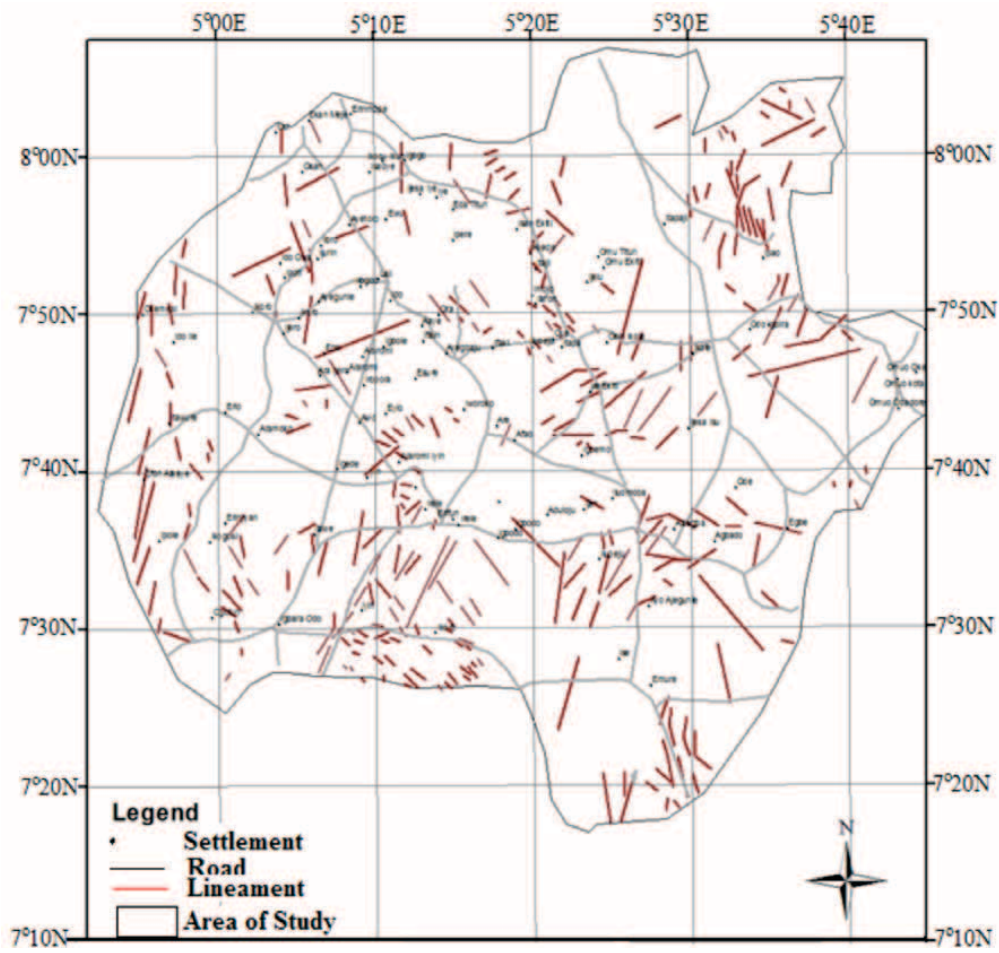


**Figure 5.** Lineament map of the study area.

The final groundwater potential map in which the study area were zoned into three categories (Very good, good-moderately good & poor) is represented in Figure 11. Furthermore, Figure 12 represents a typical weathered overburden soil in charnockite bed rock terrain at Ikere in the southern partof the study area while graphical evaluation of the highlighted zones with well depths and yield data are presented in Figures 13 and 14 respectively.

**Lineaments**

The study area is criss-crossed with lineaments characterized by dominant NW-SE and NE-SW directions while a few numbers of the lineaments also trend E-W (Figure 5) this strongly agree with result of the directional analysis presented in rose diagram (Figure 6). Lineaments cut across the entire bedrock units of the whole area. Futher evaluation revealed that migmatite has low lineament density with 0.02 km$^{-2}$ com-

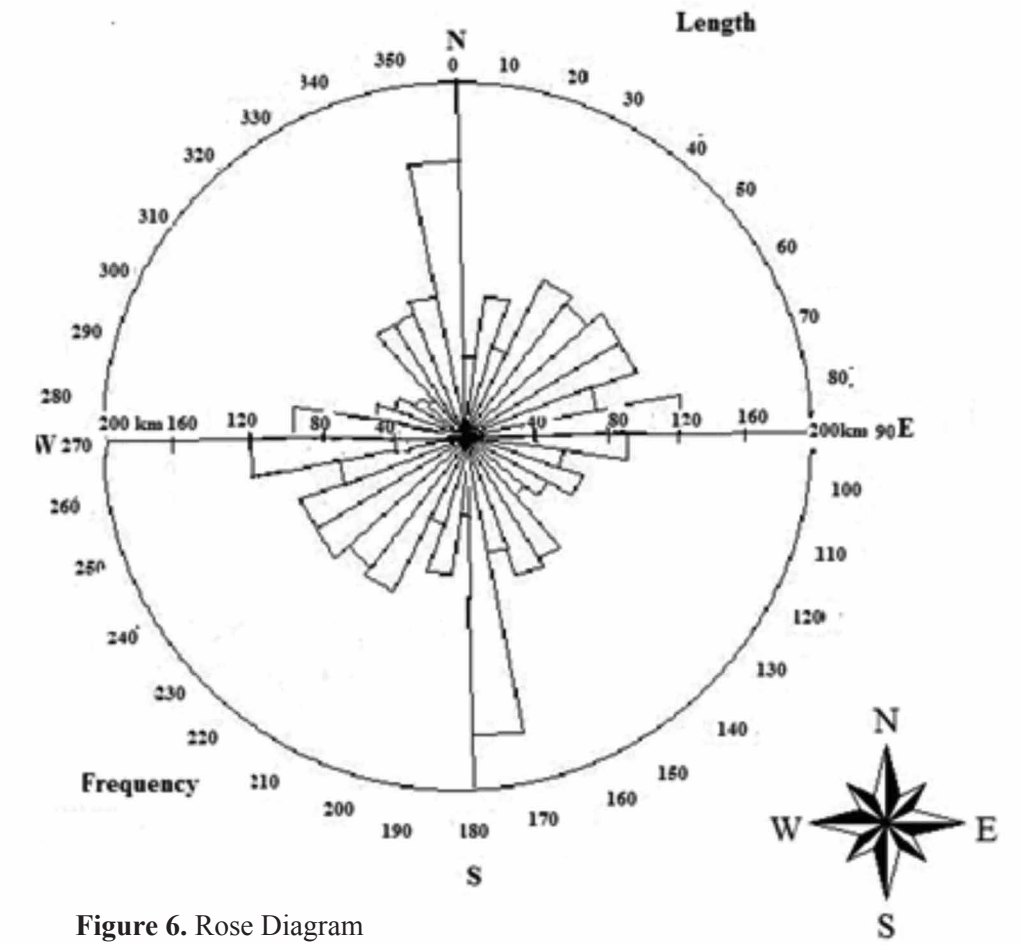


**Figure 6.** Rose Diagram

pare to quartzite, granite and charnockite with density range from 0.05 $km^{-2}$ to 0.13 $km^{-2}$. These lineament density revealed existence of more lineaments on the granitic /charnockitic rocks which might be as a result of transpressive forces exhibited during intrusion of the rocks into the parent migmatite/metasedimentary rocks. However, the lineaments in the low lying part of the study area are of significant interest with respect to groundwater occurrence because the lineaments on migmatite are mostly on the hilly and high slope areas with little or no overburden which are regarded as less significant due to possible high runoff rather than favouring vertical groudwater infiltration.

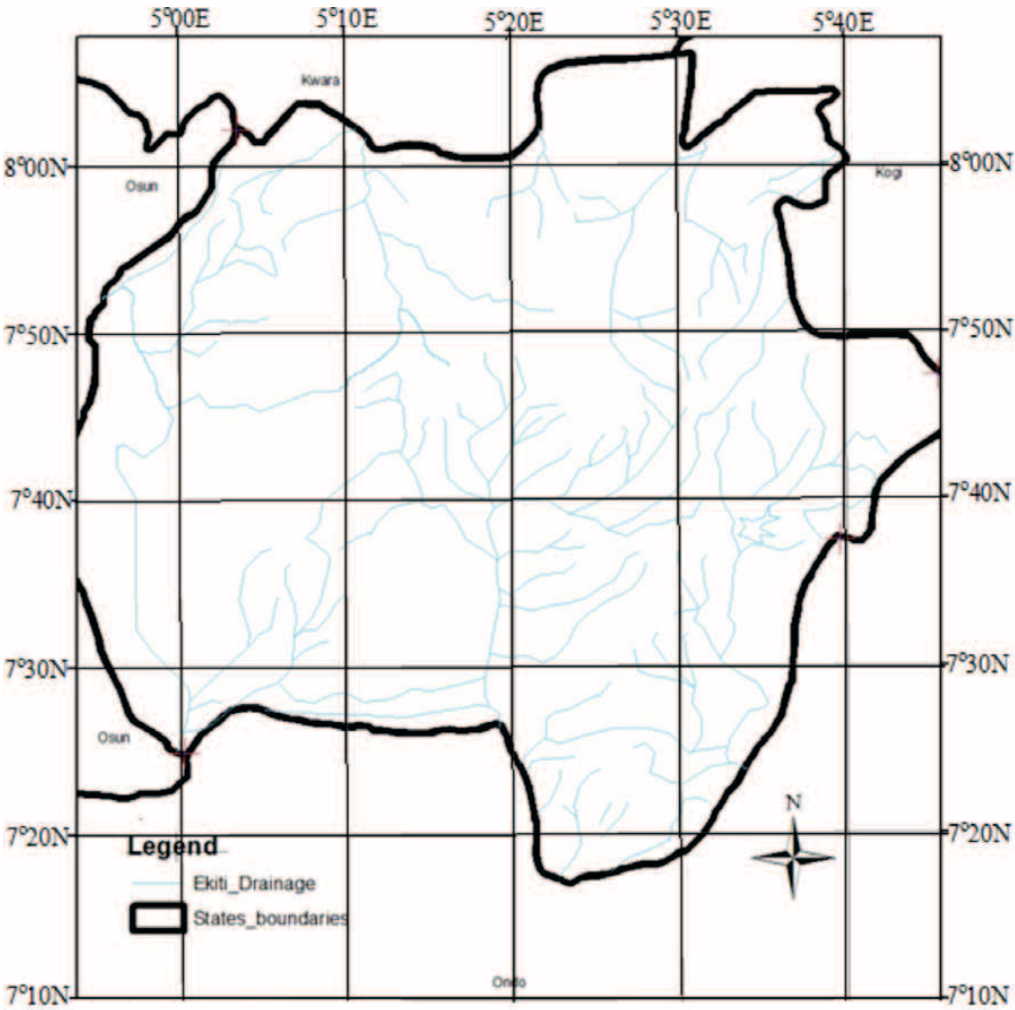


**Figure 7.** Drainage Map of the Study Area

**Drainage**

Usually, drainage patterns are said to be reflections of surface and subsurface formations while drainage density is proportional to surface run-off due to the fact that the more the drainage density, the higher the runoff. (PARASAD et al, 2008). Hence, the drainage density characterizes the runoff in an area as the volume of relative water that was unable to penetrate into the subsurface. In addition, drainage density do give

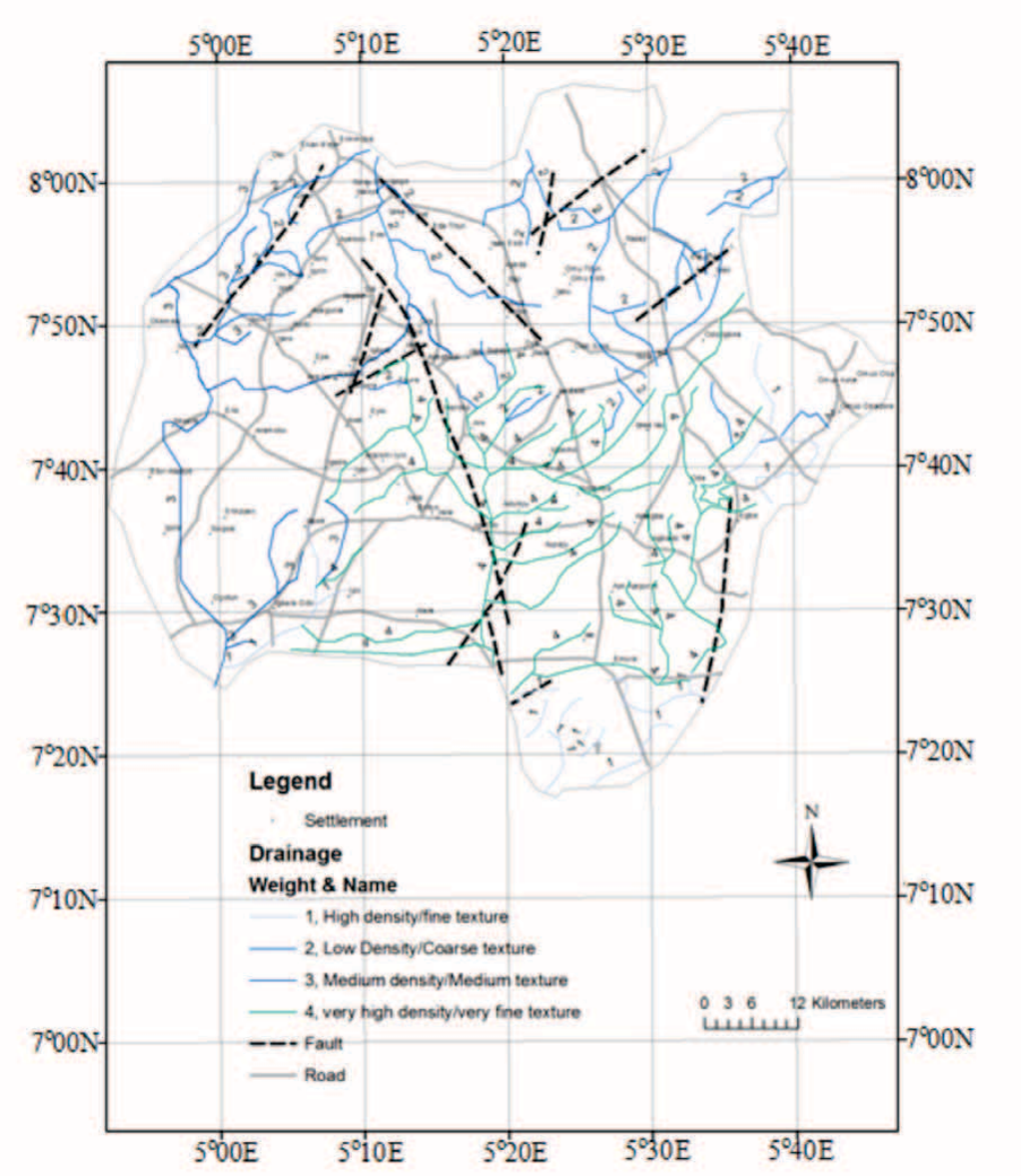


**Figure 8.** Drainage Density Map of the Study Area

indications of closing or otherwise of stream/river channels which inturn will depend on the nature and degree of weathering of the surface and subsurface lithologic units. Low drainage density therefore enhances the chance of recharge and contributes positively to groundwater availability if other groundwater occurrence conditions are favourable. In this study thematic map extracted from the topographic map shows dendritic pattern (Figure 7) while the drainage density map presented in Figure 8 reflects the infiltration characteristics with high drainage density indicating low-infiltration and the low drainage density high infiltration respectively. Most of the drainage originates from the quartzite ridge and granitic/charnockitic hills with dense drainage pattern. The lowland part of the study area that are characterized mainly by diverse rock units (porphyritic granite, fine-medium grained granite, granite gneiss and migmatite) presents low density an indication of favourable condition for vertical infiltration of runoff from surrounding hills and thus enhancing grounwater occurrence.This observation signify that groundwater occurrence in the lowland part of the study area is not only controlled by rock formations but other factors like topography and weathering as weathering products from the surrounding hills pile up to form overburden thickness aquifer while during igneous rocks intrusion fractures favourable for vertical infiltration were developed and thus additionally support groundwater occurrence.

**Slope/Geomorphology**

Results of slope and geomorphology thematic maps produced from integrated RS and GIS as presented in Figures 9 and 10 respectively revealed eight slope categories ranging from extreme slope to lowland and two main geomorphic units; hilly area and lowland area. Geomorphology is a reflection of the various landform and structural features of an area. Such landform and structural features are useful in categorizing groundwater occurrence. Generally, field observation revealed that the lowland areas are covered by thick weathered material representing alluvium matrials from the hilly areas (Figure 12). The weathered overburden revealed three principal horizons designated A, B and C. The “A” horizon is dark brown to redish lateritised soil, littered with some plant residues which implies organic soil form. The “B” horizon is subdivided into three distinct sub-units but all the three units are generally finer in texture compared to “A” horizon and of a lighter brown. The first two subunits of ‘‘B’’ horizon constitute the vadoze zone where active leaching and vertical of infiltration water occurs.The third sub-unit of the horizon constitute the phreatic zone representing the aquiferous layer.Soil horizon ‘‘C’’ is grey to white in col-

our due mainly to absence or substantial reduction of weathering activities and represents fresh parent rock which may or may not be fractured. However, when the parent rock is fractured, it compliments the overburden thickness in terms of groundwater occurrence.

The hilly areas comprise of gentle sloping surfaces with transported sediments lying between hills and plains. Additionally, the hilly areas are also characterized by presence of residual hills occuppying over 64 % of the study area (Figure 11). The ground-

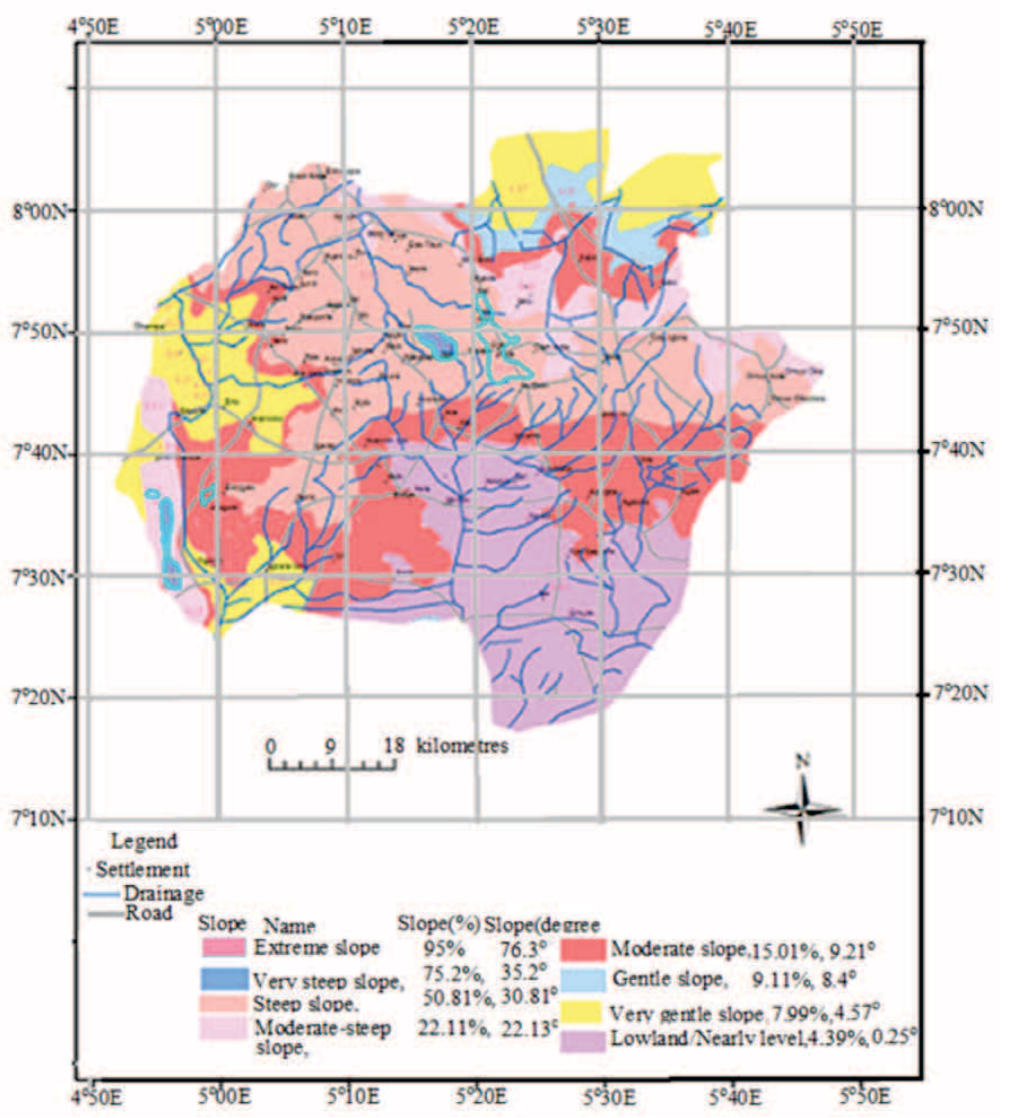

water prospect in this zone is poor. Further evaluation with respect to the slope characteristics of the study area revealed that gentle slope are indicative of slow runoff allowing more time for rainwater infitration, whereas extremly steep slope area facilitate high runoff allowing less residence time for rainwater hence, comparatively less infiltration. Extreme slope to moderately

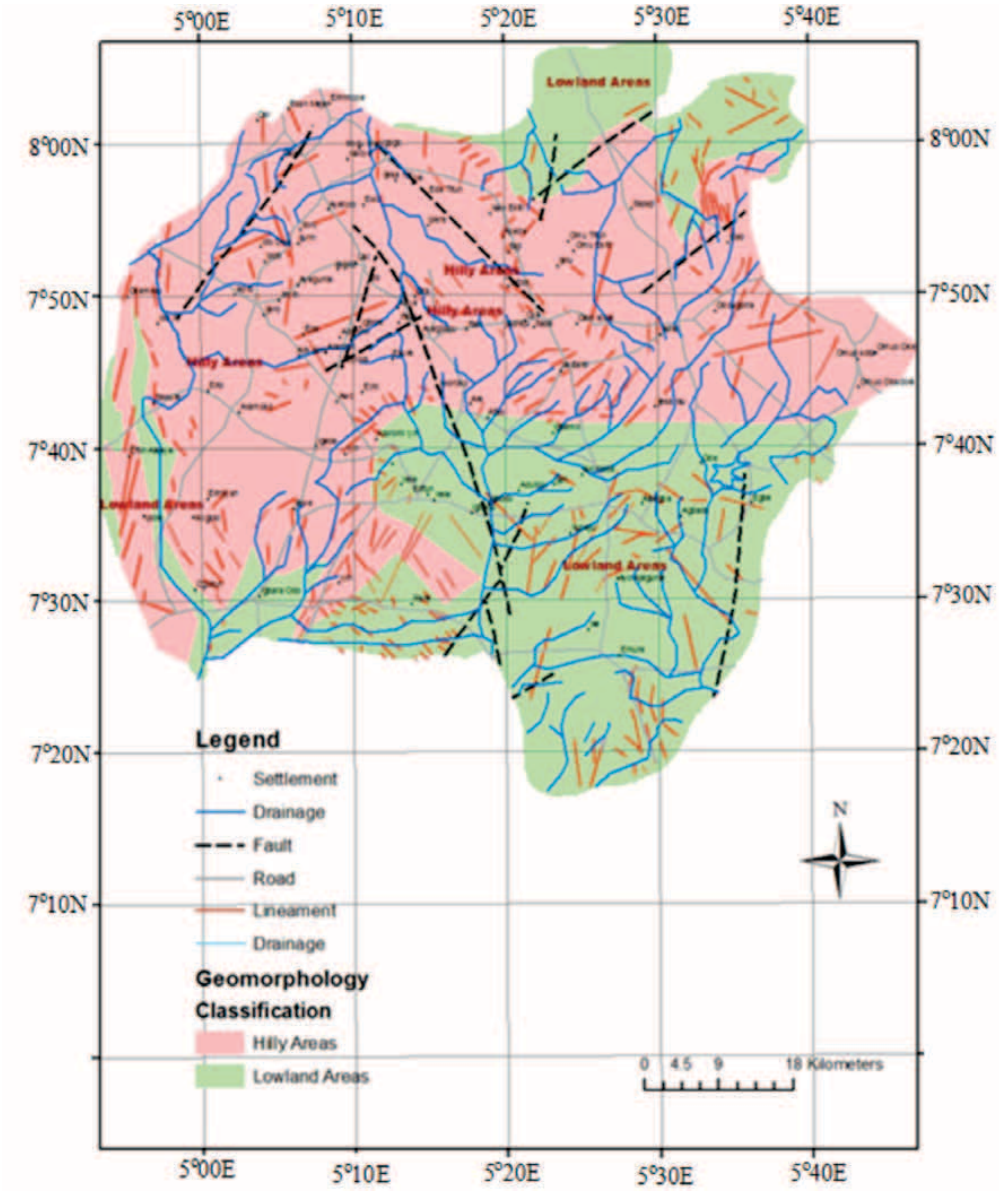


**Figure 10.** Geomorphology Map of the Study Area

steep slope occupy over 50 % of the study area and groundwater prospect in this area is poor in agreement with the earlier observation infereed from geomorphologic thematic map.

**Synthesis and Groundwater potential map of the study area**

The integration of the thematic maps resulted in the production of groundwater potential map of the study area

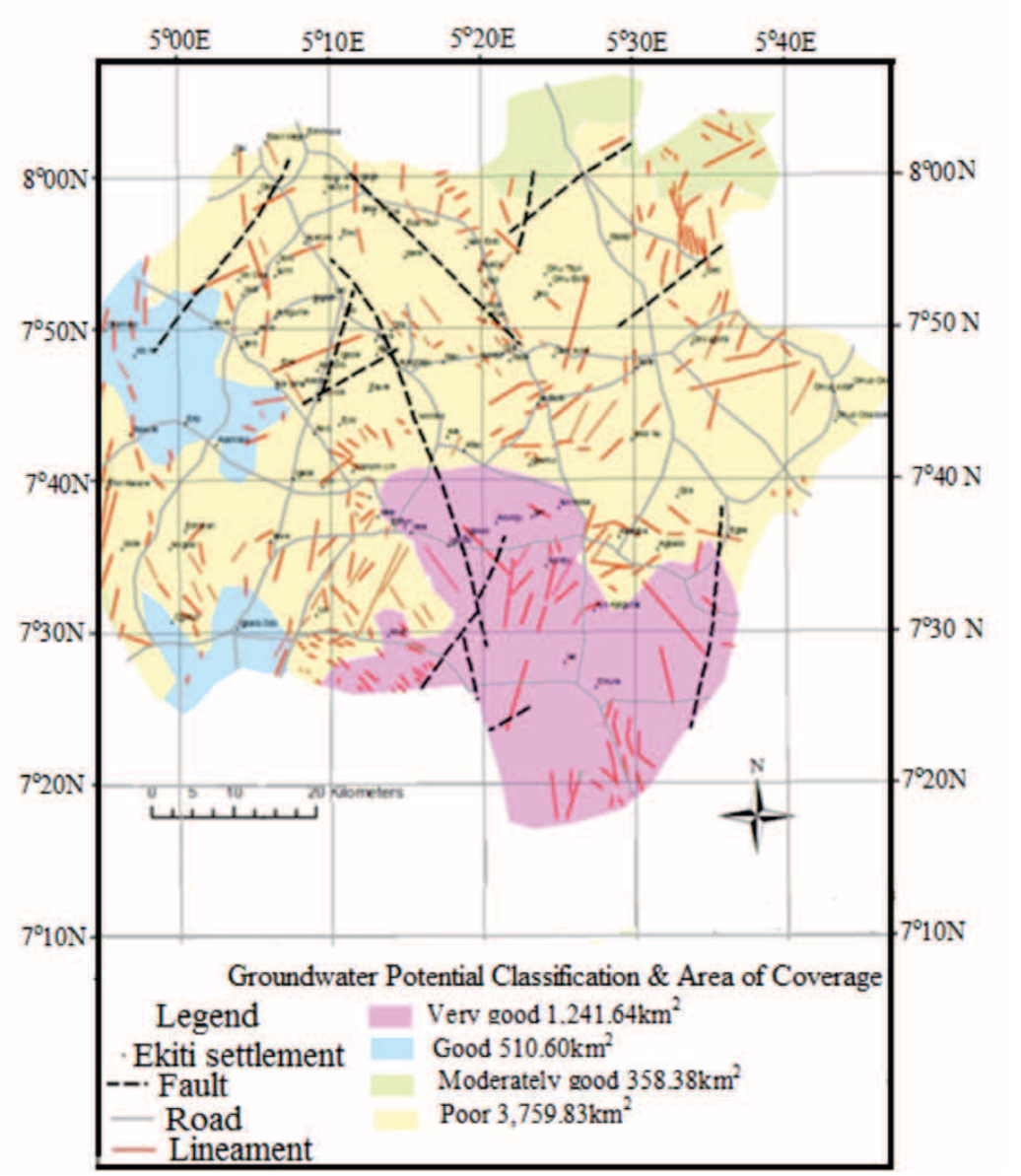


**Figure 11.** Groundwater Potential Map of the Study Area

(Figure 11). As shown in the map, the area that has very good potential for groundwater is situated in the south eastern part covering about 21.15 % of the study area. The good to moderately good potential area covers only 6.12 % while the greatest portion of the area about 64.04 % belongs to poor groundwater potential zone. The poor groundwater potential zone on the one hand is characterized majorly by migmatite and migmatite gneiss with quartzite/ quartz-schist and charnockite constituting the minority rock units while on the other hand, the very good and good to moderately good groundwater potential zones are covered majorly by granitic and charnockitic rocks with migmatite and quartzite constituting minority rock units. The various rock units cut across the different groundwater potential zones. However, the migmatite rocks that cover greater parts of poor groundwater potential zone are less fractured and in most cases covered with shallow overburden

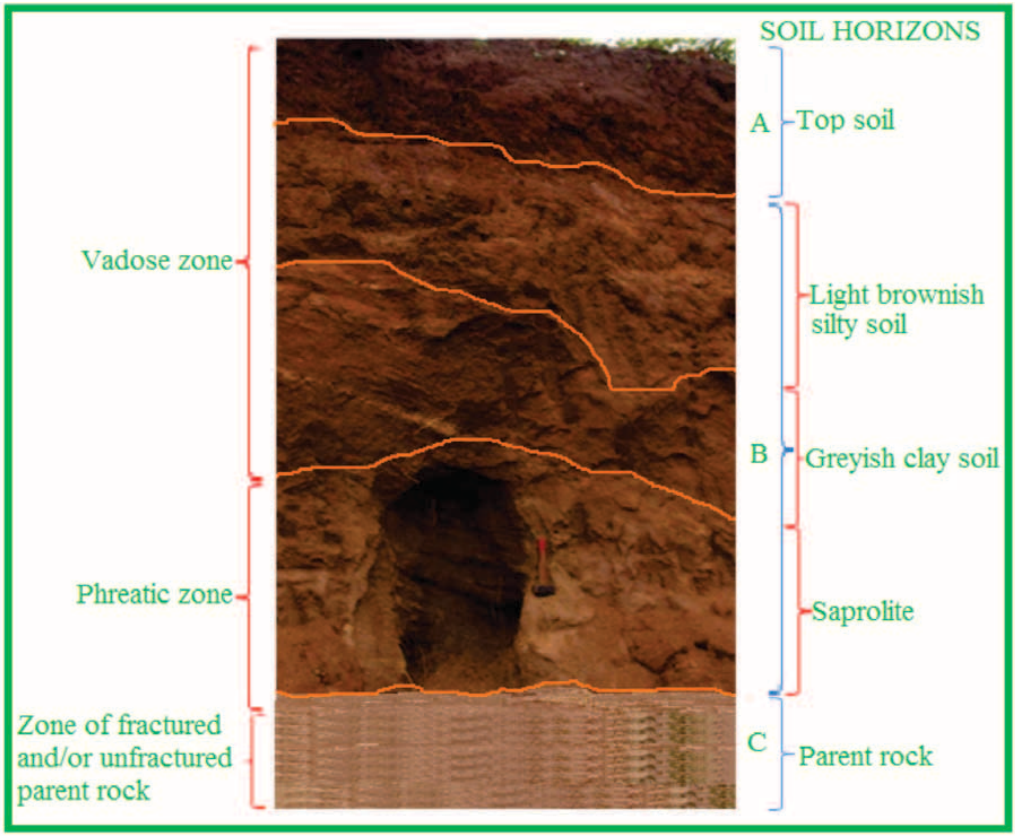


**Figure 12.** Showing weathered overburden soil in a typical charnockite bed rock terrain at Ikere

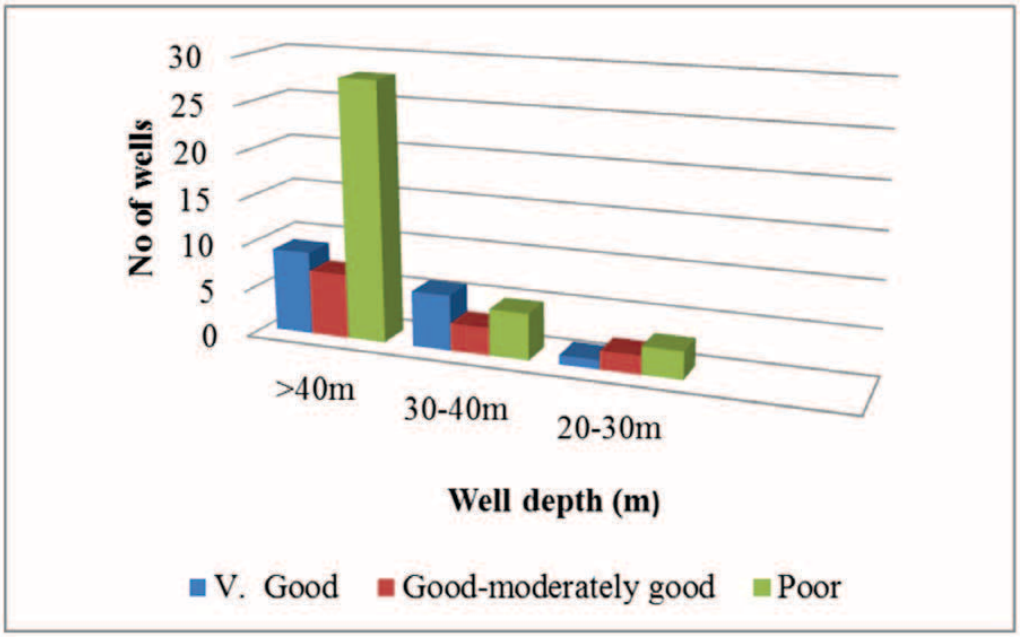


**Figure 13.** Frequency distribution of well depth with respect to groundwater potential zones.

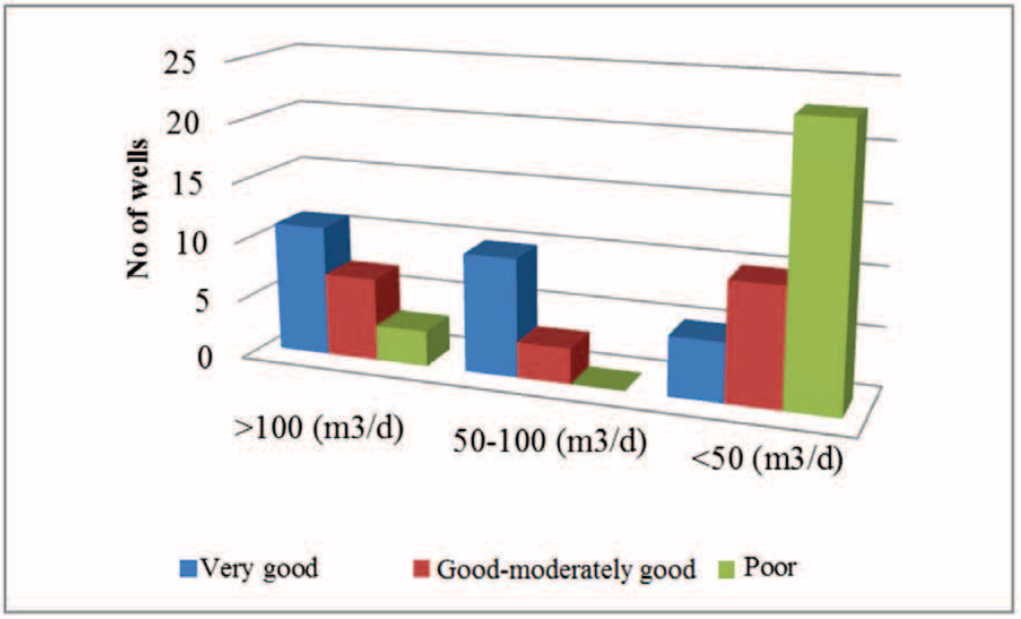


**Figure 14.** Frequency distribution of well yield with respect to groundwater potential zones

thickness when compared to the granitic and charnockitic rocks that form the major rock units of the very good and good to moderately good potential zones. Obviously, weathering, thickness of overburden mateerial as well as fracture system in the various groundwater potential zones are major factors controlling groundwater occurrence in the study area and these factors are more favoured in the very good and good to moderately good groundwater potential zones compared to the poor groundwater potential zones.

**Result validation**

In order to validate the classification of the study area into different groundwater potential zones (i.e. very good, good to moderately good and poor), bohole yield data of existing wells from Benin/Owena River Basin Development Authority (BRBDA), Ikere-Ekiti, and Federal Ministry of Water Resources, Lagos, Nigeria were collected and evaluated. The data revealed that boreholes in the study area can be categorized into high (>100 $m^3$/d), moderate (50–100 $m^3$/d) and low yield (<50 $m^3$/d). In additipon, the depth range varies from 21.3 m to 92 m while the yield range between 8.64 $m^3$/d to 354.24 $m^3$/d (Table 3). The data also revealed that 46 % of wells within granitic terrain are of high yield (>100 $m^3$/d) while 21 % of well in both migmatite and charnockitic also exhibited high yield compared to 12 % of the quartzite terrain. These are characteristics of very good to good groundwater potential zones which is consistent with the trend of the GIS-based potential zones. However, migmatite, charnockite, granite and quartzite bedrocks are characterized by 63 %, 16 %, 13 % and 3 % of the low yield (<50 $m^3$/d) wells respectively which are typical of poor groundwater potential zones in the study area.

**Table 3.** Summary of Borehole completion records in Ekiti Basement area

| S/NO | Location | *BHD*/m | *SWL*/m | Yield ($m^3$/d) | GWZ | Bedrock |
|---|---|---|---|---|---|---|
| 1 | Ogbesse | 45 | 4.1 | 86.4 | Very good | migmatite |
| 2 | Ikere (Ogoga palace) | 53 | 8.9 | 103.68 | Very good | granite |
| 3 | Ikere(Benin/Owena office) | 40 | 3.9 | 103.68 | Very good | charnockite |
| 4 | Emure(Owode) | 35 | 1 | 103.68 | Very good | granite gneiss |
| 5 | Emure(Awopegba house) | 30 | 5.7 | 69.12 | Very good | granite gneiss |
| 6 | Ise(oraye) | 45 | 4.8 | 103.68 | Very good | migmatite |
| 7 | Orun | 40 | 4.5 | 69.12 | Very good | migmatite |
| 8 | Ado(Bolorunduro) | 36 | 3.9 | 86.4 | Very good | charnockite |

| | | | | | | |
|---|---|---|---|---|---|---|
| 9 | Ado(Italaoro) | 30 | 3.3 | 86.4 | Very good | granite |
| 10 | Igede | 35 | 8 | 69.12 | Very good | granite |
| 11 | Temidire | 43.8 | 6 | 131.33 | Very good | granite |
| 12 | Ilumoba | 45 | 7 | 354.24 | Very good | migmatite |
| 13 | Ago-Aduloju | 29.6 | 2.7 | 129.6 | very good | charnockite |
| 14 | Bolorunduro | 31.3 | 3.2 | 30.24 | very good | charnockite |
| 15 | Ado-Com. School | 40 | 6.8 | 132.19 | Very good | granite |
| 16 | Aro Camp-Ikere | 42 | 3.2 | 54.43 | Very good | charnockite |
| 17 | ESGSC-Ikere | 68 | 18 | 203.04 | Very good | charnockite |
| 18 | Ado grammar school | 51.4 | 7.2 | 25.92 | Very good | granite |
| 29 | Ogbese | 48.6 | 1.5 | 283.39 | Very good | migmatite |
| 20 | Itawure | 37 | 2 | 103.68 | Good | quartzite |
| 21 | Ikoro | 60 | 9 | 112.32 | Good | migmatite |
| 22 | Egbewa | 50 | 21 | 103.68 | Good | migmatite |
| 23 | Owode | 43 | 2.1 | 175.39 | Good | granite gneiss |
| 24 | Ilupo | 26 | 4 | 103.68 | Good | granite gneiss |
| 25 | Imesi | 46.6 | 8 | 114.05 | Good | quartz-schist |
| 26 | Ijero-Ekiti | 80 | 8.1 | 304.99 | Good. | quartz-schist |
| 27 | Aramoko-Ekiti | 48 | 14.61 | 160.70 | Good | granite gneiss |
| 28 | Ogotun-Ekiti | 92 | 2 | 129.6 | Good | granite |
| 29 | Iloro-Temidire | 38 | 9.1 | 95.04 | Good | granite |
| 30 | Soso | 31.4 | 8.7 | 98.49 | Good | granite |
| 31 | Itawure | 21.3 | 5.7 | 95.04 | Good | quartzite |
| 32 | Ado-Ekiti | 74 | 2.7 | 191.81 | Good | granite |
| 33 | Ifaki | 40 | 18 | 69.12 | Poor | migmatite |
| 34 | Ijero(palace) | 50 | 6 | 69.12 | Poor | quartz-schist |
| 35 | Ipoti | 50 | 1.7 | 53.57 | Poor | migmatite |
| 36 | Epe | 31 | 12 | 69.12 | Poor | migmatite |
| 37 | Are | 40 | 4.6 | 34.56 | Poor | migmatite |
| 38 | Iworoko | 42 | 5 | 43.2 | Poor | migmatite |
| 39 | Ipoti | 50 | 11.8 | 51.84 | Poor | migmatite |
| 40 | Erinjiyan | 40 | 10 | 43.2 | Poor | quartzite |
| 41 | Igede-Ekiti | 72 | 1.3 | 114.91 | Poor | granite |

| | | | | | | |
|---|---|---|---|---|---|---|
| 42 | Orin farm settlement | 60 | 12.4 | 8.64 | poor | charnockite |
| 43 | Aba Igbira | 37.8 | 13.9 | 17.28 | poor | migmatite |
| 44 | MGHS Ifaki | 59 | 1 | 86.4 | poor | migmatite |
| 45 | Ofale community | 50 | 11 | 11.23 | poor | migmatite |
| 46 | Ipao CHC | 25.5 | 2.9 | 21.6 | poor | migmatite |
| 47 | Eda-Ile | 54.7 | 12.3 | 31.10 | poor | migmatite |
| 48 | Ilasa | 46.6 | 6.2 | 27.65 | poor | migmatite |
| 49 | Kajola | 30 | 7.2 | 17.28 | poor | migmatite |
| 50 | Ipole Iloro | 43.5 | 9.2 | 11.23 | poor | migmatite |
| 51 | Ipoti-Ekiti | 72 | 13.97 | 95.90 | poor | granite |
| 52 | Igede-Ekiti | 72 | 1.33 | 114.91 | Poor | granite |
| 53 | Otun-Ekiti | 72 | 3.89 | 102.81 | poor | migmatite |
| 54 | Ilawe-Ekiti | 89 | NN | 86.4 | poor | granite |
| 55 | Usi-Ekiti | 80 | 10.63 | 64.8 | poor | charnockite |
| 56 | Iyin-Ekiti | 72 | 9.15 | 26.78 | poor | granite |
| 57 | Ilogbo-Ekiti | 70 | 4.85 | 44.06 | poor | migmatite |
| 58 | Iworoko-Ekiti | 78 | 3.5 | 120.09 | poor | migmatite |
| 59 | Ire-Ekiti | 74 | 12.8 | 28.512 | poor | migmatite |
| 60 | Ijan-Ekiti | 70 | 1.9 | 40.61 | poor | charnockite |
| 61 | Igogo-Ekiti | 46 | 1.33 | 40.61 | poor | migmatite |
| 62 | Usi-Ekiti | 80 | 10.63 | 64.8 | poor | migmatite |
| 63 | Ajebandele | 41.5 | 3 | 17.28 | poor | migmatite |
| 64 | Ikogosi | 42 | 14.4 | 103.68 | poor | quarzite |
| 65 | Irare Fulani | 46.1 | NN | 36.29 | poor | migmatite |
| 66 | Irare community | 48.4 | 6.1 | 8.64 | poor | migmatite |
| 67 | Ogunnire School | 29 | 8.5 | 8.64 | poor | charnockite |
| 68 | Obalatan | 50.6 | 4.5 | 8.64 | poor | charnockite |
| 69 | EKSC Ayede | 23.4 | 2.1 | 21.6 | poor | migmatite |

Source: Federal Ministry of Water Resources, Lagos, Nigeria and Benin/Owena River Basin Development Authority, Ikere- Ekiti, Nigeria
NN: Not known
BHD: Borehole depth
SWL: Static water level
GWZ: Groundwater zones

Further evaluations revealed low correlation ($r$ = 0.37) between well yield and well depth suggesting that well yield depends on aquifer characteristics such as porosity, permeability and fracture system rather than depth. This is consistent with the frequency distribution of well depth with respect to groundwater potential zones (Figure 13) revealed that well yield is not controlled by depth due to the fact that wells with depth >40 m are more represented in the poor groundwater potential zone. This is a clear indication of the localized nature of weathered basement aquifer in the study area. Nonetheless, the frequency diagram of well yield distribution (Figures 14) support the early observation because wells with low yield (<50 $m^3$/d) are predominant in the poor groundwater potential zone and minimal in the good to moderately good groundwater potential zone. Thus the frequency of occurrence of high yielding wells decreases from very good groundwater potential zone to poor groundwater potential zone in agreement with the GIS evaluation of the groundwater potential of the study area.

Further evidence to support this observation is the fact that the shallowest well with depth of 21.3 m located on quartzite has a yield of 95.04 $m^3$/d well with depth of 89.0 m on a granite bedrock has a yield of 86.4 $m^3$/d. This scenario is an indication of the tendency of the unqualified local driller to drill deeper in the hard granitic and migmatite bedrocks with the hope of intersecting fractures at deeper depth. The is an indication of lack of adequate knowledge of the hydrogeological settings by these local unqualified drillers as the assumption is not always applicable in such Basement bedrock setting hence the need to use professionally trained drillers in the drilling exercise not only reduce cost but also to ensure sustainable groundwater exploitation.

## SUMMARY AND CONCLUSIONS

This study provides an integrated RS/GIS approach to groundwater potential zonation in Ekiti Basement terrain to serve as a guide for groundwater exploration and development in the study area. As part of the study approach, thematic maps were prepared and susequently integrated using Arc GIS 9.1 software to produce groundwater potential map of the study area.

The groundwater potential assessment revealed;

1) That the very good groundwater potential zones are located mainly in the south-eastern part of the study area with an area extent of 1 241.64 $km^2$ representing 21.15 % coverage. Also, the good to moderately good groundwater potential zones are concentrated in the north-

eastern and south-western parts of the study area. These zones have an area extent of 868.97 km$^2$ representing 6.12 % coverage. However, the poor groundwater potential zone with an area extent of 3 759.83 km$^2$ represents 64.04 % coverage and is variably located in the remaining portions of the study area.

2) That the very good potential groundwater zone is undelain mostltly by granitic/ charnockitic rocks while the good to moderately good groundwater potential zone is covered by quartzite/quartz-schist, granite and charnockitic rocks. The poor groundwater potential zone, however, are underlain by predominantly by migmatite/ migmatite gneiss bedrock with few charnockite and granitic rock units.
3) That fractures on the migmatite bedrocks are poorly developed with thin overburden thickness accounting for the poor groundwater occurrence in this terrain. However, the relatively moderate to thick weathered overburden units characterized the quartzite and granitic bedrocks where greater proportion of high yield (>100 m$^3$/d) are located.
4) That yield is not controlled by well depth as wells with depth >40 m are more represented in the poor groundwater potential zone compared to very good and good to moderately good groundwater potential zones. This is a clear indication of the localized nature of weathered basement aquifer in the study area.
5) That superimposition of existing groundwater yield data on the deciphered groundwater potential zones revealed more frequent occurrence of high to medium yield wells in the favourable groundwater potential zones which support the result of integrated GIS thematic maps.

In summary the overall asssessment as presented in this study highlight that mapping of groundwater potential using integrated RS/GIS approach could be an effective means of charcaterization of groundwater potential zones as well as serving as a usuful tool and guide in groundwaer exploration and development in the study area. However, further geophysical investigation to determine the aquifer characteristics and the overburden thickness of various groundwater potential zones highlighted is recommended to compliment the present study.

## References

Ademilua, O. L. & Olorunfemi, M. O. (2000): Geoelectric/Geology estimation of the groundwater potential of the Basement Complex area of Ekiti and Ondo States, Nigeria. *Journal of Techno science.* Vol. 4, pp. 4–20.

Burrough, P. A. (1986): Principles of Geographical Information Systems for

Land Resource aassessment. Clarendon Press, Oxford, U. K.

Gustafsson, P. (1993): High Resolution Satellite Data and GIS as a Tool for Assessment of the Groundwater Potential of a Semi-Arid Area. *Proceedings of the Ninth Thematic Conference on Geologic Remote sensing*. Vol. 1, pp. 609–619.

Gustafsson, P. (1994): Spot satellite data for exploration of fractured aquifers in a semi-arid area in south eastern Botswana. *Applied Hydrogeology J. Vol.* 2, pp. 9–18.

Jain, P. K. (1998): Remote sensing techniques to locate ground water potential zones in upper Urmil River basin, district Chatarpur-central India. *J Ind Soc Remote Sens. Vol.* 26, No. 3, pp. 135–47.

Krishnamurthy, J. N., Venkatesa, K., Jayaraman, V. & Manivel, M. (1996): An approach to demarcate ground water potential zones through remote sensing and geographical information system. *Int J Remote Sens. Vol.* 17, pp. 1867–1884.

Matheis, G. (1987): Nigeria Rare Metal Pegmatites and their lithologic framework. *Geol. Journ.* Vol. 22, pp. 271–291.

Oloruniwo, M. A. & Olorunfemi, M. O. (1987): Geophysical investigation for groundwater in Precambrian terrains: a case study from Ikare. Southwestern Nigeria. *Journal of African Earth Sciences. Vol.* 6, No. 6, pp.787–796.

Oyinloye, A. O. & Ademilua, O. L. (2005): The nature of aquifer in the crystalline basement rocks of Ado-Ekiti, Igede-Ekiti and Igbara-Odo areas, southwestern Nigeria. *Pak. J. sci. Ind. Res. Vol.* 48, No. 3, pp. 154–161.

Prasad, R. K., Mondal, N. C., Banerjee, Pallavi, Nandakumar, M. V. & Rao, N. Subba (2006): Groundwater potential index in a crystalline terrain using remote sensing data. *Environmental Geology. Vol.* 50, pp. 1067–1076.

Prasad, R. K., Mondal, N. C., Banerjee, Pallavi, Nandakumar, M. V. & Singh, V. S. (2008): Deciphering potential groundwater zone in hard rock through the application of GIS. *Environ. Geol.* Vol. 55, pp. 467–475.

Reboucas, A. C. & Cavalcante, I. N. (1989). Hydrogeology of crystalline rocks in Brazil. In groundwater exploration and development in crystalline basement aquifers. (Proceedings, Zimbabwe, 15–24 June, 1987, vol.1 sessions 1–5), *Commonwealth Science Council, Pall Mall, London:* 103–126.

Saraf, A. & Choudhary, P. R. (1998): Integrated remote sensing and GIS for ground water exploration and identification of artificial recharge site. *Int J Remotes sense*. Vol. 19, pp.1825–1841.

Singh, V. S. (2008): Deciphering potential groundwater zone in hard rock through the application of GIS. *Environ Geol.* Vol. 55, pp. 467–475.

Srinivasa, Rao Y. & Jugran, K. D. (2003): Delineation of groundwater potential zones and zones of groundwater quality suitable for domestic purposes using remote sensing and GIS *Hydrogeol. Sci. J. Vol.* 48, pp. 821–833.

USGS – General Interest Publication "Groundwater" – retrieved from http://pubs.usgs.gov/edu/waterdistribution.html.

# Influence of the heat treatment and extrusion process on the mechanical and microstructural properties of the AISi1MgMn Alloy

# Vpliv toplotne obdelave in postopka iztiskanja na mehanske in mikrostrukturne lastnosti zlitine AISi1MgMn

Matej Steinacher[1], Vukašin Dragojević[2] & Anton Smolej[1]

[1]University of Ljubljana, Faculty of Natural Science and Engineering, Department for Materials and Metallurgy, Aškerčeva 12, Ljubljana, Slovenia
[2]Impol, Aluminium Industry, Slovenska Bistrica, Slovenia

*Corresponding author. E-mail: matej.steinacher@omm.ntf.uni-lj.si

**Received:** August 17, 2011 **Accepted:** November 2, 2011

**Abstract:** The paper describes the influence of homogenization temperatures (480 °C/5 h and 560 °C/6 h), methods of cooling rate after homogenization annealing and various extrusion processes (conventional extrusion K, press-quenching PQ, billet quenching BQ) upon the microstructural and mechanical properties of AlSi1MgMn (AA6082) alloy at industrial producing conditions. The mechanical properties of extruded rods from homogenized billets at 560 °C/6 h are higher after the extrusion processes PQ and BQ than the mechanical properties of the rods from homogenized billets at lower temperature. The rods, produced by process K, have higher tensile stress and yield stress in comparison to processes PQ and BQ. The reason is the distribution of $Mg_2Si$ phase during the homogenization annealing and subsequent BQ and PQ treatment of the alloy.

**Povzetek:** Članek opisuje vpliv homogenizacijskega žarenja (480 °C/5 h in 560 °C/6 h), način ohlajanja po homogenizacijskem žarenju in različne postopke iztiskanja (navadno iztiskanje K, gašenje na iztiskalnici PQ in gašenje okroglic BQ) na mikrostrukturne in mehanske lastnosti zlitine AlSi1MgMn (AA6082), ki je bila izdelana in predelana v industrijskih razmerah. Mehanske lastnosti palic iz drogov, homogeniziranih pri 560 °C/6 h in iztiskanih po postopkih PQ in BQ, so viš-

*Preliminary notes*

je kot mehanske lastnosti palic iz drogov, homogeniziranih pri nižji temperaturi. Palice, ki so bile izdelane po tehnologiji K, imajo višje mehanske lastnosti v primerjavi s postopkoma PQ in BQ. Vzrok je porazdelitev faze $Mg_2Si$ med homogenizacijskim žarenjem in nadaljnjo BQ- in PQ-obdelavo zlitine.

**Key words:** AlSi1MgMn alloy, homogenization, extrusion
**Ključne besede:** zlitina AlSi1MgMn, homogenizacija, iztiskanje

## INTRODUCTION

Investigated AlSi1MgMn alloy belongs to the AA6xxx (AlMgSi) series of aluminium alloys, where magnesium and silicon are the principal alloying elements. The commercial alloys of this type contain the mass fractions 0.5 % to 1.5 % of Si and 0.5 % to 1.5 % of Mg and are used in great quantities and they are universal aluminium alloys which can be extruded into sections, rods and tubes. Their characteristics are high workability, strength properties, corrosion resistance and machinability. Their mechanical and technological properties depend on the chemical composition and heat treatment of castings i. e. cast blanks and extruded pieces.[1, 2]

Heat treatment of castings consists of the homogenization annealing where principal factors are temperature and time of annealing, and the cooling rate of material to the ambient temperature. The way of cooling influences the precipitation of those alloying elements which are in solid solution during the homogenization annealing. The size and the distribution of secondary precipitates influence the stress required for deformation, extrusion rate, surface quality, and mechanical properties of extruded pieces. Optimal properties of semiproducts depend also on the reheating of homogenized castings to the temperature of the extrusion process.[2]

The influence of the cooling after the homogenization on the extrusion rate was widely investigated, but findings were often controversial.[3–8] It is known that $Mg_2Si$ precipitates have to be fine and uniformly distributed in the matrix.[8]

The conventional extrusion process of the alloy includes the homogenization annealing of as-cast billets, cooling from the annealing temperature by air fans (H) or by water sprays (HP), heating to the forming temperature, extrusion, separated solution treatment in the salt bath, quenching, and artificial aging.[9] Recently, the development of the extrusion of the 6xxx series alloys combined different technological

processes. The processes of separated solution annealing and quenching were replaced by the press-quenching process (PQ). This process contains extrusion and quenching on the extrusion press. Due to its reduced number of operations and efficiency of working heat, this process has great economic and ecological advantages.

The billet quenching process (BQ) is an upgrade of extrusion process PQ and includes the technological processes of preheating above the solvus temperature and cooling billets with water sprays to the forming temperature. At the preheating of billets above the solvus temperature, the $Mg_2Si$ phase dissolves in the solid solution. During cooling of billets with water sprays to the forming temperature, the $Mg_2Si$ phase does not precipitate and so all the Mg and Si remain in the solid solution. The extrusion process BQ includes the following technological processes the homogenization annealing of as-cast billets, cooling from the annealing temperature by air fans or by water sprays, preheating of billets above the solvus temperature, cooling with water sprays to the forming temperature, extrusion, quenching on the extrusion press and artificial aging. The new extrusion process BQ was first used for extrusion of Al-Cu alloys.[10, 11]

The present paper describes the influence of the homogenization annealing and the modified billet-quenching process (BQ process) on the microstructual and mechanical properties of the AlSi1MgMn alloy. The BQ process includes the preheating of billets before extrusion above the solvus temperature with subsequent water cooling to the forming temperature. The comparison of BQ process was made at various forming temperatures and extrusion rates with the extrusion processes K and PQ.

## Experimental procedure

The tested alloy was semicontinuously casted with HotTop-AirSlip system into billets with diameter of 228 mm, Table 1. The billets were in the first example homogenization annealed 5 h at 480 °C and in the second example 6 h at 560 °C in the gas furnace at industrial conditions. Cooling after the completed annealing was achieved by two cooling rates: ≈116.6 °C/min (water sprays, HP) and ≈200 °C/h (air fans, H). Then the billets were cut, tested with X-ray and extruded (20 MN direct press machine) into rods (diameter 20 mm) at various extrusion processes (K, PQ and BQ), Figure 1.

At the extrusion process BQ, the billets were preheated above the solvus temperature and cooled with water sprays to the forming temperature. Preheating time of the billets above the solvus temperature was 6 min and cooling times were 4 s, 8

**Table 1.** Chemical composition of investigated alloy (*w*/%)

| Si | Fe | Cu | Mn | Mg | Cr | Zn | Ti | Pb | Bi | Al |
|---|---|---|---|---|---|---|---|---|---|---|
| 0.8599 | 0.2022 | 0.0236 | 0.4778 | 0.6911 | 0.0547 | 0.0220 | 0.0286 | 0.0032 | 0.0019 | rest |

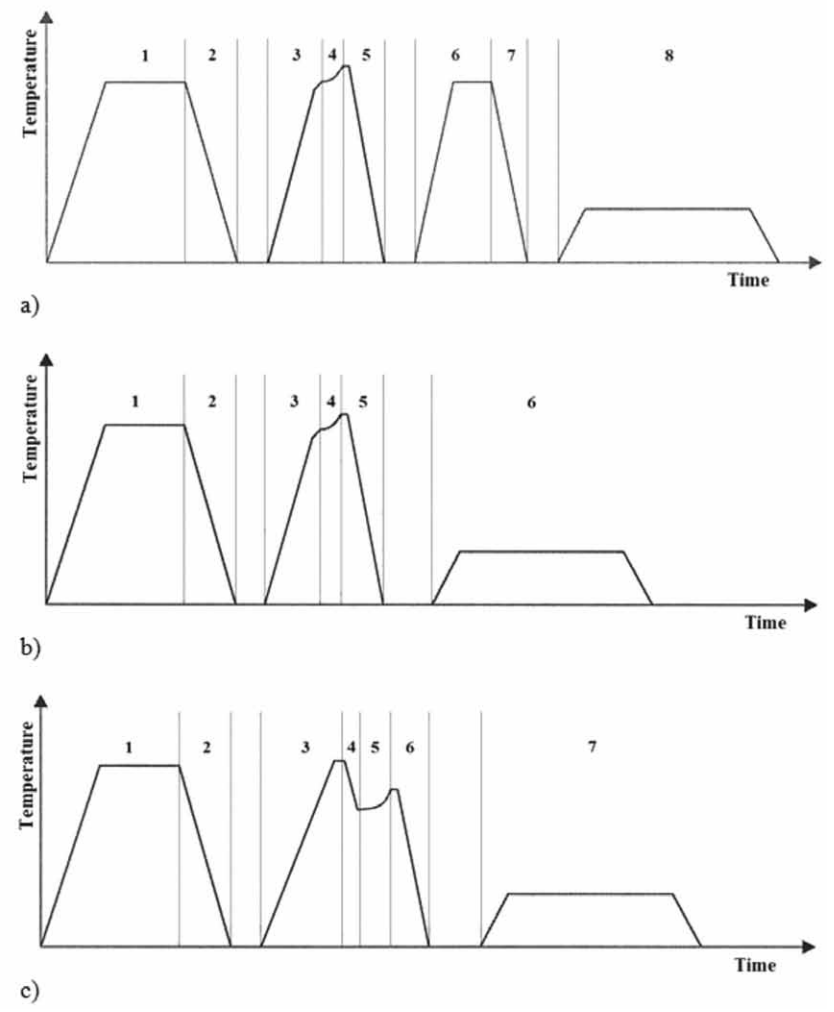


**Figure 1.** Scheme of the extrusion processes a) conventional, K (1-homogenization, 2-cooling, 3-reheating, 4-extrusion, 5-cooling, 6-solution treatment, 7-quenching and 8-artifical aging), b) press-quenching, PQ (1-homogenization, 2-cooling, 3-reheating, 4-extrusion, 5-quenching and 6-artifical aging) and c) billet-quenching, BQ (1-homogenization, 2-cooling, 3-preheating above the solvus temperature, 4-cooling to the forming temperature, 5-extrusion, 6-quenching and 7-artificial aging)

s, 12 s and 16 s. After the quenching on the extrusion press, the rods were artificially aged for 16 h at 150 °C.

Mechanical properties were tested by Zwick Z 400 tensile testing machine and Brinell hardness number by Zwick ZHU250. Microstructures were analyzed by JEOL JSM-5610 scanning electron microscope and Leica MEF4M optical microscope.

## Results and discussion

### *Mechanical properties*

At extrusion process K, the rods exceed mechanical properties specified by EN standard to heat treatment T6, because the extrusion process K is similar to the heat treatment T6, Table 2. The rods from the homogenized billets at the temperature of 480 °C/5 h have higher values of $R_m$ and $R_{p0.2}$ for 2 %, same values of HB and lower values $A_5$ for 7 % than the rods from the homogenized billets at the temperature of 560 °C/6 h, Figure 2.

At extrusion process PQ, the rods from the homogenized billets at the temperature of 480 °C/5 h, have lower values of $R_m$ for 3 %, HB for 2 %, $A_5$ for 12 % and higher values of $R_{p0.2}$ for 3 % than the rods from the homogenized billets at the temperature of 560 °C/6 h, Figure 2.

At extrusion process BQ, the rods from the homogenized billets at the temperature 480 °C/5 h, have lower values of $R_m$ for 6 %, $R_{p0.2}$ for 2 %, $A_5$ for 8 % and *HB* for 2 %, than the rods from the homogenized billets at the temperature of 560 °C/6 h. The extruded temperatures of billets after cooling do not have significant effect on the mechanical properties, Figure 2.

The rods, extruded with process K, have higher values of $R_m$ for 5 %, $R_{p0.2}$ for 13 % and lower values of $A_5$ and HB for 8 % then the rods extruded with process PQ and BQ. The impact of homogenization annealing on the mechanical properties is very questionable at the extrusion process K, because process K contains of separated soluble annealing in salt bath and quenching in water. During the separated soluble annealing in salt bath at the temperature of 525 °C the whole $Mg_2Si$ phase dissolves in the solid solution. Therefore the rods have higher

**Table 2.** Prescribed mechanical properties of the alloy AlSi1MgMn after the heat treatment T6[12]

| $R_m$/(N mm$^{-2}$) | $R_{p0.2}$/(N mm$^{-2}$) | HB | $A_5$/% |
|---|---|---|---|
| min. 310 | min. 260 | 85 | 8 |

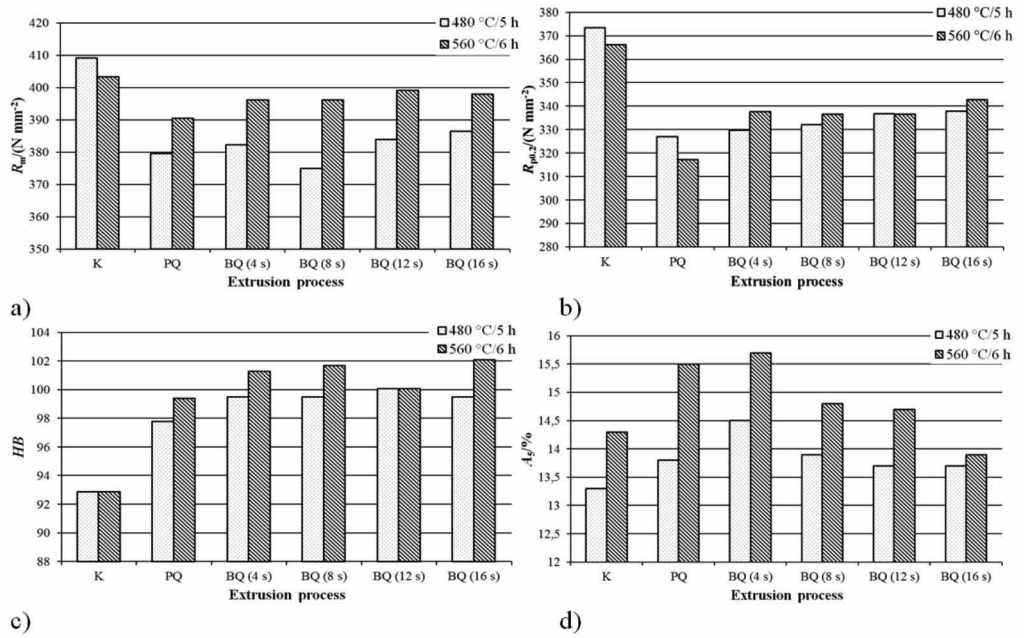


**Figure 2.** Mechanical properties of the extruded rods at different extrusion processes a) tensile strength, $R_m$, b) yield stress, $R_{p0.2}$, c) Brinell hardness, HB and d) elongation, $A_5$

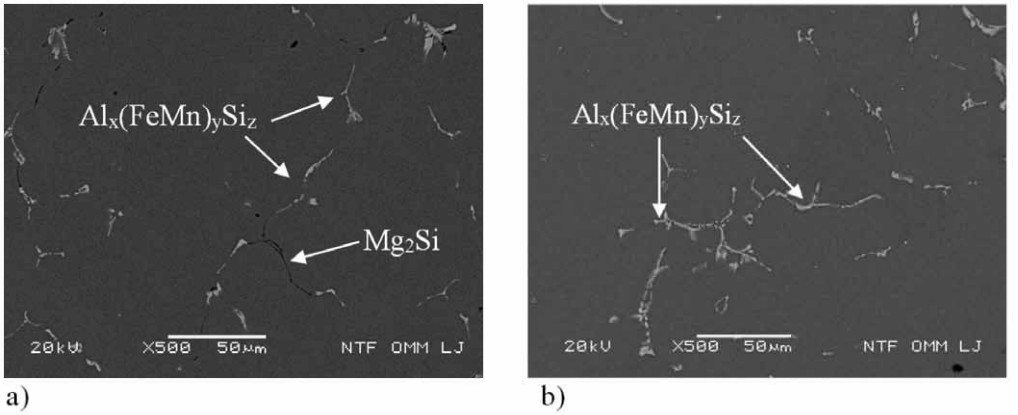


**Figure 3.** Back scattered electron micrographs of a) homogenized alloy at temperature of 480 °C/5 h and b) homogenized alloy at temperature of 560 °C/6 h

mechanical properties. The methods of cooling after homogenization annealing (H or HP) do not affect mechanical properties of the rods, Figure 2.b)

***Microstructural properties***

Microstructure of as cast billets is composed of matrix $\alpha_{Al}$ and intermetallic phases $Mg_2Si$ and $Al_x(FeMn)_ySi_z$. The

$Mg_2Si$ phase does not fully dissolve in the solid solution during homogenization annealing at the temperature of 480 °C/5 h, Figure 3 a. Therefore all Si and Mg can not contribute at precipitation hardening. At homogenizing temperature of 560 °C/6 h the $Mg_2Si$ phase fully dissolves, Figure 3 b, while the $Al_x(FeMn)_ySi_z$ phase does not change during homogenization annealing.

Distributions of the eutectic and iron-enriched phases are similar in all rods and they are oriented in the direction of extrusion, Figure 4.

The rods that were soluble annealed in salt bath (process K) have edge zone, this is recrystallized zone on the surface of rods, Figure 5 a. Size of the edge zone is up to 3.5 mm. Solution anneal in salt bath and quenching in water increase the edge zone, because solution anneal courses above threshold of recrystallization. On the surface of rods occurs static recrystallization, because on the surface the degree of deformation is higher. During extrusion, courses process of dynamic recovery and consequently formation of subgrains. These subgrains brake static recrystallization. But on the surface of rods there are some places where static

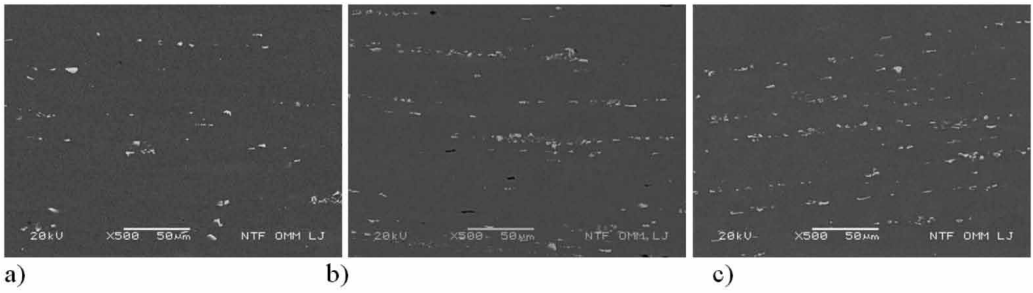


**Figure 4.** Back scattered electron micrographs of the extruded rods in longitudinal section from billets that were homogenized at the temperature of 480 °C/5 h a) process K, b) process PQ and c) process BQ (4 s)

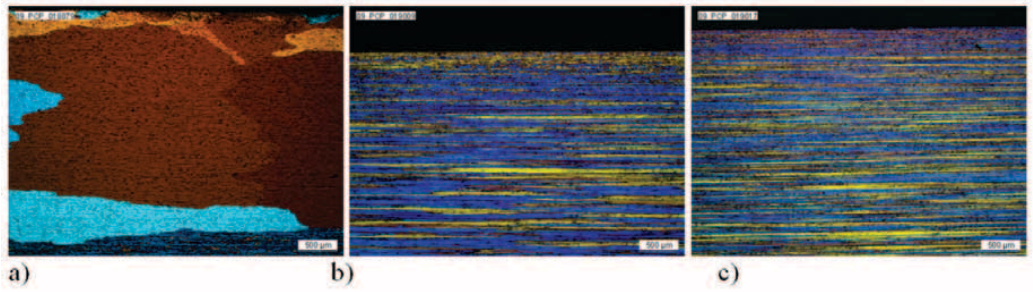


**Figure 5.** Polarized light micrographs of the extruded rods in longitudinal section a) process K, b) process PQ and c) process BQ (4 s)

recrystallization courses and causes formation of extremely large grains. At extrusion processes PQ and BQ, the rods do not have edge zone, Figure 5 b and c.

## Conclusions

Results show that the rods extruded with different processes K, PQ and BQ have similar mechanical properties. The homogenization annealing of the billets at lower temperature (480 °C/5 h) is unsuitable for investigated alloy, because the $Mg_2Si$ phase does not fully dissolve in the solid solution. The extrusion processes PQ and BQ have higher economic and ecological priority, than the process K. Process BQ was done at lower extrusion temperatures than processes K and PQ, therefore the speed of extrusion can be increased.

## References

[1] Totten, G. E. & Scott Mackenzie, D. (2003): Handbook of Aluminum: Physical metallurgy and processes, *New York, Basel,* Vol. 1, pp. 266–280.

[2] Smolej, A., Soković, M., Kopač, J. & Dragojević, V. (1995): Influence of heat treatment on the properties of the free-cutting AlMgSiPb alloy. *Journal of Materials Processing Technology.* Vol. 53, Is. 1–2, pp. 373–384.

[3] Raiso, O. (1992): The Effect of Compositional and Homogenisation Treatment on Extrudability of AlMgSi Alloys, In: *The Effect of Microstructure on the Extrudability of Some AlMgSi Alloys (Second Edition), Hydro Aluminium Sundalsöra,* pp. 31.

[4] Sperry, P. R. (1984): Correlation of Microstructure in 6XXX Extrusion Alloys with Process Variables and Properties, In: *Proceedings of Third International Aluminium Extrusion Technology Seminar (Second Edition), Atlanta*, Vol. 1, 21–29.

[5] Langerweger, J. (1982): Metallurgische Einflüsse auf Produktivität beim Strangpressen von AlMgSi-Werkstoffen. *Aluminium 58*. pp. 21.

[6] Marchive, D. (1983): High Extrudability Alloys in the 6000 Series. *Light Metal Age.* Vol. 41, Is. 3–4, pp. 6–10.

[7] Lang, G. & CASTLE, A. F. (1978): Effect of Rate of Cooling after Homogenisation on Direct-Extrusion Parameters of 6063 (Al-Mg-Si) Billet. *Metals Technology*. pp. 434–438.

[8] Hains, R. W. (1984): Press Quenching of Aluminium Alloys, *Proceedings of Third International Aluminium Technology Seminar (Second Edition)*, *Atlanta*, Vol. 1, pp. 81.

[9] Sheppard, T. (1999): Extrusion of Aluminium Alloys, *Kluwert Academic Publishers, Dordrecht,* pp. 420.

[10] Barbič, R. (2009): The Effect of In-

tensive Billet Cooling on Press Quenching and Properties of Al-Cu Alloys, *Doctoral thesis, University of Ljubljana, Faculty of Natural Sciences and Engineering, Department for Materials and Metallurgy, Ljubljana*.

[11] Barbič, R., Dragojević, V. & Smolej, A. (2010): Billet quenching extrusion process as efficient and reliable replacement for conventional extrusion of Al-Cu alloys. *Materials Science and Technology.* Vol. 26, No. 1, pp. 58–65.

[12] Europäisches KOmitte für Normung, Aluminium und Aluminiumlegirungen-Stranggepresste Stangen, *Rohren und Profile-Teil 2: Mechanische Eingeschaften*, 1997, EN 755-2.

# Petdeset let delovanja Metalurškega instituta “Kemal Kapetanović” v Zenici

Dne 25. oktobra se je na Metalurškem institutu "Kemal Kapetanović" v Zenici odvijal slavnostni dogodek – praznovanje 50-letnice delovanja.

Metalurški institut "Kemal Kapetanović" v Zenici deluje kot znanstvenoraziskovalna institucija že polnih 50 let. Institut je bil osnovan v času, ko so intenzivna rast proizvodnje in tehnološke zahteve pri proizvodnji jekla pokazale, da je stopnja raziskav in razvoja presegla nivo, ki ga je do tedaj uspel zagotavljati Oddelek tehnične kontrole Železarne Zenica.

Na čelu s prof. dr. Kemalom Kapetanovićem, kot glavnim zagovornikom osnovanja instituta, je leta 1961 institut začel svoje delo. Institut je imel jasno vizijo, perspektivo ter potrebo po izpolnitvi velikih pričakovanj celotne tedanje družbe.

Velika pozornost je bila posvečena osnovnemu konceptu raziskovalnega dela. Prevladala je orientacija, da se institut prvenstveno osredini na področji aplikativnega in razvojnega dela za potrebe črne metalurgije, primarno pa za potrebe tedanje Železarne Zenica.

Ta koncept je omogočil institutu hitro vključevanje v reševanje problematike proizvodnje, po orientaciji in programu dela pa ni prihajal v kolizijo z drugimi raziskovalnimi centri v bivši skupni državi. Za tako opredelitev je imel institut svetle vzore v zahodnoevropskih državah z visoko razvito metalurgijo, kot so npr. Nemčija, Avstrija, Švedska, ...

Metalurški institut "Kemal Kapetanović" si je pridobil velik ugled tako v poslovnem kot tudi političnem svetu. Vključevanje v številne pomembne projekte zunaj Bosne in Hercegovine je v tem času afirmiralo institut ne samo na področju bivše skupne države, temveč tudi širše. Vzpostavljeni so bili številni kontakti s priznanimi svetovnimi institucijami znanja, kar je močno prispevalo k dvigu ugleda instituta.

S ciljem prilagoditi se tedanjim sistemskim zakonom in zahtevam trga je institut leta 1991 z izdajo internih delnic začel aktivnosti pri reorganizaciji instituta kot delniške družbe z mešanim lastništvom. Težko obdobje po neljubih dogodkih na

tleh bivše skupne države je institutu prinesel nove preizkušnje v boju za obstanek. Človeški viri, kot ključni vir znanstvenoraziskovalne institucije, so se v tem času izredno oslabili, predvsem zaradi izredno slabih razmer za delo in edukacijo. Novi časi so prinesli spremembe, ki so imele pomemben vpliv na delo in politiko instituta. Sprememba družbenega sistema, načina poslovanja oziroma prehoda iz planskega na tržno gospodarstvo je prisilil institut v borbo za lastni obstoj. Institut je v tem času pokazal svojo pravo moč in našel pot preživetja s spremljanjem potreb trga ter prilagoditvijo njegovim zahtevam, predvsem pri utrjevanju poslovnih odnosov s srednjimi in majhnimi podjetji ter reševanju njihovih problemov. V tej smeri je bila leta 1997 sprejeta odločitev o začetku projekta uvajanja sistema menedžmenta kakovosti v laboratorije instituta v skladu s standardom EN 45001 ter o gradnji internetne mreže.

V obdobju 1998 do 2006 se je pomembno povečala vloga in pomen instituta za gospodarstvo Bosne in Hercegovine. Institut je pridobil prve akreditacije svojih laboratorijev v skladu z evropskimi standardi, povečal se je interes majhnih in

**Slika 1.** Praznovanje 50-letnice Metalurškega instituta "Kemal Kapetanović"

srednje velikih podjetij za delo in storitve instituta tako v Bosni in Hercegovini kot tudi širše, prav tako se je obnovilo tudi prekinjeno sodelovanje z velikimi poslovnimi sistemi.

Zeniško-dobojski kanton je konec leta 2006 kot lastnik kapitala prevzel pravice in obveznosti ustanovitelja Metalurškega instituta "Kemal Kapetanović" ter potrdil njegov status organizacijske enote Univerze v Zenici. Tako se je institut vključil v visokošolsko institucijo s ciljem povezave znanstvenoraziskovalnega dela, izobraževanja in gospodarstva.

Leto 2011 pomeni za institut petdeset let njegovega obstoja in delovanja. Glede na razmere in okolje, v katerem je deloval in deluje še danes, lahko rečemo, da je bil zelo uspešen. Z gotovostjo lahko zapišemo, da je Metalurški institut "Kemal Kapetanović" pustil pomemben pečat v obdobju 1961–2011. Pokazal je, da so moč znanja, volja in upornost nujni za razvoj družbe in gospodarstva.

Vizija instituta je nadaljevati tradicijo uspešnega poslovanja in obstanka v tem prostoru. Institut želi biti iniciator in nosilec razvoja ter uvajanja novih tehnologij in materialov, dviga kakovosti proizvodov ter konzultantska institucija predvsem za podjetja zeniško-dobojskega kantona. Institut želi v naslednjem obdobju pridobiti več državnih merilnih laboratorijev ter biti podpora Univerzi v Zenici pri vzgoji dodiplomskih in podiplomskih študentov ter mladih strokovnjakov iz industrije. S pridobitvijo mednarodnih akreditacij za določene laboratorijske storitve v letošnjem letu je institut ustvaril realne pogoje, da ponudi svoje znanje in storitve tudi zunaj Bosne in Hercegovine.

Institut je v zadnjih letih vzpostavil tudi pristne odnose na znanstvenoraziskovalnem in poslovnem področju s slovenskimi institucijami znanja ter podjetji.

Več informacij o Metalurškem institutu "Kemal Kapetanović" v Zenici lahko dobite na njihovi spletni strani www.miz.ba oziroma po elektronski pošti miz@miz.ba ter telefonu: 00 387 32 247 999 in faksu 00 387 247 980.

Borut Kosec, Univerza v Ljubljani, Naravoslovnotehniška fakulteta
Milenko Rimac, Metalurški institut "Kemal Kapetanović"

# Author`s Index, Vol. 58, No. 3


| | |
|---|---|
| Chen Jiawen | jiawen.chenn@gmail.com |
| Choubey V. K. | |
| Dragojević Vukašin | vukasin.dragojevic@impol.si |
| Gojić Mirko | gojic@simet.hr |
| Kanduč Tjaša | tjasa.kanduc@gmail.com |
| Kosec Borut | borut.kosec@omm.ntf.uni-lj.si |
| Kosec Ladislav | ladislav.kosec@ntf.uni-lj.si |
| Kožuh Stjepan | |
| Lamut Martin | martin.lamut@space.si |
| Lazić Ladislav | lazic@siscia.simet.hr |
| Purandara B. K. | purandarabk@yahoo.com |
| Rimac Milenko | |
| Smolej Anton | anton.smolej@omm.ntf.uni-lj.si |
| Steinacher Matej | matej.steinacher@omm.ntf.uni-lj |
| Talabi Abel O. | soar_abel@yahoo.com |
| Tijani Moshood N. | mn.tijani@mail.ui.edu.ng |
| Venkatesh B. | |
| Zavšek Simon | simon.zavsek@rlv.si |
| Žula Janja | janja.zula@rlv.si |

# INSTRUCTIONS TO AUTHORS

**RMZ-MATERIALS & GEOENVIRONMENT** (RMZ- Materiali in geookolje) is a periodical publication with four issues per year (established 1952 and renamed to RMZ-M&G in 1998). The main topics of contents are Mining and Geotechnology, Metallurgy and Materials, Geology and Geoenvironment.

**RMZ-M&G** publishes original Scientific articles, Review papers, Preliminary notes, Professional papers **in English**. In addition, evaluations of other publications (books, monographs,...), In memoriam, Professional remarks and reviews are welcome. The Title, Abstract and Key words in Slovene will be included by the author(s) or will be provided by the referee or the Editorial Office.

**** Additional information and remarks for Slovenian authors:***
*Only Professional papers, Publications notes, Events notes, Discussion of papers and In memoriam, will be exceptionally published in the Slovenian language.*

**Authorship and originality** of the contributions. Authors are responsible for originality of presented data, ideas and conclusions as well as for correct citation of data adopted from other sources. The publication in RMZ-M&G obligate authors that the article will not be published anywhere else in the same form.

## Specification of Contributions

*RMZ-M&G will publish papers of the following categories:*

*Full papers (optimal number of pages is 7 to 15, longer articles should be discussed with Editor prior to submission). An abstract is required.*

- **Original scientific papers** represent unpublished results of original research.
- **Review papers** summarize previously published scientific, research and/or expertise articles on the new scientific level and can contain also other cited sources, which are not mainly result of author(s).

- **Preliminary notes** represent preliminary research findings, which should be published rapidly.
- **Professional paper**s are the result of technological research achievements, application research results and information about achievements in practice and industry.

*Short papers (the number of pages is limited to 1 for Discussion of papers and 2 pages for Publication note, Event note and In Memoriam). No abstract is required for short papers.*

- **Publication notes** contain author's opinion on new published books, monographs, textbooks, or other published material. A figure of cover page is expected.
- **Event notes** in which descriptions of a scientific or professional event are given.
- **Discussion of papers (Comments)** where only professional disagreements can be discussed. Normally the source author(s) reply the remarks in the same issue.
- **In memoriam** (a photo is expected).

**Supervision and review of manuscripts.** All manuscripts will be supervised. The referees evaluate manuscripts and can ask authors to change particular segments, and propose to the Editor the acceptability of submitted articles. Authors can suggest the referee but Editor has a right to choose another. **The name of the referee remains anonymous.** The technical corrections will be done too and authors can be asked to correct missing items. The final decision whether the manuscript will be published is made by the Editor in Chief.

## The Form of the Manuscript

The manuscript should be submitted as a complete hard copy including figures and tables. The figures should also be enclosed separately, both charts and photos in the original version. In addition, all material should also be provided in electronic form on a diskette or a CD. The necessary information can conveniently also be delivered by E-mail.

## Composition of manuscript is defined in the attached Template

The original file of Template is available on RMZ-Materials and Geoenvironment Home page address:

**http://www.rmz-mg.com**

**References** - can be arranged in two ways:
- first possibility: alphabetic arrangement of first authors - in text: (Borgne, 1955), or
- second possibility: [1] numerated in the same order as cited in the text: example[1]

Format of papers in journals:

Le Borgne, E. (1955): Susceptibilite magnetic anomale du sol superficiel. *Annales de Geophysique*, 11, pp. 399–419.

Format of books:

Roberts, J. L. (1989): Geological structures, *MacMillan*, *London*, 250 p.

**Text** on the hard print copy can be prepared with any text-processor. The electronic version on the diskette, CD or E-mail transfer should be in MS Word or ASCII format.
**Captions of figures and tables** should be enclosed separately.
**Figures (graphs and photos)** and tables should be original and sent separately in addition to text. They can be prepared on paper or computer designed (MSExcel, Corel, Acad).
**Format.** Electronic figures are recommended to be in CDR, Al, EPS, TIF or JPG formats. Resolution of bitmap graphics (TIF, JPG) should be at least 300 dpi. Text in vector graphics (CDR, Al, EPS) must be in MSWord Times typography or converted in curves.
**Color prints.** Authors will be charged for color prints of figures and photos.
**Labeling** of the additionally provided material for the manuscript should be very clear and must contain at least the lead author's name, address, the beginning of the title and the date of delivery of the manuscript. In case of an E-mail transfer the exact message with above asked data must accompany the attachment with the file containing the manuscript.

**Information** about RMZ-M&G:
Editor in Chief prof. dr. Peter Fajfar (phone: ++386 1 4250-316) or
Secretary Barbara Bohar Bobnar, univ. dipl. ing. geol. (phone: ++386 1 4704-630),
Aškerčeva 12, 1000 Ljubljana, Slovenia
or at E-mail addresses:
peter.fajfar@ntf.uni-lj.si,
barbara.bohar@ntf.uni-lj.si

**Sending of manuscripts.** Manuscripts can be sent by mail to the **Editorial Office** address:

- RMZ-Materials & Geoenvironment
  Aškerčeva 12,
  1000 Ljubljana, Slovenia

or delivered to:

- **Reception** of the Faculty of Natural Science and Engineering (for RMZ-M&G)
  Aškerčeva 12,
  1000 Ljubljana, Slovenia
- E-mail - addresses of Editor and Secretary
- You can also contact them on their phone numbers.

*These instructions are valid from August 2009*

# NAVODILA AVTORJEM

**RMZ-MATERIALS AND GEOENVIRONMENT** (RMZ- Materiali in geookolje) – kratica RMZ-M&G - je revija (ustanovljena kot zbornik 1952 in preimenovana v revijo RMZ-M&G 1998), ki izhaja vsako leto v štirih zvezkih. V reviji objavljamo prispevke s področja rudarstva, geotehnologije, materialov, metalurgije, geologije in geookolja.

**RMZ- M&G objavlja izvirne znanstvene, pregledne in strokovne članke ter predhodne objave samo v angleškem jeziku. Strokovni članki so lahko izjemoma napisani v slovenskem jeziku.** Kot dodatek so zaželene recenzije drugih publikacij (knjig, monografij …), nekrologi In Memoriam, predstavitve znanstvenih in strokovnih dogodkov, kratke objave in strokovne replike na članke objavljene v RMZ-M&G v slovenskem ali angleškem jeziku. Prispevki naj bodo kratki in jasni.

**Avtorstvo in izvirnost** prispevkov. Avtorji so odgovorni za izvirnost podatkov, idej in sklepov v predloženem prispevku oziroma za pravilno citiranje privzetih podatkov. Z objavo v RMZ-M&G se tudi obvežejo, da ne bodo nikjer drugje objavili enakega prispevka.

## Vrste prispevkov

*Optimalno število strani je 7 do 15, za daljše članke je potrebno soglasje glavnega urednika.*
**Izvirni znanstveni članki** opisujejo še neobjavljene rezultate lastnih raziskav.
**Pregledni članki** povzemajo že objavljene znanstvene, raziskovalne ali strokovne dosežke na novem znanstvenem nivoju in lahko vsebujejo tudi druge (citirane) vire, ki niso večinsko rezultat dela avtorjev.
**Predhodna objava** povzema izsledke raziskave, ki je v teku in zahteva hitro objavo.
**Strokovni članki** vsebujejo rezultate tehnoloških dosežkov, razvojnih projektov in druge informacije iz prakse.
**Recenzije** publikacij zajemajo ocene novih knjig, monografij, učbenikov, razstav …(do dve strani; zaželena slika naslovnice in kratka navedba osnovnih podatkov - izkaznica).

**In memoriam** (do dve strani, zaželena slika).
**Strokovne pripombe** na objavljene članke ne smejo presegati ene strani in opozarjajo izključno na strokovne nedoslednosti objavljenih člankov v prejšnjih številkah RMZ-M&G. Praviloma že v isti številki avtorji prvotnega članka napišejo odgovor na pripombe.
**Poljudni članki**, ki povzemajo znanstvene in strokovne dogodke (do dve strani).

**Recenzije.** Vsi prispevki bodo predloženi v recenzijo. Recenzent oceni primernost prispevka za objavo in lahko predlaga kot pogoj za objavo dopolnilo k prispevku. Recenzenta izbere Uredništvo med strokovnjaki, ki so dejavni na sorodnih področjih, kot jih obravnava prispevek. Avtorji lahko sami predlagajo recenzenta, vendar si uredništvo pridržuje pravico, da izbere drugega recenzenta. **Recenzent ostane anonimen**. Prispevki bodo tudi tehnično ocenjeni in avtorji so dolžni popraviti pomanjkljivosti. Končno odločitev za objavo da glavni in odgovorni urednik.

## Oblika prispevka

Prispevek predložite v tiskanem oštevilčenem izvodu (po možnosti z vključenimi slikami in tabelami) ter na disketi ali CD, lahko pa ga pošljete tudi prek E-maila. Slike in grafe je možno poslati tudi risane na papirju, fotografije naj bodo originalne.

## Razčlenitev prispevka:

Predloga za pisanje članka se nahaja na spletni strani:

http://www.rmz-mg.com/predloga.htm

**Seznam literature** je lahko urejen na dva načina:
-po abecednem zaporedju prvih avtorjev ali
-po [1]vrstnem zaporedju citiranosti v prispevku.

Oblika je za oba načina enaka:
Članki:

> Le Borgne, E. (1955): Susceptibilite magnetic anomale du sol superficiel. *Annales de Geophysique*; Vol. 11, pp. 399–419.

Knjige:

ROBERTS, J. L. (1989): Geological structures, *MacMillan*, *London*, 250 p.

**Tekst** izpisanega izvoda je lahko pripravljen v kateremkoli urejevalniku. Na disketi, CD ali v elektronskem prenosu pa mora biti v MS Word ali v ASCII obliki.
**Naslovi slik in tabel** naj bodo priloženi posebej. Naslove slik, tabel in celotno besedilo, ki se pojavlja na slikah in tabelah, je potrebno navesti v angleškem in slovenskem jeziku.
**Slike** (ilustracije in fotografije) in tabele morajo biti izvirne in priložene posebej. Njihov položaj v besedilu mora biti jasen iz priloženega kompletnega izvoda. Narejene so lahko na papirju ali pa v računalniški obliki (MS Excel, Corel, Acad).
**Format** elektronskih slik naj bo v EPS, TIF ali JPG obliki z ločljivostjo okrog 300 dpi. Tekst v grafiki naj bo v Times tipografiji.
**Barvne slike.** Objavo barvnih slik sofinancirajo avtorji
**Označenost** poslanega materiala. Izpisan izvod, disketa ali CD morajo biti jasno označeni – vsaj z imenom prvega avtorja, začetkom naslova in datumom izročitve uredništvu RMZ-M&G. Elektronski prenos mora biti pospremljen z jasnim sporočilom in z enakimi podatki kot velja za ostale načine posredovanja.

**Informacije** o RMZ-M&G: urednik prof. dr. Peter Fajfar, univ. dipl. ing. metal. (tel. ++386 1 4250316) ali tajnica Barbara Bohar Bobnar, univ. dipl. ing. geol. (tel. ++386 1 4704630), Aškerčeva 12, 1000 Ljubljana
ali na E-mail naslovih:
peter.fajfar@ntf.uni-lj.si
barbara.bohar@ntf.uni-lj.si

**Pošiljanje prispevkov**. Prispevke pošljite priporočeno na naslov **Uredništva:**

- RMZ-Materials and Geoenvironment
  Aškerčeva 12,
  1000 Ljubljana, Slovenija

oziroma jih oddajte v

- **Recepciji** Naravoslovnotehniške fakultete (pritličje) (za RMZ-M&G)
  Aškerčeva 12,
  1000 Ljubljana, Slovenija
- Možna je tudi oddaja pri uredniku oziroma pri tajnici.

*Navodila veljajo od avgusta 2009.*

# TEMPLATE

## The title of the manuscript should be written in bold letters (Times New Roman, 14, Center)

## Naslov članka (Times New Roman, 14, Center)

Name Surname[1], …. , & Name Surname[X] (Times New Roman, 12, Center)

[x] University of ..., Faculty of ..., Address…, Country ... (Times New Roman, 11, Center)

*Corresponding author. E-mail: ... (Times New Roman, 11, Center)

**Abstract** (Times New Roman, Normal, 11): The abstract should be concise and should present the aim of the work, essential results and conclusion. It should be typed in font size 11, single-spaced. Except for the first line, the text should be indented from the left margin by 10 mm. The length should not exceed fifteen (15) lines (10 are recommended).

**Izvleček** (Times New Roman, navadno, 11): Kratek izvleček namena članka ter ključnih rezultatov in ugotovitev. Razen prve vrstice naj bo tekst zamaknjen z levega roba za 10 mm. Dolžina naj ne presega petnajst (15) vrstic (10 je priporočeno).

**Key words:** a list of up to 5 key words (3 to 5) that will be useful for indexing or searching. Use the same styling as for abstract.
**Ključne besede:** seznam največ 5 ključnih besed (3–5) za pomoč pri indeksiranju ali iskanju. Uporabite enako obliko kot za izvleček.

### Introduction (Times New Roman, Bold, 12)

Two lines below the keywords begin the introduction. Use Times New Roman, font size 12, Justify alignment.

There are two (2) admissible methods of citing references in text:

1. by stating the first author and the year of publication of the reference in the parenthesis at the appropriate place in the text and arranging the reference list in the alphabetic order of first authors; e.g.:
   "Detailed information about geohistorical development of this zone can be found in: Antonijević (1957), Grubić (1962), ..."
   "… the method was described previously (Hoefs, 1996)"
2. by consecutive Arabic numerals in square brackets, superscripted at the appropriate place in the text and arranging the reference list at the end of the text in the like manner; e.g.:
   "... while the portal was made in Zope environment. [3]"

## Materials and methods (Times New Roman, Bold, 12)

This section describes the available data and procedure of work and therefore provides enough information to allow the interpretation of the results, obtained by the used methods.

## Results and discussion (Times New Roman, Bold, 12)

Tables, figures, pictures, and schemes should be incorporated in the text at the appropriate place and should fit on one page. Break larger schemes and tables into smaller parts to prevent extending over more than one page.

## Conclusions (Times New Roman, Bold, 12)

This paragraph summarizes the results and draws conclusions.

## Acknowledgements (Times New Roman, Bold, 12, Center - optional)

This work was supported by the ****.

**References (Times New Roman, Bold, 12)**

In regard to the method used in the text, the styling, punctuation and capitalization should conform to the following:

FIRST OPTION - in alphabetical order

Casati, P., Jadoul, F., Nicora, A., Marinelli, M., Fantini-Sestini, N. & Fois, E. (1981): Geologia della Valle del'Anisici e dei gruppi M. Popera - Tre Cime di Lavaredo (Dolomiti Orientali). *Riv. Ital. Paleont.*; Vol. 87, No. 3, pp. 391–400, Milano.

Folk, R. L. (1959): Practical petrographic classification of limestones. *Amer. Ass. Petrol. Geol. Bull.;* Vol. 43, No. 1, pp. 1–38, Tulsa.

SECOND OPTION - in numerical order

[1] Trček, B. (2001): *Solute transport monitoring in the unsaturated zone of the karst aquifer by natural tracers.* Ph. D. Thesis. Ljubljana: University of Ljubljana 2001; 125 p.

[2] Higashitani, K., Iseri, H., Okuhara, K., Hatade, S. (1995): Magnetic Effects on Zeta Potential and Diffusivity of Nonmagnetic Particles. *Journal of Colloid and Interface Science, 172*, pp. 383–388.

Citing the Internet site:

CASREACT-Chemical reactions database [online]. Chemical Abstracts Service, 2000, updated 2. 2. 2000 [cited 3. 2. 2000]. Accessible on Internet: http://www.cas.org/CASFILES/casreact.html.

**Texts in Slovene (title, abstract and key words) can be written by the author(s) or will be provided by the referee or by the Editorial Board.**

# PREDLOGA ZA SLOVENSKE ČLANKE

## Naslov članka (Times New Roman, 14, Na sredino)

## The title of the manuscript should be written in bold letters (Times New Roman, 14, Center)

Ime Priimek[1], …, Ime Priimek[X] (Times New Roman, 12, Na sredino)

[X]Univerza…, Fakulteta…, Naslov…, Država… (Times New Roman, 11, Center)

*Korespondenčni avtor. E-mail: ... (Times New Roman, 11, Center)

**Izvleček** (Times New Roman, Navadno, 11): Kratek izvleček namena članka ter ključnih rezultatov in ugotovitev. Razen prve j bo tekst zamaknjen z levega roba za 10 mm. Dolžina naj ne presega petnajst (15) vrstic (10 je priporočeno).

**Abstract** (Times New Roman, Normal, 11): The abstract should be concise and should present the aim of the work, essential results and conclusion. It should be typed in font size 11, single-spaced. Except for the first line, the text should be indented from the left margin by 10 mm. The length should not exceed fifteen (15) lines (10 are recommended).

**Ključne besede:** seznam največ 5 ključnih besed (3–5) za pomoč pri indeksiranju ali iskanju. Uporabite enako obliko kot za izvleček.
**Key words:** a list of up to 5 key words (3 to 5) that will be useful for indexing or searching. Use the same styling as for abstract.

### Uvod (Times New Roman, Krepko, 12)

Dve vrstici pod ključnimi besedami se začne Uvod. Uporabite pisavo Times New Roman, velikost črk 12, z obojestransko poravnavo. Naslovi slik in tabel (vključno z besedilom v slikah) morajo biti v slovenskem jeziku.

**Slika (Tabela) X.** Pripadajoče besedilo k sliki (tabeli)

Obstajata dve sprejemljivi metodi navajanja referenc:

1. z navedbo prvega avtorja in letnice objave reference v oklepaju na ustreznem mestu v tekstu in z ureditvijo seznama referenc po abecednem zaporedju prvih avtorjev; npr.:

"Detailed information about geohistorical development of this zone can be found in: Antonijević (1957), Grubić (1962), ..."

"… the method was described previously (Hoefs, 1996)"

ali

2. z zaporednimi arabskimi številkami v oglatih oklepajih na ustreznem mestu v tekstu in z ureditvijo seznama referenc v številčnem zaporedju navajanja; npr.;

"... while the portal was made in Zope[3] environment."

## Materiali in metode (Times New Roman, Krepko, 12)

Ta del opisuje razpoložljive podatke, metode in način dela ter omogoča zadostno količino informacij, da lahko z opisanimi metodami delo ponovimo.

## Rezultati in razprava (Times New Roman, Krepko, 12)

Tabele, sheme in slike je treba vnesti (z ukazom Insert, ne Paste) v tekst na ustreznem mestu. Večje sheme in tabele je po treba ločiti na manjše dele, da ne presegajo ene strani.

## Sklepi (Times New Roman, Krepko, 12)

Povzetek rezultatov in sklepi.

**Zahvale (Times New Roman, Krepko, 12, Na sredino - opcija)**

Izvedbo tega dela je omogočilo ……

**Viri (Times New Roman, Krepko, 12)**

Glede na uporabljeno metodo citiranja referenc v tekstu upoštevajte eno od naslednjih oblik:

PRVA MOŽNOST (priporočena) - v abecednem zaporedju

Casati, P., Jadoul, F., Nicora, A., Marinelli, M., Fantini-Sestini, N. & Fois, E. (1981): Geologia della Valle del'Anisici e dei gruppi M. Popera – Tre Cime di Lavaredo (Dolomiti Orientali). *Riv. Ital. Paleont.*; Vol. 87, No. 3, pp. 391–400, Milano.

Folk, R. L. (1959): Practical petrographic classification of limestones. *Amer. Ass. Petrol. Geol. Bull.;* Vol. 43, No. 1, pp. 1–38, Tulsa.

DRUGA MOŽNOST - v numeričnem zaporedju

[1] Trček, B. (2001): *Solute transport monitoring in the unsaturated zone of the karst aquifer by natural tracers.* Ph. D. Thesis. Ljubljana: University of Ljubljana 2001; 125 p.

[2] Higashitani, K., Iseri, H., Okuhara, K., Hatade, S. (1995): Magnetic Effects on Zeta Potential and Diffusivity of Nonmagnetic Particles. *Journal of Colloid and Interface Science, 172*, pp. 383–388.

Citiranje spletne strani:

CASREACT-Chemical reactions database [online]. Chemical Abstracts Service, 2000, obnovljeno 2. 2. 2000 [citirano 3. 2. 2000]. Dostopno na svetovnem spletu: http://www.cas.org/CASFILES/casreact.html.

**Znanstveni, pregledni in strokovni članki ter predhodne objave se objavijo v angleškem jeziku. Izjemoma se strokovni članek objavi v slovenskem jeziku.**

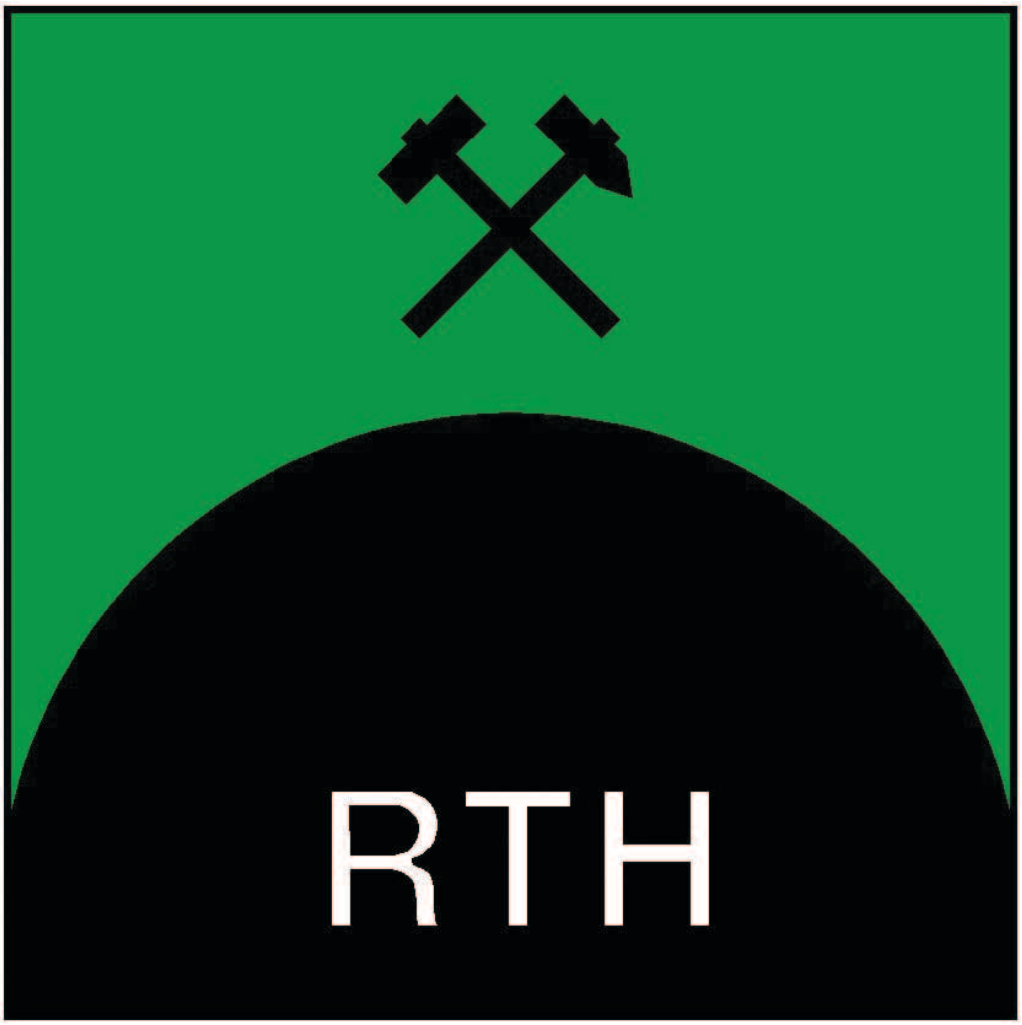
RTH

Slovenčeva 93
SI 1000 Ljubljana

tel.: +386 (1) 560 36 00
fax: +386 (1) 534 16 80
www.irgo.si

# IRGO

## Inženirska geologija
## Hidrogeologija
## Geomehanika
## Projektiranje
## Tehnologije za okolje
## Svetovanje in nadzor

# Če se premakne, boste izvedeli prvi

## Leica Geosystems rešitve za opazovanje premikov


- **Geodetski senzorji**
  samodejni tahimetri, GPS in GNSS senzorji
- **Geotehnični senzorji**
  senzorji nagiba, Campbell datalogger
- **Drugi senzorji**
  meteo, senzorji nivoja
- **Programska oprema**
  za zajem in obdelavo podatkov, analizo opazovanj, alarmiranje, predstavitev rezultatov

geo servis

Authorized Leica Geosystems Distributor

- when it has to be **right**

Leica Geosystems

Geoservis, d.o.o.
Litijska cesta 45, 1000 Ljubljana
t: (01) 586 38 30, i. www.geoservis.si